



Calhoun: The NPS Institutional Archive DSpace Repository

Theses and Dissertations

1. Thesis and Dissertation Collection, all items

1972

Optimization of waterjet propulsion pumps for hydrofoil application.

Percival, Robert Clayton.

Massachusetts Institute of Technology

<http://hdl.handle.net/10945/16289>

Downloaded from NPS Archive: Calhoun



Calhoun is the Naval Postgraduate School's public access digital repository for research materials and institutional publications created by the NPS community.

Calhoun is named for Professor of Mathematics Guy K. Calhoun, NPS's first appointed -- and published -- scholarly author.

Dudley Knox Library / Naval Postgraduate School
411 Dyer Road / 1 University Circle
Monterey, California USA 93943

<http://www.nps.edu/library>

OPTIMIZATION OF WATERJET PROPULSION
PUMPS FOR HYDROFOIL APPLICATION

Robert Clayton Percival

OPTIMIZATION OF WATERJET PROPULSION
PUMPS FOR HYDROFOIL APPLICATION

by

Robert Clayton Percival

B.S., U. S. Naval Academy

(1966)

SUBMITTED IN

PARTIAL FULFILLMENT

OF THE REQUIREMENTS FOR THE

DEGREE OF OCEAN ENGINEER

AND MASTER OF SCIENCE

at the

MASSACHUSETT'S INSTITUTE OF

TECHNOLOGY

June, 1972

OPTIMIZATION OF WATERJET PROPULSION
PUMPS FOR HYDROFOIL APPLICATION

by

Robert Clayton Percival

Submitted to the Department of Ocean Engineering on May 12, 1972, in partial fulfillment of the requirements for degrees of Ocean Engineer in Ocean Engineering and Master of Science in Mechanical Engineering.

ABSTRACT

The problem of finding the optimal waterjet propulsion pump for a hydrofoil of given configuration and displacement is examined from the point of view of least weight. Included in the propulsion pump study are the gear weight for matching the waterjet pump to the specified prime mover(s) and fuel weight for a specified range and speed.

From the current waterjet pump designs, two competing design approaches were selected: (1) Multi-parallel double suction impeller centrifugal pump with up to ten impellers and (2) Axial pump with an inducer impeller followed by axial stages when required by the pump head and net positive suction head. Because of the hydrofoil's drag to speed characteristics with its take off hump, the pump design problem requires an efficient reliable pump that meets the cavitation conditions at take off. Both designs satisfy these requirements.

From the required flow rate and system losses each pump design is solved for size and weight with the choice of optimum pump being the lightest design for that particular set of overall system parameters. Each pump design is directly related to the cavitation condition at the take off point which is the design point. The value of Thoma's cavitation criterion is closely related to the pump selection. As the value decreases the selection of pump shifts from the centrifugal to the axial design. The actual selection for a given design point is a trade off between the pump, gear, and fuel weights where the centrifugal design has the heavier fuel and lighter gear weight.

Thesis Supervisor: A. Douglas Carmichael

Title: Professor of Ocean Engineering

Acknowledgments

The author wishes to thank Prof. A. D. Carmichael who as the advisor gave much needed guidance and whose door was always open.

The author also wishes to express his appreciation to the U. S. Navy for making the educational experience possible and to his wife for giving the needed encouragement over the last three years.

Table of Contents

Title Page	1
Abstract	2
Acknowledgments	3
Table of Contents	4
List of Tables	6
List of Figures	7
List of Symbols	9
Chapter 1. Introduction	13
Chapter 2. Waterjet Propulsion	16
Chapter 3. Waterjet Pump Design	19
3.1 Basic Theory	19
3.2 Principles of Similitude	22
3.3 Specific Speed	23
3.4 Pump Characteristics	24
3.5 Impeller Types	25
3.6 Cavitation	27
3.7 Pump Design Problem	31
3.8 Centrifugal Pump Design	33
3.9 Inducer Design	40
3.10 Axial Pump Design	43
Chapter 4. Gear Design	48
Chapter 5. Prime Movers	52
Chapter 6. Integrated System Results	56
Chapter 7. Conclusions	62
Chapter 8. Recommendations	63



References	65
Tables	69
Figures	74
Appendix A. Development of Cavitation Parameters	93
Appendix B. Development of Specific Speed as a Function of Head and Flow Coefficients	96
Appendix C. Sample Calculations for the Centrifugal Pump Design	98
Appendix D. Sample Calculations for Axial Pump Design ..	102
Appendix E. Fuel Weight Calculation Method	105
Appendix F. Program Flow Diagram	106
Appendix G. Program Listing	115

List of Tables

<u>Table No.,</u>	<u>Title</u>	<u>Page</u>
1.	Performance Characteristics of Marine Gas Turbines	69
2.	Reduction Gear Minimum Weight Equations	70
3.	Sample Pump Solutions	71

List of Figures

<u>Fig. No.</u>	<u>Title</u>	<u>Page</u>
1.	Propulsion Efficiency vs Jet Velocity Ratio	74
2.	Hydrofoil Drag as a Function of Speed	75
3.	Impeller Flow Velocity Diagram	76
4.	Inducer Stage Performance Map	77
5.	K_h as a Function of K_q for the Axial Pump Design	78
6.	Centrifugal Pump Flow Rate vs Head For Changes in Specific Speed	79
7.	Centrifugal Pump Efficiency Curves for Various Values of Specific Speed	80
8.	Pump Impeller Profiles for Range in Specific Speed	81
9.	Relative Inlet Angle as a Function of Suction Specific Speed	82
10.	Centrifugal Pump Section for One Impeller	83
11.	Centrifugal Pump Section Dry Weight to Exit Diameter Ratio as a Function of Specific Speed	84
12.	Width Ratio as a Function of Specific Speed	85
13.	Centrifugal Pump Design Chart	86
14.	Centrifugal Pump Head Curve Coefficients as a Function of Non-Dimensional Specific Speed	87
15.	Inducer Stage Axial Pump Design	88
16.	Inducer Plus One Axial Stage, Axial Pump Design	89
17.	Theoretical Head Coefficient vs Flow Coefficient for Values of Diffusion Factor	90
18.	Inducer Inlet Flow Coefficient and Head Coefficient as a Function of Non-Dimensional Specific Speed for Various Designs	91

<u>Fig. No.</u>	<u>Title</u>	<u>Page</u>
19.	Gear Weight to Input Torque Ratio as a Function of Reduction Gear Ratio for $Fac=1.0$	92
20.	Percent of SHP vs Percent of SFC with Respect to Normal Power Approximation for a Gas Turbine	93

List of Symbols

<u>Symbol</u>	<u>Description</u>	<u>Unit</u>
Δ	Hydrofoil displacement	tons
D	Drag	lbs
L	Lift	lbs
T	Thrust	lbs
P	Power	ft-lbs/sec
τ	Torque	ft-lbs
ω	Angular velocity	rad/sec
v_j	Waterjet velocity	ft/sec
v_o	Hydrofoil velocity	ft/sec
Q	Flow rate	ft ³ /sec
N	Pump speed	rpm
A_j	Jet area	ft ²
Ain	Pump inlet area	ft ²
Lp	Pump length	ft
n	Number of double suction impellers	
H	Pump head	ft
Hth	Euler pump head	ft
Hsv	Net positive suction head	ft
ΔH_L	Total system head loss	ft
Ha	Atmospheric head	ft
h_v	Vapor pressure	ft
p	Static pressure	lb/ft ²

σ_p	Cavitation number with respect to impeller relative velocity at tip	
σ_T	Thoma's cavitation criterion	
K_q	Flow rate similarity condition	
K_h	Head similarity condition	
K_p	Power similarity condition	
N_s	Specific Speed	$\frac{\text{rpm (cfs)}^{\frac{1}{2}}}{\text{ft}^{3/4}}$
n_s	Non-dimensional specific speed	
S	Maximum suction specific speed	
ϕ	Flow coefficient	
ψ	Head coefficient	
D_{xy}	Pump diameter	ft
r	Radius ratio with respect to impeller tip radius	
V	Absolute flow velocity	ft/sec
W	Relative flow velocity	ft/sec
U	Tangential flow velocity	ft/sec
β	Relative flow angle	
α	Absolute flow angle	
DF	Diffusion factor	
c/s	Blade solidity	
K_D	Loss coefficient	
Ka	Blockage coefficient	
C_w	Pump weight coefficient	
C_L	Pump length coefficient	
η_h	Pump hydraulic efficiency	
η_m	Pump mechanical efficiency	

η_v	Pump volumetric efficiency	
η_p	Pump efficiency	
η_g	Gear efficiency	
M_o	Gear ratio	
m_g	First reduction or idler gear ratio	
$\Sigma F d^2/c$	Reduction gear weight factor	
N_p	Prime mover output speed	rpm
SHP	Shaft horsepower	shp
SFC	Specific fuel consumption	lbs/SHP-HR
C_{Fs}	SFC constant	
W_D	Dry pump weight	lb
W_w	Pump entrained water weight	lb
W_F	Fuel weight	lb
W_6	Gear weight	lb
ρ	Density	lb ^m /ft ³
g	Gravitational constant	

Subscripts

1	Impeller inlet
2	Impeller exit
h	Impeller hub
s	Impeller shroud
θ	Tangential component
m	Meridinal component
D	Design point

Chapter 1 INTRODUCTION

Waterjet propulsion is not a new ship propulsor and has been used or tested on a variety of ship types ranging from the three thousand ton naval destroyer to the small pleasure planing craft. Besides pleasure craft, waterjets have been most successfully used by river patrol craft in South Vietnam.

The large ocean going hydrofoil has brought renewed interest to waterjet propulsion because of the unique propulsion problems presented by the hydrofoil. Propeller propulsion with the power transmission through the strut has posed many problems to the designer and is currently considered to be unreliable. The waterjet has been demonstrated as a feasible and reliable system on the hydrofoil Tucumcari (PGH-2). Low overall efficiency and high plant weight are still problems to the system.

The current contract by the U.S. Navy for a waterjet hydrofoil in the two hundred ton range has caused increased interest and development work by industry on waterjet systems. Also, considerable work has been done on waterjets for surface effect ships which also encounter the same transmission problems and high craft speeds.

To the pump designer the waterjet system requires a departure from the normal practice of pump design and has made adapting off-the-shelf pumps to hydrofoils a difficult process. It has also created entirely new designs or caused adaptation of radical pump types from other fields.

Because of its low specific weight and small size, the aircraft derivative gas turbine has become the principle prime mover for the hydrofoil in its foil born mode. Even when British engines are included, the selection of gas turbines with respect to a shaft horsepower is very limited in the ranges from five to ten thousand and fifteen to twenty thousand shaft horsepower.

The problem of matching a given prime mover to the optimum pump type and number of each is a complex and not well understood problem. The problem has been studied to define the design parameters and how they relate to give the optimum design based on least system weight. The weight of the propulsion package will include: pump, gear, and engine dry weight; ducting and piping; entrained water above the water line; and fuel weight for a given hydrofoil range at constant craft speed. The problem is bound by the hydrofoil configuration, size, and speed. The configuration will be similar to the PGH-2 with the two after struts containing the inlet nacelles with the prime mover(s) and pump(s) located internally in the craft. The maximum number of engines and pumps will be two per strut. Only subcavitating foil speeds will be examined, therefore, limiting the cruise speed to fifty knots. A range in displacement from fifty to one thousand tons will be considered.

The pump design problem will be to establish the lightest pump, gear, and fuel weight combination for a

given set of waterjet propulsion parameters. All of the system components will be from tested designs. The pump design will be studied in detail while the gear and prime mover will only be studied for their weight growth and relationship to the overall problem. These designs will be incorporated in a computer design program. This program will be a subroutine in an optimization program for the overall waterjet propulsion system.

Chapter 2 WATERJET PROPULSION

The waterjet propulsion system may be considered as four sub-systems: inlet nacelle, ducting, pumping machinery, and nozzle. In order to understand the selection of pumping machinery, its interaction with the three other areas is required.

Using the mass average form, the thrust delivered by the system:

$$T = \rho Q (V_j \cos\alpha - V_o) \quad (2.1)$$

where $\cos\alpha$ is the depression angle of the nozzle. In the equilibrium state the thrust equals the drag for a given craft speed.

The velocity ratio, V_j/V_o , is the primary independent variable for system evaluation. Put into the momentum equation and neglecting the depression angle gives:

$$T = \rho Q V_o (V_j/V_o - 1) \quad (2.2)$$

Figure (1) taken from Levy's report¹ is a typical study of propulsive efficiency versus the jet velocity ratio for values of system loss coefficient where the losses are approximated by:

$$\Delta H_L = K_D V_j^2 / 2g \quad (2.3)$$

The studies show a flattening out of the efficiency curve to the right of the maximum efficiency for a given loss coefficient. This fact leads to a jet velocity higher than that at maximum efficiency because of the large decrease in

entrained water weight for a small decrease in system efficiency. This curve illustrates why systems designed on maximum efficiency tend to be heavy.

The shape of the hydrofoil drag versus speed curve, see figure (2), illustrates one of the basic design problems. In its displacement or hull born mode, the hydrofoil drag increases with speed to a maximum value just prior to flying. This point will be referred to as take off and typically represents the maximum value of drag. Just after take off the drag drops off and then increases with craft speed. For the typical subcavitating foil system, the take off speed is about one half the foil born cruise speed, ie., for a 45 knot cruise speed, take off speed is 22 knots.

To allow for acceleration, the available thrust at take off is assumed to be 25 percent greater than the equilibrium thrust at the take off point.

The main system parameters are selected outside the pump design problem. They set the required flow rate and system losses. From the parameters and losses the required pump head can be calculated:

$$H = V_j^2/2g - V_o^2/2g + \Delta H_L + h_\ell \quad (2.4)$$

Also the net positive suction head, which is the head above vapor pressure, at the pump inlet is found for use in cavitation considerations for the pump. It is given by:

$$H_{SV} = V_o^2/2g - \Delta H_L + H_a - h_\ell - h_v \quad (2.5)$$

It is these values of flow rate, pump head, and net positive suction head along the drag curve that drive the pump design.

Chapter 3. WATERJET PUMP DESIGN

Section 3.1 Basic Theory

The pumping machinery suitable for waterjet propulsion are turbomachines since other types are too heavy. Turbo-machinery covers a large range of pumps which can be classified by the flow path through the pump with respect to the rotating axis and grouped into three types: centrifugal, mixed flow, and axial.

The principle by which the pump transmits energy to the fluid is the conservation of angular momentum. In the case of steady flow, the change in net flux of angular momentum through the rotating impeller is equal to the torque, τ , on the impeller. Referring to the velocity diagram, Figure (3), :

$$\tau = \int_2 \rho r_2 V_2 \cos \alpha_2 dQ - \int_1 \rho r_1 V_1 \cos \alpha_1 dQ \quad (3.1)$$

For uniform flow across the impeller this reduces to the form:

$$\tau = \rho Q (r_2 V_2 \cos \alpha_2 - r_1 V_1 \cos \alpha_1) \quad (3.2)$$

The power required by the pump is:

$$P = \tau \omega = \rho Q g H \quad (3.3)$$

Combining equations (3.2) and (3.3) gives Euler's equation for the theoretical head, H_{th} , developed by an impeller without hydraulic losses:

$$H_{th} = 1/g (\omega r_2 V_2 \cos \alpha_2 - \omega r_1 V_1 \cos \alpha_1)$$

$$H_{th} = 1/g (U_2 V_{\theta 2} - U_1 V_{\theta 1}) \quad (3.4)$$

Euler's equation further reduces to the form:

$$H_{th} = 1/g (U_2 V_{\theta 2}) \quad (3.5)$$

when there is no prewhirl to the flow at the impeller inlet. This is a good approximation for most pump impellers with no inlet guide vanes and a uniform flow profile.

From equation (3.5), the theoretical head to capacity curve can be produced which gives an idea of the pump characteristics with respect to discharge angle from the impeller with the assumption that fluid angle, β_2 , leaving the rotor remains constant:

$$V_{\theta 2} = U_2 - V_{m2} \cot \beta_2$$

$$H_{th} = U_2^2/g (1 - V_{m2}/U_2 \cot \beta_2) \quad (3.6)$$

The flow rate is proportional to V_{2m} . This gives a linear relation of head to flow rate.

The definitions of velocity diagram angles varies considerably in the published literature. Figure (3) is based on definitions used by Stepanoff² and will be carried throughout.

For example, a centrifugal impeller with back sloping blades, where β_2 is less than 90° , and constant pump speed, produces a theoretical head proportional to Q :

$$H_{th} \propto C_1 - C_2 Q \cot \beta_2 \quad (3.7)$$

This gives a negative slope straight line. The power to capacity can also be shown:

$$P \propto Hth Q$$

$$P \propto C_1 Q - C_2 Q^2 \cot \beta_2 \quad (3.8)$$

Equation (3.8) gives a convex curve with some maximum power point. This fact could explain why back sloping impellers are often used.

Euler's equation for head also leads to definitions of pump efficiency. Efficiencies are divided into three groups: Hydraulic, volumetric, and mechanical. Only the hydraulic efficiency effects the pump head and is defined as the ratio of pump head to theoretical head:

$$\eta_h = H/Hth \quad (3.9)$$

The hydraulic losses are caused by skin friction along the direction of flow and eddies. The prediction of hydraulic losses is usually not accurate for a new design.

Volumetric efficiency is a measure of the leakage losses or losses in capacity.

Mechanical efficiency is the measure of losses in power that are not related to the head. They include disk friction and bearing losses. The total pump efficiency is the product of the three groups:

$$\eta_p = \eta_h \eta_v \eta_m \quad (3.10)$$

$$\eta_p = \frac{g \rho Q H}{550 \text{ SHP}} \quad (\text{English units}) \quad (3.11)$$

Section 3.2 Principles of Similitude

The current state of preliminary pump design is based on several established similarity conditions for geometrically similar pump designs. These relate two of our design input pumps; head, H , and capacity, Q , with pump size and speed.

Relating the fluid dynamic forces by the velocity triangles at the same geometric point on an impeller gives the flow coefficient:

$$\phi = V_m / U|_A = V_m / U|_B \quad (3.12)$$

where V_m is proportional to Q/D^2 and U is proportional to ND gives the similarity conditions:

$$K_q = Q/ND^3 = \text{constant} \quad (3.13)$$

which relates capacity to size and speed.

From Euler's equation the forces on the pump are proportional to head:

$$H_{th} = U_2 V_{\theta 2} / g \quad (3.14)$$

where $V_{\theta 2} \propto U_2$. Therefore, the head is proportional to tangential velocity squared. Put in non-dimensional form gives the head coefficient:

$$\psi = H / U^2 / g \quad (3.15)$$

substituting $N^2 D^2$ for U^2 gives the dynamic similarity that relates head to size and speed:

$$K_h = H / N^2 D^2 = \text{constant} \quad (3.16)$$

Since power is proportional to the product of head and flow rate, a similarity condition can be established from the above two:

$$K_p = P / N^{3/5} D^5 = \text{constant} \quad (3.17)$$

The basic similarity conditions are only good if the hydraulic losses of the impellers being compared are a constant fraction of the pump head, i.e., no Reynolds number effects. In practice, the assumption is good especially for the range in pump size that the hydrofoil will be utilizing.

The flow and head coefficients are important parameters in pump design. This fact will be treated in detail in the following section.

Section 3.3 Specific Speed

By combining the two similarity conditions to get a condition relating head, capacity, and pump speed:

$$K_q^{1/2} / K_h^{3/4} = N Q^{1/2} / H^{3/4} \quad (3.18)$$

This parameter is specific speed, N_s , and is used in three different sets of units:

$$N_s (\text{gpm}) = N (\text{rpm}) Q (\text{gpm})^{1/2} / H (\text{ft})^{3/4} \quad (3.19)$$

$$N_s (\text{cfs}) = N (\text{rpm}) Q (\text{cfs})^{1/2} / H (\text{ft})^{3/4} \quad (3.20)$$

$$n_s = N (\text{rps}) Q (\text{cfs})^{1/2} / (g H)^{3/4} \quad (3.21)$$

Due to usage, the non-dimensional form, n_s , is not as common as the dimensional forms. In order to handle comparisons, the following conversions are given:

$$Ns(\text{cfs}) = Ns(\text{gpm})/21.2$$

$$ns = Ns(\text{gpm})/17150$$

$$ns = Ns(\text{cfs})/811.3$$

Section 3.4 Pump characteristics

Pump characteristics are given in the form of a head versus capacity curve and an efficiency versus capacity curve. Both curves are for a given pump speed.

Since the similarity conditions, K_q , and, K_h , hold along a constant specific speed or efficiency line, the pump performance map can be constructed from one speed line; figure (4) is given as an example. A plot of K_h versus K_q , figure (5), is another form of the same information and is sometimes more useful.

The specific speed of a pump is usually at the point of best efficiency, BEP. Once the design is established from the operating requirements at BEP, the pump characteristics at off design can be found from the performance map.

Assuming the normalized head curve with respect to BEP is parabolic:

$$H/H_D = A (Q/Q_D)^2 + B Q/Q_D + C \quad (3.22)$$

and converting to a K_h versus K_q curve:

$$K_h = A' K_q^2 + B' K_q + C' \quad (3.23)$$

the original curve becomes:

$$H/H_D = A (Q/Q_D)^2 + B Q/Q_D N/N_D + C (N/N_D)^2 \quad (3.24)$$

In the case of the hydrofoil, knowing the design point, the head, and the flow rate for the off design, the off design pump speed can be found by solving the above quadratic equation.

Another aspect of the pump performance curves is their general shape with respect to impeller type and specific speed. The hydraulic losses produce a curve rather than the linear relationship given by Euler's equation for head. Figures (6) and (7) are examples of changes in performance curves for a range of specific speeds for centrifugal pump impellers ².

To explain the change in slope of the head curve at the best efficiency point, examine the design curves in figure (10). As the specific speed increases the flow coefficient also increases. When the capacity, ie., V_m , is increased for a constant pump speed, the percentage change in the tangential velocity component is much smaller for small values of ϕ_2 than large values of ϕ_2 . Therefore, for high values of specific speed, the head term, which is proportional to the tangential velocity component, drops off sharply with an increase in flow rate.

Section 3.5 Impeller Types

Turbomachinery can be classified by three basic impeller types based on the flow path through the impeller with respect to the rotating axis. Also impellers are further classified by specific speed. Although each type could

theoretically cover a broad range of specific speed, usage has dictated certain ranges for each impeller type to achieve the best efficiency. These ranges are only general and there is definitely a large overlap in each type³.

In the centrifugal impeller, the fluid exits radially with respect to the rotating axis by changing the flow direction 90 degrees through the impeller. The specific speed range is from 24 to 189. This indicates that the centrifugal pump is used for high head and lower flow rate applications.

The mixed flow impeller has an exit flow path somewhere between the radial and axial direction. Its range is from 189 to 472.

As the name suggest, the axial pump flow path is parallel with the pump axis. Its specific speed range is 472 to 708. The axial pump is used for higher flow rate and lower head conditions where additional stages are added to cover higher head requirements. Much of the axial gas turbine compressor design work has influenced the axial pump design.

All three of the impeller types are represented in waterjet propulsion. For small craft application, Jacuzzi builds a pump with one mixed flow impeller and Buehler uses a two stage axial design. The current hydrofoil, PGH-2, uses a centrifugal pump with two double suction impellers operating in parallel on one shaft. By splitting the flow, the centrifugal pump can handle the large flow rates.

Further discussion of the pump types with their design parameters and performance characteristics is covered in the design section.

Section 3.6 Cavitation

In classical fluid dynamics, cavitation occurs when the local static pressure of the fluid is equal to the vapor pressure:

$$P + \frac{1}{2}\rho V^2 = P_v + \frac{1}{2}\rho V^2 \quad (3.25)$$

To the pump designer, cavitation imposes severe limitations. The vapor bubbles forming along the pump impeller can cause impeller damage by collapsing and impinging on the surface eroding the metal. This process can also cause vibration and noise in the pump. A fall off in pump head is caused by a more developed vapor cavity.

The third input to the design problem, net positive suction head, H_{sv} , is the most important for cavitation considerations since it gives the total head above vapor pressure at the impeller inlet:

$$H_{sv} = h - h_v + V_{m1}^2 / 2g \quad (3.26)$$

The point at which cavitation occurs for given types of impellers is determined from experimentation. The point where there is a three percent drop in head is most common and will be used here. Incipient cavitation would have already occurred at this condition.

Prandtl's cavitation number in terms of relative inlet velocity at the impeller shroud is:

$$\sigma_p = \frac{P - Pv}{\frac{1}{2} \rho W_{sl}^2} \quad (3.27)$$

Substituting in the equation for H_{sv} gives:

$$H_{sv} = \frac{W_{sl}^2}{2g} + K_1 \frac{V_{ml}^2}{2g} \quad (3.28)$$

where K_1 is taken to be 1.1 to account for impeller eye conditions. This equation relates the velocity inlet triangle, ϕ_1 , to H_{sv} for a given cavitation number. If σ_p is the critical value, then the minimum value of H_{sv} is determined.

There is another cavitation constant used in pump design that was first introduced by Thoma². Thoma said that there is an experimental ratio between the inlet velocity head at capacity cut off and the pump head. This was first used for low N_s pumps. Thoma's constant is defined:

$$\sigma_T = H_{sv}/H \quad (3.29)$$

and is constant for a given N_s for conditions approaching cavitation while the similarity conditions still hold. There is also a Reynolds number effect but some uncertainty exists how this effect changes in σ_T . A recent study⁴ of large centrifugal impellers shows σ_T increasing with impeller size which is contrary to what theory suggests.

A third parameter is found by applying the similarity

conditions to H_{sv} that were applied to pump head. This is a suction specific speed and relates H_{sv} to N , and Q :

$$S = NQ^{1/2} H_{sv}^{-3/4} \quad (3.30)$$

S is expressed in the same units as N_s with the same conversions holding.

Suction specific speed is a useful parameter for it relates the cavitation limitations to specific speed:

$$N_s = S \sigma_T^{3/4} \quad (3.31)$$

For example, if a limiting value of S is used and Thoma's criterion is determined from the pump requirements, then the pump specific speed is set.

When suction specific speed is expressed in terms of cavitation number, inlet flow coefficient, and inlet geometry, as developed in appendix A, some insight is given into the influence of cavitation on the pump design:

$$S = \frac{\frac{60}{\pi} \{ \frac{\pi}{4} (1 - r_{h1}^2) \}^{1/2}}{\phi_1 \{ 1/2g (1 + \sigma_p + \frac{\sigma_p}{\phi_1^2}) \}^{3/4}} \quad (3.32)$$

Figure (9) is a plot of the above equation and shows how there is an optimum value of ϕ_1 , ie., inlet angle, for a given value of cavitation number. Also, it shows that a minimum value of hub to tip ratio gives a maximum value of S .

Wislicenus⁵ states that for commercial pump operation, a value of σ_p for cavitation free operation is 0.4. However, the Hydraulic Institute uses S equal to 8500, which corresponds to a σ_p of 0.2 as the limit. Specially designed pumps, which will be covered in detail, have reached values of S equal to 34,000. As figure (9) shows, these pumps have low values of ϕ_1 and τ_p and operate in the cavitation region.

Cavitation is the primary limit to hydrofoil waterjet pump design. Furthermore, because of the increased losses and lower ram head, the take off point is the critical point for cavitation and, therefore, drives the pump design.

Section 3.7 Pump Design Problem

The curve of hydrofoil drag to ship's speed establishes a two point design problem for the pump designer. One point is at takeoff and the second at cruise. The takeoff point requires the pump to maintain head and avoid cavitation damage and the cruise point requires good pump efficiency. There is a choice of designing at either point and checking the other for cavitation and efficiency. Since the inlet conditions are critical for establishing good performance against cavitation, the takeoff point is chosen as the design point.

Current approaches to pump design for waterjet propulsion can be put in three categories:

- (1) The first design is the centrifugal double suction impellers in parallel on one shaft.

This design is demonstrated by the (PGH-2) pump which was built by Byron-Jackson.

⁴ Lockheed has also recommended this design.

The design approach is to reduce the flow rate per impeller. This raises the pump speed and decreases the impeller size. This design will be covered in detail.

- (2) The second design approach is to have a two speed multi-stage pump. The first stage operates at a lower RPM which allows the pump to meet the inlet cavitation requirement. The remaining stages have a higher

speed and produce the majority of pump head. This design is being developed by both Aerojet and Garrett. The disadvantages are the special gear arrangement and double shaft. This arrangement is feasible but requires development to insure reliability. This design will not be covered since it is similar in size and weight to the third design.

- (3) The third approach is the single speed multi-stage pump with the first stage being an inducer which operates at a suction specific speed approaching 30,000. This design has been built and tested by Pratt and Whitney and by Rocketdyne. The inducer has proven both efficient and reliable, after early problems in the inducer design.

The pump design section of the optimization program will calculate the design parameters, size, and weight for both the centrifugal, multi-parallel, double suction impeller design and the axial inducer design. The lightest weight pump including entrained water, gear, and fuel weight is sub-optimized within the overall program.

Each pump design will be established at the design point, ie., take off point. From the relationships of Thoma's cavitation criterion, specific speed, suction specific speed, and design coefficients to the required flow rate and head at take off, the pump size and weight

are established for each design. Any other point along the drag curve will be considered an off design point and the pump speed and efficiency are calculated from the pump characteristic head and efficiency curves. The following design sections are based on current pump designs incorporating realistic values of suction specific speed at the takeoff point.

Section 3.8 Centrifugal Pump Design

For hydrofoil application, the centrifugal pump has been selected by several pump designers and manufacturers. They use multi-parallel, double suction impellers on one shaft and in one pump casing. The PGH-2, which has one pump with two double suction impellers, has demonstrated that the design is both reliable and efficient.

The multi-parallel design has several advantages over the single stage pump design when both are operating near the same suction specific speed. Given the operating conditions, they both have the same N_s for one impeller:

$$N_s = S_{\sigma_T}^{3/4} \quad (3.33)$$

For the double suction design, the specific speed will be for one impeller, i.e., one half of a double impeller. With, n , being the number of double suction impellers, as n increases and impeller size decreases:

$$N = \frac{N_{sH}^{3/4}}{Q^{1/2}} (2n)^{1/2} \quad (3.34)$$

This reduces gear weight and produces a long narrow pump

design when six to ten double suction impellers are used.

The number of double suction impellers depends on output speed from the prime mover and available space and machinery configuration in the hydrofoil. For design purposes, a maximum of ten impellers is used.

The program objective in the pump design is to establish the pump size and weight. The pump dry weight is a function of the pump geometry and its size. The geometry reflects both the specific speed and the type of discharge system that is used in the design. The design is based on the pump model (ref.4) that was developed specifically for waterjet propulsion. Since the pump configuration and discharge system (Fig. 10) is established the weight is only a function of size and specific speed.

By letting the impeller exit diameter, D_{2s} , represents the size, the dry weight is:

$$\frac{W_D}{D_{2s}^x} = F(N_s) \quad (3.35)$$

The value of x is somewhere between two and three depending on the growth and casing thickness. From the stress analysis in reference (4) the minimum casing thickness is much less than the thickness used for economical casting techniques. Therefore, it is assumed that for the range in pump head experience in hydrofoil design, the casing thickness is a constant. This fact gives $x = 2$. This relationship is further supported by the Peerless pumps¹ plotted in figure(11). Even though their weight is heavier than

the waterjet pump designs, they demonstrate that equation (3.35) for $x = 2$ is representative.

Knowing the head coefficient of the pump establishes the exit diameter since pump speed is known:

$$D_{2s} = \frac{60}{\pi N} (gH/\psi_2)^{\frac{1}{2}} \quad (3.36)$$

However, the head coefficient is not constant over the range of specific speed but varies slightly with N_s . By substituting into the definition of specific speed, a relationship can be found between the head coefficient, flow coefficient, and pump geometry term at impeller exit. From appendix B:

$$n_s = \frac{1}{\pi^{\frac{1}{2}}} (Ka b/D_{2s})^{\frac{1}{2}} \phi_2^{\frac{1}{2}} / \psi_2^{3/4} \quad (3.37)$$

where Ka is the blockage factor.

From current pump design practice the impeller discharge angle is a constant in the range of 22 degrees to 23 degrees for good pump performance. By setting β_2 constant, the specific speed can be expressed as a function of ϕ_2 and b/D_{2s} where:

$$\psi_2 = n_h (1 - \phi_2 \cot \beta_2) \quad (3.38)$$

assuming no inlet prewhirl and a value of hydraulic efficiency. The plot of equation (3.37) for values of β_2 and specific speed is often used as a design chart for centrifugal pump design^{2,6}. However, before this plot can be completed something must be known about the impeller width ratio, b/D_{2s} , with respect to N_s . As illustrated in figure (12), the impeller exit width and blade curvature change

considerably as N_s is increased. Both the curves from the literature^{2,7} and values of width ratio from current designs show the same slope of b/D_{2s}^2 with respect to specific speed (Fig.12). By establishing the width ratio the design chart (Fig. 13) can be completed and the head coefficient for a given specific speed can be found giving the impeller exit diameter.

From figure (11), the pump weight for a single section is established from the three current designs available:

$$W_D = C_w N_s D_{2s}^2 \quad (3.39)$$

where $C_w = 3.32$ for a single discharge volute.

Following current practices for light weight pump construction, the casing is cast from aluminum with a titanium impeller and steel pump shaft. From the Lockheed report⁴ a typical weight breakdown for an eight double suction impeller pump with an $N_s = 57.2(1210)$:

Pump case	2260 lbs.
Impellers	832
Shaft	627
Bearings	431
Misc.	350
<hr/>	
Total	4500 lbs.

For good pump efficiency the impeller inlet angle was taken equal to the exit angle, ie., $\beta_1 = \beta_2$. The requirement for higher suction specific speed causes a smaller value of inlet angle to be used. In order to study the possibil-

ity of increasing the suction specific speed for the double suction impeller design, Lockheed⁴ tested two impellers with different configurations. Using the normal configuration for inlet ducting and a five bladed impeller with an inlet blade angle of 13 degrees and an exit angle of 22 degrees, a suction specific speed of 13,800 (gpm) with a H_{sv} of 31 feet was obtained. This relationship of low flow coefficient to high S was established in section (3.6). For current centrifugal design an inlet of 13 to 15 degrees is considered a minimum. Therefore, for this design, β_1 was set at 14 degrees, $\phi_1 = 0.25$. By knowing the blockage and hub to tip ratio at the inlet, the flow coefficient can be used to find the inlet diameter:

$$D_{ls} = \frac{240}{K_a \pi^2 \phi_1 N (1 - r_{hl}^2)} \frac{Q/n}{R_{hl}}^{1/3} \quad (3.40)$$

For the multi-parallel design the minimum hub diameter is established by the pump shaft requirements to handle the input torque. A value of $r_{hl} = 0.5$ will be used which corresponds to designs established by Lockheed⁴. A detailed design would require an increase in r_{hl} for increases in the number of double suction impellers. As the number of impellers increases, Q per impeller decreases, thereby decreasing D_{ls} , but the power transmitted remains constant, holding R_{hl} minimum constant.

The centrifugal pump length is scaled from the impeller

inlet diameter, D_{1s} . The pump length is based on the section length for one impeller (Fig. 10) plus the shaft and bearing supports at the pump ends. The section length is governed by the inlet system. Letting the average inlet velocity at the pump base be equal to 75 percent of the impeller inlet velocity, v_{ml} , gives the impeller section inlet area:

$$A = \frac{Q/N}{0.75v_{lm}}$$

$$A = \frac{Q/N \cdot 60}{0.75\pi N D_{1s} \phi_1} \quad (3.41)$$

By letting the rectangular inlet be:

$$A = L_x L_y \quad (3.42)$$

where:

L_x - pump section length

L_y - pump section width

by letting:

$$L_y = C_L L_x$$

where:

$$C_L = 0.866$$

then:

$$L_x = \sqrt{A/C_L}$$

The total pump length is then:

$$L_p = nL_x + L_x \quad (3.43)$$

The pump efficiency is then found by scaling for Reynolds number from a standard value of $\eta_p = 0.88$ when $D_{2s} = 2.33$ feet. The efficiency scaling law is based on a method used by Byron Jackson ⁹:

$$\frac{1-\eta_h}{1-\eta_h'} = \left(\frac{D' 2s}{D_{2s}} \right)^{0.165} \quad (3.44)$$

The centrifugal pump off design point characteristics are found by assuming parabolic head and efficiency curves. The head curve for the centrifugal design changes with changes in specific speed. The off design pump speed is found by using equation (3.24) where the coefficients are a function of specific speed. This relationship is plotted in figure (14).

Section 3.9 Inducer Design

The problem of pumping the cryogenic liquids for rocket engines created the need for an impeller that is generally referred to as an inducer. The rocket fuel pump was required to match a high rpm input, usually a vapor turbine, to handle the high flow rates and to be as small and light weight as possible. In order to reduce size, the pump speed must be increased. This requires an increase in inlet suction specific speed for a given pump head and net positive suction head at the pump inlet. To increase S a special inducer impeller was put in front of a centrifugal impeller raising the H_{sv} for the centrifugal impeller.

The same requirements for the rocket pump are also present for the hydrofoil waterjet pump. Therefore, the inducer design has been adapted to the waterjet pump application.

The design goal is to operate at the highest possible suction specific speed, ie., high rpm, without reducing pump efficiency or reliability. The inlet geometry and, therefore, pump size is governed by the equation (3.32) developed in appendix A. As stated in the cavitation section, low values of cavitation number, hub to tip ratio, and inlet flow coefficient are required to achieve high values of suction specific speed at the pump inlet.

Figure (9) shows that there is an optimum inlet blade angle, ie., ϕ_1 , for a required suction specific speed.

Taking the derivative of equation (3.32) with respect to ϕ_1 gives the optimum value of ϕ_1 for a given value of σ_p , see appendix A. Achieved values of σ_p are determined experimentally and depend on the amount of impeller loading along the blade. The ratio of maximum inlet relative velocity to actual relative velocity at the tip can be put as a function of cavitation number:

$$\sigma_p = \left(\frac{W_{1S}}{W_{max}} \right)^2 - 1 \quad (3.45)$$

For low values of σ_p , $\frac{W_{max}}{W_{1S}}$ approaches 1, ie., no loading at the impeller inlet. For $S = 30,000$, a very low value of σ_p is required. If $r_{h1} = 0.3$ and $\sigma_p = 0.03$, then the optimum value of ϕ_1 is 0.166 from equation (3.32) and a theoretical suction specific speed of 26,000 should be achieved.

From the inlet analysis, the inducer size and inlet geometry are fixed. The outlet is fixed by the second stage design. Typically, the next stage has a lower suction specific speed impeller and, therefore, its inlet flow coefficient is much higher. If the second stage has the same tip diameter, then the meridional velocity must be much larger. This causes the hub to tip ratio to increase by a factor of two or larger through the inducer. Some designs also decrease the impeller tip diameter through the inducer. This improves flow to the second stage and decreases its tip speed. This is carried out when there

is a large change in flow coefficient.

The blade shape of the impeller is very critical to its performance. Several design methods are in the literature, references (10) to (16), but the best designs have been achieved through experimental and developmental work ^{10, 11}.

The major problem in adapting the inducer type impeller for hydrofoils is in preventing cavitation damage while not sacrificing cavitation performance. Since a rocket is only a short duration vehicle, maintaining pump head was the primary concern and some impeller erosion was acceptable.

There are several current designs by industry of successful uses of the inducer impeller. Sponsored by the Joint Surface Effect Ship Project Office, both Pratt and Whitney ¹¹ and Rocketdyne ¹⁰ have developed and tested pumps that have good cavitation performance and resistance to cavitation damage. Since both of these inducers have approximately the same minimum σ_T and specific speed, they will be used as the basis of the first stage of the axial pump design. The impeller parameters used are:

$$N_s = 149.5$$

$$r_{h1} = 0.3$$

$$r_{h2} = 0.7$$

$$\psi_2 = 0.4$$

$$\phi_2 = 0.11$$

$$\sigma_{T\min} = 0.055$$

Section 3.10 Axial Pump Design

The axial pump consists of the inducer impeller discussed in section 3.9 followed by axial stages when needed (Fig. 15 and Fig. 16). The inducer can be used in front of any of the three impeller types. The axial stage was selected because for many cases only the inducer impeller is required to handle the pump head and σ_T . This fact is due to the speed restriction imposed by the subcavitating foils. Only by going to very high jet velocity ratios does the pump head exceed 700 feet. The axial stage design is the lightest weight due to the inlet matching and discharge nozzle associated with the design. The nozzle section can be as short as 0.65 times the inlet diameter. These two factors give advantages over the centrifugal design where the discharge system is a large part of the pump weight and the mixed flow pump where a change in tip diameter and flow direction require a longer and more complex problem of matching the stages.

The axial stage design consists of a stator row and rotor. Patterned after the axial compressor design, the design has a higher hub to tip ratio, a higher flow coefficient, and a lower head coefficient than the inducer stage. A series of detailed designs and tests, references (17) through (19), give three designs with hub-tip ratios of

0.4, 0.7, and 0.8 with increasing blade loading as the hub-tip ratio increases.

The axial stage must be matched to the inducer. From the inducer exit hub to tip ratio and the ratio of inlet to exit tip diameters, the axial stage inlet flow coefficient can be calculated:

$$\phi_{1 \text{ axial}} = C \phi_{1 \text{ inducer}}$$

$$C = \frac{\{Ka D_{1S}^2 (1-r_{h1}^2)\}_{\text{inducer}}}{\{Ka D_{1S}^2 (1-r_{h1}^2)\}_{\text{axial}}} \quad (3.46)$$

For Ka and D_{1S} to be constant for both designs if $\phi_{1I} = 0.11$ then $\phi_{1A} = 0.196$. If the tip diameter is decreased through the inducer as in the Rocketdyne design, the r_{h1} is increased for the inducer raising the flow coefficient. From the axial designs, the parameter diffusion factor is used as a measure of rotor blade loading:

$$DF = 1 - \frac{W_{2S}}{W_{1S}} + \frac{R_{S2} V_{\theta 2} - R_{S1} V_{\theta 1}}{c/s W_1 (R_{S2} + R_{S1})} \quad (3.47)$$

for $R_{S2} = R_{S1}$, DF reduces to:

$$DF = 1 - \frac{W_2}{W_{1S}} + \frac{\Delta V_{\theta}}{2(c/s)W_1} \quad (3.48)$$

As shown in figure (17) the diffusion factor gives the relationship between impeller loading and flow and head coefficients. Because of the high head inducer design, a DF of around 0.5 is used giving $\psi_2 = 0.2$. Using esta-

blished values of solidity, $c/s = 1.01$ for the $r_{h1} = 0.7$; the preliminary design is established from the flow and head coefficients.

Figure (19) is a plot of head and flow coefficients versus specific speed for inducer designs available in the literature^{10, 11, 12, 13}. Since the higher head inducers, which are the Rocketdyne and Pratt and Whitney designs, are in a narrow range of specific speed; this specific speed value is used for the inducer design. By using one inducer the design approach to the axial pump is modified by letting σ_T determine the suction specific speed.

Depending on Thoma's cavitation criterion, the take off suction specific speed can vary up to a maximum value. When the maximum S is exceeded, an additional axial stage is added to the pump design.

Using flow rate and pump head, pump speed is calculated. Inlet diameter is calculated from N and flow coefficient.

To determine the number of stages both σ_T and head coefficient must be used. When either the minimum value of σ_T or maximum value of S are exceeded, the number of stages increases.

Pump length and dry weight are a function of the number of stages and inlet diameter:

$$L_p = C_L D_{s1} \quad (3.49)$$

$$W_{Dt} = C_w D_{1S}^x \quad (3.50)$$

where x is less than three and greater than two. Pratt & Whitney sets $X = 2.2$ and other sources¹ set X at 2.5 for more conventional designs. Since a series of pump sizes is not available for this design, a value of $X = 2.3$ will be used. Scaling from the Rocketdyne pump weight, the coefficients are:

<u>No. Stages</u>	<u>C_w</u>	<u>C_L</u>
1	347.1	1.79
2	393.5	1.71
3	439.9	2.03

The off design operating points are calculated by applying the similarity conditions to the characteristic head curve. Figure (4) is the map for the inducer design and was generated from equation (3.24). From the off design rpm, the ratio of off design to design flow coefficients is calculated. If the flow coefficient ratio is much less than 1.0, stall is possible; and if it is greater than 1.0, cavitation is more likely or a higher H_{sv} is required. Since off design points are at a higher craft speed, ie., increased ram head, the off design cavitation problem does not occur. From test cases run, there has not been a significant change in ϕ_1 from the take off to cruise operating point.

Pump efficiency based on measured results is set at 91% for a 3.66 foot impeller diameter. The efficiency is scaled for larger and smaller pump sizes using equation

(3.44). The off design efficiency is found by assuming the efficiency curve with respect to flow rate to be parabolic.

Chapter 4 REDUCTION GEAR DESIGN

The lightest weight gear design is the gas turbine's integral gear box, and therefore, when available it should be used. When a reduction gear is required to match the pump speed to the prime mover output shaft speed, a gear design based more on aircraft than marine practice is designed.

The purpose of the gear design is to give the weight growth associated with changes in pump speed and different engine-pump combinations.

Three different gear designs are incorporated in the program to handle the possible range in gear ratio and the various engine to pump combinations. When the number of engines equals the number of pumps, a planetary gear is incorporated because it has the lightest weight. For an unequal number of pumps and engines a combining gear is required to match either two engines to one pump or one engine to two pumps. This gear is based on a single reduction offset gear with idler design for gear reduction ratios less than twelve and a double reduction double branch design for higher gear ratios.

The gear weight determination is based on a method developed by Willis²⁰. The method uses the assumptions that the gear weight is proportional to the solid rotor volume, Fd^2 , and the rotor volume is a function of input torque, gear ratio, and K factor where K factor is uniform for all gears:

SHP and output speed, N_p , the gear weight is calculated by:

$$W_G = 0.35 \frac{126,000}{K} \frac{SHP}{N_p} \frac{(\sum F_d)^2}{C} \quad (4.5)$$

For the planetary offset gear designs, the K factor equals 500. This requires a hardness of $R_c = 60$ which implies a hardened and ground gear. In order to have a light weight and relatively small gear, the high K factor is essential. To demonstrate the feasibility of a large planetary gear, Curtiss Wright built a 40,000 SHP gear for the U.S. Navy.

The offset combining gear design is based on a single input and output shaft design times a constant to account for the added pinion and idler gear in the case of the two engine one pump combination or the added bull gear for the two pump one engine combination. For the two pinion gear design the weight would be less if the total SHP were used because the power is divided decreasing the pinion and idler size. However, the value of SHP used in the program is always SHP per engine. Therefore, the weight increases by a factor of 1.3. For the two bull gear design the weight is 1.7 times that of the single shaft design.

The double reduction gear design is included in order to cover entire range of gear ratio. Current marine locked train double reduction gears are too heavy for hydrofoil application. Therefore, a light weight gear design of higher K factors requires development. Because the K

$$d^2 F = \tau/2k \left(\frac{m_g + 1}{m_g} \right)^3 \quad (4.1)$$

For each gear type an expression of the overall gear ratio, M_o , and the first reduction or idler gear ratio when applicable is developed and set equal to the weight factor:

$$\frac{\Sigma Fd^2}{\tau/2k} = \frac{\Sigma Fd^2}{C} \quad (4.2)$$

An example of the design method is the single offset gear with idler where the weight factor is equal to:

$$\frac{\Sigma Fd^2}{C} = 1 \frac{1}{m_g} + m_g + m_g^2 + M_o + \frac{M_o}{m_g} \quad (4.3)$$

To find the lightest gear design the value of m_g is determined by taking the derivative of the right hand side of equation (4.3) with respect to m_g and set equal to zero.

For the offset design this reduces to:

$$2m_g^3 + m_g^2 = \frac{M_o^2 + 1}{2} \quad (4.4)$$

Similar expressions are developed for all gear types and are summarized in table (2).

From the weight factor, gear weight is found by determining the desired K factor which is a measure of compressive tooth stress and corresponds to the surface hardness. An allocation factor, AF, is also used to adapt the general design method to particular applications.

For hydrofoils, $AF = 0.35$. Therefore, for a given engine

factor used in the design method is an average value and also to bias the problem against the larger gear, a lower K factor value of 300 is used. This value would still require a harden gear for the first reduction pinion and gear.

For the planetary and offset gears, the gear efficiency is set at 0.98. For the double reduction gear $\eta_g = 0.95$.

Figure (19) illustrates the influence of gear ratio on gear weight for the four designs. The gear weight divided by input torque is plotted versus the gear ratio. From the figure it is clear that the planetary gear is by far the lightest design.

Chapter 5 PRIME MOVERS

The aircraft derivative gas turbine is the predominant prime mover for hydrofoil craft. Table (1) is a list of British and American engines that have been marinized and are, therefore, suitable for hydrofoil propulsion. The list is not all-inclusive but gives the range of power available. For example, the Rolls Royce Olympus is not included but the FT4 and LM2500 engines cover that particular power range.

A confusing aspect of comparing gas turbines is the different power ratings. For this problem, only the maximum intermittent power and the normal power ratings are used. Another commonly used term is maximum continuous power which lies between the two listed ratings. The inlet ambient temperature plus inlet and exhaust losses also effect the power ratings. The three common ambient temperatures used by manufacturers are 60° F, 80° F, and 100° F. The table reflects the current United States Navy practice using 100° F inlet temperature as the standard.

Some engines are available with an integral reduction gear. The Proteus engine is listed for the 1500 rpm and 1000 rpm versions of output shaft speed.

The matching of gas turbine to craft displacement is critical for an optimum propulsion plant weight to displacement ratio. Because of the existing gaps in available engine sizes, ideal matching of engine power to required power is not possible for all displacements. Instead of determi-

ning craft size by mission and required payload, the availability of a gas turbine or combination of gas turbines should be a primary consideration in the decision of craft size.

The engine size, efficiency and output rpm all have an impact on the overall design. However, the single largest weight component that the engine influences is fuel weight. Depending on the required hydrofoil range, the fuel weight can be a significant percentage of the overall propulsion plant weight. The fuel weight is calculated for a constant cruise speed assuming that the lift to drag ratio is constant and the system losses are only a function of the jet velocity head term.

The measure of engine efficiency is given in terms of specific fuel consumption, SFC. A characteristic of the gas turbine's performance is that its minimum SFC is at maximum power. The SFC then drops off as the power decreases. For the fuel calculation, the relationship of SFC to SHP is approximated by:

$$SFC = C_{FS} / (SHP)^n \quad (5.1)$$

where $n = \frac{1}{4}$ for SHP from normal power to 70 percent of normal and $n = 3/4$ for the range from 70 percent downward. Figure (20) shows this approximation with respect to an actual gas turbine curve.

The fuel consumption for constant SHP for a time Δt is:

$$W_F = SFC \cdot SHP \cdot \Delta t$$

$$W_F = C_{FS}^{(1-n)} \Delta t \quad (5.2)$$

However, for the case of constantly decreasing SHP as the fuel is burned, the fuel weight solution is not straight forward. The required SHP at any time is a function of displacement and system losses if D/L and V_o are held constant. As developed in Appendix E:

$$SHP = \frac{\rho g Q H}{550 \eta_p \eta_g} \quad (5.3)$$

$$SHP = \frac{\gamma A_j V_j}{550 \eta_p \eta_g} (h_l + (1+K_D) \frac{V_j}{2g} - \frac{V_o^2}{2g}) \quad (5.4)$$

$$\text{where: } V_j = -\frac{V_o}{2} + \left\{ \frac{V_o^2}{4} + \Delta (D/L) \frac{1}{\rho A_j} \right\}^{\frac{1}{2}} \quad (5.5)$$

For solving by computer, a discrete step approach was used. The total fuel was then the sum of the intervals:

$$W_F = \sum_{i=1}^N W_{Fi} \quad (5.6)$$

For a range of 750 n. miles, the difference in fuel for $N = 20$ or $N = 40$ was less than one half of a percent, therefore, 20 intervals is used for the calculations.

As would be expected if the shaft horsepower per prime mover is less than 70% of normal power at full load, at the end of 750 n. miles the required SHP will only be 50% of

normal power for a craft speed of 45 knots. As figure (20) demonstrates, the SFC in the 70% to 50% range is much increased. These relationships will be further discussed in the chapter on integrated system results.

The engine output shaft speed is important for gear weight. The lightest gear is the integral box and is treated as part of the engine weight.

The last area of engine influence in design is the number of prime movers. The design method only treats the cases of 1, 2, or 4 engines. When the number of engines increases, provided a sacrifice in SFC is not required, the design weight tends to improve mainly due to the decrease in pump weight and water weight. However, multiple engines also offer advantages in flexibility and reliability. For example, if one engine out of four could be shut down during cruise, then the SHP per engine of the other three would increase and total engine hours would decrease.

The detailed design problems of engine and pump installation including auxiliary systems have not been treated. Since the particular engine choice is outside of the problem, its auxiliary weights will not change. A detailed study of the best engine and pump arrangement given the number and type would prove worthwhile for future study.

Chapter 6 INTEGRATED SYSTEMS RESULTS

The waterjet system is most strongly influenced by the choice of gas turbine for a particular hydrofoil displacement. As already discussed in chapter 5, the propulsion system weight to displacement ratio varies considerably with displacement primarily due to the availability of gas turbines over a broad range in power.

In order to analyze the design program results and its choice of optimum pump and design parameters, it must be remembered that the craft displacement and choice of gas turbine are inputs to the program and, therefore, are not optimized. Most of the analysis of the design program was carried out on a hydrofoil of 400 ton displacement because of the availability of published figures of estimated losses and weight data for that particular size hydrofoil. Computations were also made for 80 tons, 200 tons, and 750 tons of displacement.

The program selects the lightest pump, gear, and fuel weight combination for a given operating condition. Although the size and performance of the nacelle and structural diffusion are important in defining the operating conditions, the jet velocity ratio gives the clearest indication of what type pump will be selected and what weight is driving the optimization program. As figure 1 illustrates there is a value of V_j/V_o for maximum propulsive efficiency and values to the right of this point decrease the propulsive efficiency thereby increasing the required power.

As stated earlier, the optimum design point will be for higher values of V_j/V_o than the maximum efficiency point. The results support this fact except when the problem is bounded. From table (3), it is seen that the 400 ton hydrofoil went to a high optimum value of V_j/V_o (2.83) for the case of the FT4C-2 gas turbine where there was no power limitation. For the other 400 ton cases using one engine, the upper horsepower limit at take off limited the V_j/V_o to some value less than 2.83. If two engines were used splitting the horsepower so that only 50% of normal power would be required at cruise, the SFC to SHP relationship will drive the V_j/V_o value very high as in the FT4A-2 example for two engines and two pumps where $V_j/V_o = 3.80$.

The pump selection can also be related to the jet velocity ratio when no bounds are present. The losses increase with V_j/V_o ; therefore, the value of Thoma's cavitation criterion, σ_T , decreases. As a general rule for high values of σ_T (greater than .1) the centrifugal pump is selected. For low values of σ_T (less than 0.05) the axial design is selected. In the region between these values of σ_T , the pump size, gear weight, and fuel weight or problem bounds can enter into the selection process.

Since the primary objective of multi-parallel design is to increase pump speed, the rpm for the centrifugal pump is higher than the axial design and, therefore, the gear weight can be the predominant factor in selecting the

centrifugal pump design. Pump speed can also be a bound for small hydrofoil displacements when the axial pump, due to its fixed specific speed, cannot achieve a gear ratio of one or greater and is eliminated.

The fuel weight component for the same v_j/v_o is a function of pump efficiency. The axial design is generally three percent more efficient, and therefore, the axial pump requires less fuel than the centrifugal pump. Depending on the range, the fuel weight can also be a determining factor in the pump selection.

The comparison of the pump weight component is a function of σ_T and pump size. Because the centrifugal pump specific speed is proportional to σ_T , the difference in pump weights decreases as σ_T decreases until a cross over point is reached.

The relationship in pump diameter also affects the difference in pump weight. For the same operating conditions, if the number of pumps is increased, the axial pump becomes lighter when compared to the centrifugal design. However, this decrease in weight of the axial pump can be offset by increases in gear weight especially if the increase in pumps cause a shift from a planetary to a combining reduction gear.

The problem bounds are quite often the determining factors in setting the v_j/v_o and therefore in selecting the pump type. The primary bound is available engine horsepower. Depending on the relationship between maximum

intermittent power and normal power, either maximum intermittent power can be a limit at take off or normal power can be a limit at cruise. It is even possible for the difference in pump efficiency to be a determining factor in selecting the axial pump for high values of σ_T because the centrifugal design is rejected due to required cruise power.

The cross over region between the pump designs can be changed by adjusting the values of maximum suction specific speed and the maximum number of centrifugal impellers. For example, if the maximum suction specific speed for the centrifugal design is increased to 10,000; the specific speed would increase for the same values of σ_T and the cross over point from the centrifugal to axial pump will lower.

As table 3 illustrates there is a large variation in the design parameters at the optimum point for different displacement and engine selections. There are several explanations for this variation. First is the maximum available horsepower, which limits the jet velocity ratio. By increasing the jet velocity, the required power is increased. If not enough power is available, the design will reach a maximum value of jet velocity ratio before an optimum point is reached.

The second case is the installed engine power greatly exceeds the full load cruise power. As in the example of the 200 ton hydrofoil with an LM2500 gas turbine installed,

the optimum point is driven to a very high value of jet velocity ratio typically greater than three. This fact is explained by referring to the gas turbine performance characteristics, figure (20). When the required power at full load is less than 70% of the normal engine power, the SFC to SHP relationship is such that lower fuel weights can be achieved at higher values of SHP, ie., v_j/v_o . Also, the high jet velocity ratio gives low entrained water weight. If the range were reduced or set to zero, a very different optimum point would be selected by the program.

In summary, the choice of the lightest pump design is directly related to the optimum point parameters that the program selects. This selection is a very complex trade off between the system components. Only the cases that can be directly attributed to the pump or prime mover have been dealt with here. However, from data points already run, if no power limitation exists, the value of jet velocity ratio at the optimum design point is greater than the maximum propulsive efficiency point and usually higher than 2.0.

The selection of pump type is primarily dependent on the system losses, ie., Thoma's cavitation criterion, σ_T . Where for very low values of σ_T (less than 0.05) only the inducer design is selected due to the poor cavitation conditions which cause the centrifugal design to go to very small values of specific speed. However, as the cavitation

conditions improve, the centrifugal design becomes more competitive and is usually selected for values of σ_T greater than 1.0.

In the middle range of σ_T near the cross over point, the pump selection is more arbitrary. Other factors of the design problem such as arrangement of machinery and weight distribution should then enter into the pump selection process.

Chapter 7. CONCLUSIONS

From the study of waterjet pumps for hydrofoil propulsion several conclusions to the design approach can be made. The first conclusion is that the take off point cavitation condition establishes the pump design. If only a conventional impeller design, with respect to suction specific speed, is used, the specific speed for one impeller is established by the required pump head and net positive suction head at the pump inlet. From sample cases run for $S_{max} = 424.5(9000)$, the specific speed range was from 49 to 118. This specific speed range specifies a centrifugal type impeller especially at the lower end of the range where the optimum point is more likely to be established. To design for a single impeller pump at the low required value of specific speed would give a large diameter slow speed pump which would require a large reduction gear.

In order to get a light weight pump design, the three design approaches stated in section 3.1 have been tried by industry. All three design approaches are an attempt to increase the pump speed and, therefore, decrease the pump size and weight.

The selection of the optimum pump design from the two selected design approaches is very closely related to Thoma's cavitation criterion, σ_T , as discussed in chapter 7. Changes or improvements to either or both of the pump designs would only shift the cross over point and should not alter the overall outcome of the propulsion pump problem.

Chapter 8. RECOMMENDATIONS

The waterjet pump problem has only been approached from the point of view of least weight for a given hydrofoil displacement. It would be beneficial to study waterjet propulsion if the problem were approached from the view point of lightest propulsion system weight for a required payload and the optimum propulsion system and hydrofoil displacement for a specified gas turbine.

Since the program only solves the preliminary design for two design approaches, the updating of the current program as more developed work becomes available and the inclusion of the two speed pump design approach if development proves the design feasible should be accomplished. In the jet velocity ratio range where the two designs are nearly equal in weight, a detailed pump design study concentration on the engine and pump arrangement, location of jet nozzle, and details of the auxiliary propulsion systems is needed.

As stated, the pump selection is limited by the choice of gas turbine. Only in the case of proper matching of engine power to displacement is a true optimum design achieved. Any further work should approach the problem from the view point of gas turbine selection and further study the problem when a good matching is not possible.

The centrifugal multi-parallel impeller design always requires less gear reduction than the inducer design. When a combining gear is required, this fact produces the centrifugal pump as the optimum design over a larger range of σ_T .

References

1. Levy, J. and Meggit, P.J., Study of Waterjet Propulsion for 400-Ton Hydrofoil Ship, Naval Ship Research and Development Center, Report 4366, October 1971.
2. Stepanoff, A.J., Centrifugal and Axial Flow Pumps Theory, Design, and Application, John Wiley & Sons, New York, 1957.
3. Hydraulic Institute Standards, Hydraulic Institute, New York, 1965, p. B(I)-2.
4. Waterjet Propulsion System Study, Report No. 2 Pump Selection and Design, Lockheed Contract NObs-88605, September 1965.
5. Wislicenus, G.F., Fluid Mechanics of Turbomachinery, Dover Publications, New York, 1965.
6. Kasai, T., Hydraulic Design of Centrifugal Pump Impellers Based on the Specific Speed, Pump Design and Testing, Proceedings of Symposium at National Engineering Laboratory, Glasgrow, April 1965, p. 51.
7. Addison, H., Centrifugal and Other Rotodynamic Pumps 3rd ed., Chapman & Hall, London, 1966.
8. Blom, Development of the Hydraulic Design for the Grand Coulee Pumps, Trans. ASME, Vol. 72, 1950, p. 53.
9. Kittredge, C.P., Estimating the Efficiency of Prototype Pumps from Model Tests, ASME, Paper No. 67-WA/FE -6, 1967.
10. Wong, G.S., Full Scale Design and Experimental Model Testing of a Waterjet Pump for a 500 Ton CAB Test Craft, Vol. I, Prepared for Joint Surface Effects Program Office, Washington, D.C., January 1971.
11. Humphries, G.E., et. al., FT12-1 Waterjet Cavitation Damage Study Find Report of Phase I Scale Model Testing, Pratt & Whitney Aircraft, Contract MA 4489, June 1971.
12. Sandercock, D.M. and Crouse, J.E., Design and Overall Performance of a Two-Stage Axial-Flow Pump with a Tandem-Row Inlet Stage, NASA TN D-2879, June 1965.
13. Mullan, P.J., An Investigation of Cavitating Inducers for Turbopumps, Report No. 53, Gas Turbine Laboratory, MIT, May 1959.

14. Brown, L.E., Design and Performance of the PB-1 Axial Flow Pump Impeller, Symposium on Pump Machinery for Marine Propulsion, ASME Fluids Conference, May 1968, p. 84.
15. Sandercock, D.M., et. al., Cavitation and Non-Cavitation Performance of an 80.6° Flat Plate Helical Inducer at Three Rotational Speeds, NASA TN-D1439, November 1962.
16. Arcand, L., The Performance of Two Axial Flow Water Pumps, ASME Fluids Conference, Symposium on Pumping Machinery for Marine Propulsion, Phil., May 1968.
17. Crouse, J.E., et. al., Design and Overall Performance of an Axial Flow Pump Rotor with a Blade Tip Diffusion Factor of 0.43, NASA TN D-2295, May 1964, pp. 2-21.
18. Crouse, J.E. and Miller, M.J., Design and Overall Performance of an Axial Flow Pump Rotor with a Blade Tip Diffusion Factor of 0.66, NASA TN D-3024, September 1965.
19. Crouse, J.E., et. al., Investigation of the Performance of an Axial-Flow Pump Stage Designed by the Blade-Element Theory, NASA, TN D-1109, 1961
20. Chironis, E.P. ed., Gear Design and Application, McGraw-Hill Book Co., New York, 1967.
21. Acosta, A.J. and Bowerman, R.D., An Experimental Study of Centrifugal Pump Impellers, Trans. ASME, Vol. 81, 1957, pp. 1821-1839.
22. Arcand, L., The Performance of Two Axial Flow Waterjet Pumps, Symposium on Pumping Machinery for Marine Propulsion, ASME Fluids Conference, May 6, 1968, p. 103.
23. Arcand, L. and Comolli, C., Optimization of Water Jet Propulsion for High Speed Ships, J. Hydronautics, Vol. 2, #1, pp. 2-8, 1968.
24. Brandau, J.H., Performance of Water Jet Propulsion Systems - A Review of the State-of-the-Art, J. Hydronautics, Vol. 2, #2, April 1968.
25. Crouse, J.E., Miller, Sandercock, Summary of Experimental Investigation of Three Axial Pump Rotors Tested in Water, ASME, Paper No.66 -WA/FE-24, 1966.

26. Crouse, J.E., et al., Investigation of Performance of an Axial-Flow-Pump Stage Designed by the Blade-Element Theory-Design and Overall Performance, NASA TN D-591, 1961.
27. Davis, H., et. al., The Influence of Re on the Performance of Turbomachinery, Trans. ASME, Vol. 73, No. 5, July 1951, pp. 499-509.
28. Fang, K.S. and Koolhof, F., Determination of NPSH on Large Centrifugal Pumps and Thoma's Law of Similarity, ASME, 1971 Cavitation Forum, p. 4.
29. Study of Propulsion Transmission Systems for 500-Ton 80 Knot Hydrofoil Ship, Gibbs & Cox Inc., New York, November 1962.
30. Hatte, R. and Hughs, J. P., Selection of Hydrofoil Waterjet Propulsion Systems, Paper 66-732, AIAA, August 1966.
31. Holl, J.W. and Wislicenus, Scale Effects on Cavitation, Trans. ASME, J. Basic Eng., Vol. 83, Series D, No. 3, September 1961, pp. 385-398.
32. Jekat, W.K., Reynolds Number and Incidence-Angle Effects on Inducer Cavitation, ASME, Paper 66-WA/FE-31, 1966.
33. Johnson, V.E., Waterjet Propulsion for High Speed Hydrofoil Craft, AIAA Paper 64-306, June 1964.
34. Kasai, T. and Takamatu, Y., Cavitation Aspects and Suction Performances of Centrifugal Pumps. Symp. on Cavitation and Hydraulic Machinery, September 1962, p. 417.
35. Kovats, A., Some Conditions of Cavitation Free Operation of Centrifugal and Mixed Flow Pumps Having Low NPSH, ASME. Cavitation Forum, 1968, p. 23.
36. Levy, J., The Design of Waterjet Propulsion Systems for Hydrofoil Craft, Marine Technology, Vol. 2, #1, January 1965.
37. Levy, J., Feasibility Study of Water-Jet Propulsion Systems for a 500 Ton Hydrofoil Ship, Aerojet-General Corp., AD 654-719, April 1962.
38. Levy, J. and Davis, S., Analytical Study of Unconventional Pumps for Waterjet Propulsion, Report #3522, Aerojet-General Corp., for NRSDC, March 1968.

39. Miller, M. J. and Soltis, R.F., Detailed Performance of Radial-Bladed Centrifugal Pump Impeller in Water, NASA TN-D 4613, 1968.
40. Pradhan, A.V. and Caine, G. H., Design and Test Results for Low NPSH, ASME, Cavitation Form, 1969.
41. Ross, C.C., Principles of Rocket Turbo Pump Design, J. Am. Rocket Society, No. 84, March 1951, pp. 21-33.
42. Ross, C.C. and Banerian G., Some Aspects of High-Suction Specific Speed Pump Inducers, Trans. ASME, Vol. 78, November 1956, pp. 1716-1721.
43. Stenning, A.H., The Design of Axial Inducers for Turbopumps, Gas Turbine Lab Report #44, MIT, February 1958.
44. Stepanoff, A.J., Pumps and Blowers Selected Advanced Topics, John Wiley & Sons, New York 1965, pp. 56-68.
45. Stepanoff, A.J. and Stahl, H.A., Cavitation Criterion for Dissimilar Centrifugal Pumps, ASME Paper No. 61-WA-139, 1961.
46. Stripling, L.B. and Acosta, A.J., Cavitation in Turbo Pumps, Trans. ASME, J. of Basic Eng., Vol. 84, No. 3, September 1962, pp. 339-356.
47. Strom-Tejsen, J., Day, W.G., Study of Air Cushion Vehicle Propulsion System Part 3, Transmission Design and Performance, NSRDC, TND Report 378-Ho8, January 1971.
48. Varley, F.A., Effects of Impeller Design and Surface Roughness on the Performance of Centrifugal Pumps, Proceedings of the Inst. of Mechanical Engineering, London, Vol. 175, No. 21, 1961, pp. 955-989.
49. Wislicenus, G.F., Critical Considerations of Cavitation Limits of Centrifugal and Axial-Flow Pumps, Trans. ASME, Vol. 78, No. 8, November 1956, p. 1707.
50. Wright, M.K., Design Comments and Experimental Results for Cavitation-Resistant Inducers up to 40,000 Suction Specific Speed, Trans. ASME, April 1964, p. 176.
51. Yedidiah, S.H., Energy Transfer in Centrifugal Pumps, ASME Paper No. 67-FE-22, 1967.

Table 1. Performance Characteristics of Marine Gas Turbines

No.	Turbine	Normal SHP at 100°F	SFC at Normal Power	Max. Int. % SHP @ 100°F	RPM	Engine Dry Weight (lb.)
1	TF 35	2220	0.59	2840	14500	1050
2	TF 40	2850	0.55	3060	14500	1050
3	Proteus	2800	0.63	3510	1500*	3200
4	Proteus	2800	0.63	3510	1000*	3300
5	Tyne RM-1A	3320	0.49	4250	3110*	2800
6	Tyne RM-1C	4160	0.47	5300	3110*	2800
7	FT12A-3	2220	0.79	2840	9000	1010
8	LM1500	12500	0.575	14000	5500	7500
9	LM2500	22200	0.41	22500	3400	10500
10	FT4A-2	19150	0.52	24200	3600	14200
11	FT4A-12	21750	0.52	26950	3600	14200
12	FT4C-2	27600	0.48	34400	3600	14200

* Integral R. Gear output

Table 2. Reduction Gear Weight Equations

<u>Gear Type</u>	<u>Gear Ratio Equation m_g</u>
Simple Offset	$2m_g^3 + m_g^2 = 1$
Offset with Idler	$2m_g^3 + m_g^2 = M_o^2 + 1$
Double-Reduction Double-Branch	$2m_g^3 + \frac{2m_g^2}{\frac{M_o}{M_o+1}} = \frac{M_o^2 + 1}{2(\frac{M_o}{M_o+1})}$
Planetary	$2m_s^3 + m_s^2 = \frac{0.4(M_o - 1)^2 + 1}{b}$
<u>Gear Type</u>	<u>Total Weight Fraction $\Sigma F_d/c =$</u>
Simple Offset	$1 + 1/m_g + m_g + m_g^2$
Offset with Idler	$1 + 1/m_g + m_g + m_g^2 + M_o^2/m_g + M_o^2$
Double-Reduction Double-Branch	$\frac{1}{2} + 1/2m_g + 2m_g + m_g^2 + m_g^2/M_o + M_o^2/2m_g + M_o/2$
Planetary	$1/b + 1/bm_s + m_s + m_s^2 + \frac{0.4 (M_o - 1)^2}{b m_s} + \frac{0.4 (M_o - 1)^2}{b}$

Table 3 Sample Pump Solutions

* Weight per pump

No	Disp (tons)	V _O (Kts)	Range (n.mi)	Engine (No)	Pump (No)	No.	Stages/n	Cruise			σ_T
								V _j /V _O	Q	H _{SV}	
1	54	45	600	Proteus (1)	Cent. (1)	1	2.65	33	581	100	.176
2	196	48	600	LM2500 (1)	Axial (2)	2	2.80	97	742	100	.137
3	400	42	500	LM2500 (1)	Cent. (1)	10	1.75	852	177	95	.538
4	400	42	1000	LM2500 (1)	Cent. (1)	10	1.74	848	174	94	.551
5	400	42	500	FT4A-12 (1)	Cent. (1)	10	2.21	478	323	92	.287
6	400	42	500	FT4A-12 (1)	Cent. (2)	10	2.10	549	283	96	.337
7	400	42	500	FT4C-2 (1)	Axial (1)	3	2.83	308	569	91	.160
8	400	42	500	FT4C-2 (1)	Axial (2)	3	2.81	313	560	91	.162
9	750	40	2000	LM2500 (2)	Axial (2)	2	2.25	911	323	73	.226
10	750	50	2000	FT4C-2 (2)	Axial (1)	2	2.75	416	774	100	.142

Table 3 (continued)

No	Take Off				Pump Parameters									
	V_j/V_o	Q	H	H _{SV}	c_T	N _S	S	D _{1s}	D _{2s}	L _P	N _{cr}	N _{to}	η_p	η_p to
1	5.58	.34	705	35	.049	44.2	429.5	1.17	2.25	3.08	1341	1459	.873	.875
2	5.90	102	906	26	.029	149.5	1265	1.67	1.67	2.85	1877	2040	.898	.903
3	3.31	804	209	38	.181	118	424.5	1.75	2.27	25	985	1021	.878	.879
4	3.29	804	209	37	.185	115.8	424.5	1.76	2.32	25	958	999	.877	.879
5	4.63	499	417	34	.082	65.2	424.5	1.41	2.52	21	1083	1205	.880	.882
6	4.28	558	353	37	.106	78.7	1265	1.03	1.66	15	1578	1717	.873	.873
7	6.28	341	772	31	.041	149.5	1265	4.12	4.12	8	—	906	.900	.917
8	6.21	346	757	31	.041	149.5	1265	2.94	2.94	6	—	1266	.896	.912
9	4.53	915	379	20	.053	149.5	1265	5.33	5.33	6	532	561	.920	.92
10	5.68	429	910	27	.030	149.5	1265	4.75	4.79	8	681	725	.917	.919

Table 3 (continued)

* weight per pump

Pump Parameters		W _T /Δ	W _D *	W _W *	W _F
No	SHP _{cr}	SHP _{to}			
1	2549	3219	.24	0.59	0.00
2	9518	12184	.21	0.57	2.70
3	20436	22659	.29	9.54	.60
4	20307	22492	.39	9.74	44.8
5	20830	28085	.27	6.49	.66
6	21187	26866	.31	3.40	84.25
7	23156	34186	.21	5.09	.66
8	23252	34148	.25	2.34	55.59
9	19029	22446	.58	8.24	56.31
10	20881	25258	.54	2.76	3.81
				2.00	17.7
					340.13

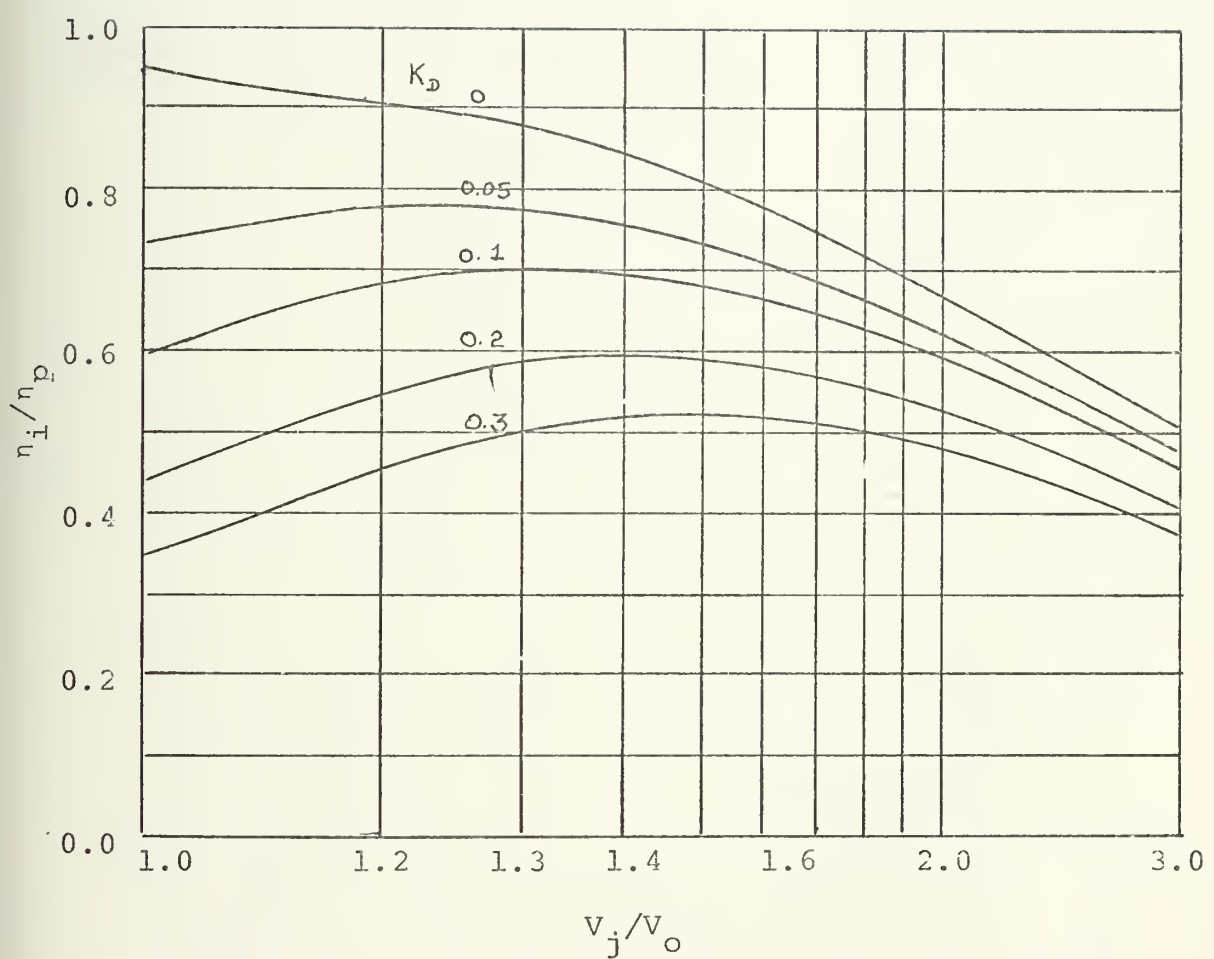


Figure 1. Propulsive Efficiency versus Jet Velocity Ratio for Values of Loss Coefficient

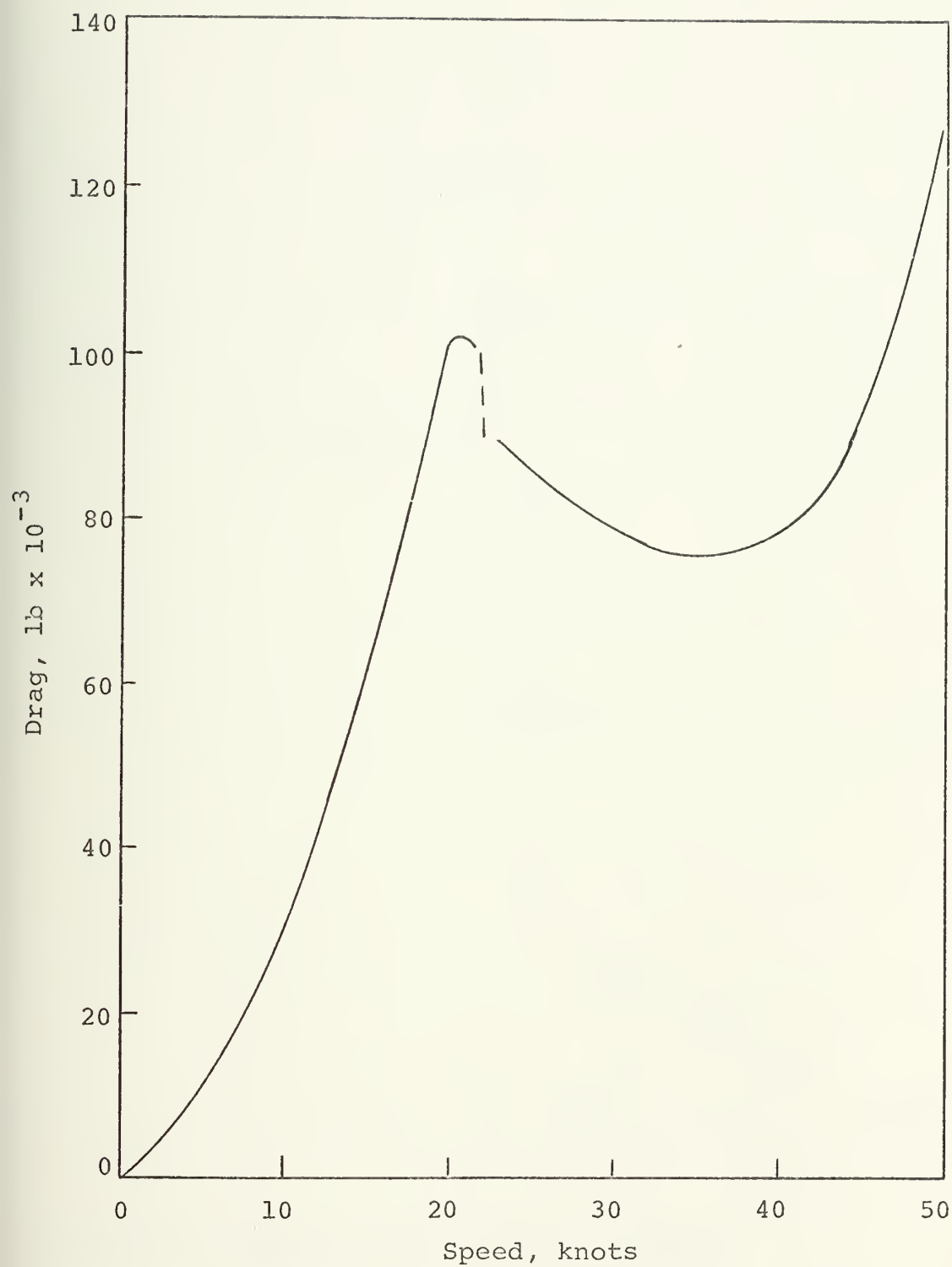


Figure 2. Hydrofoil Drag as a Function of Speed

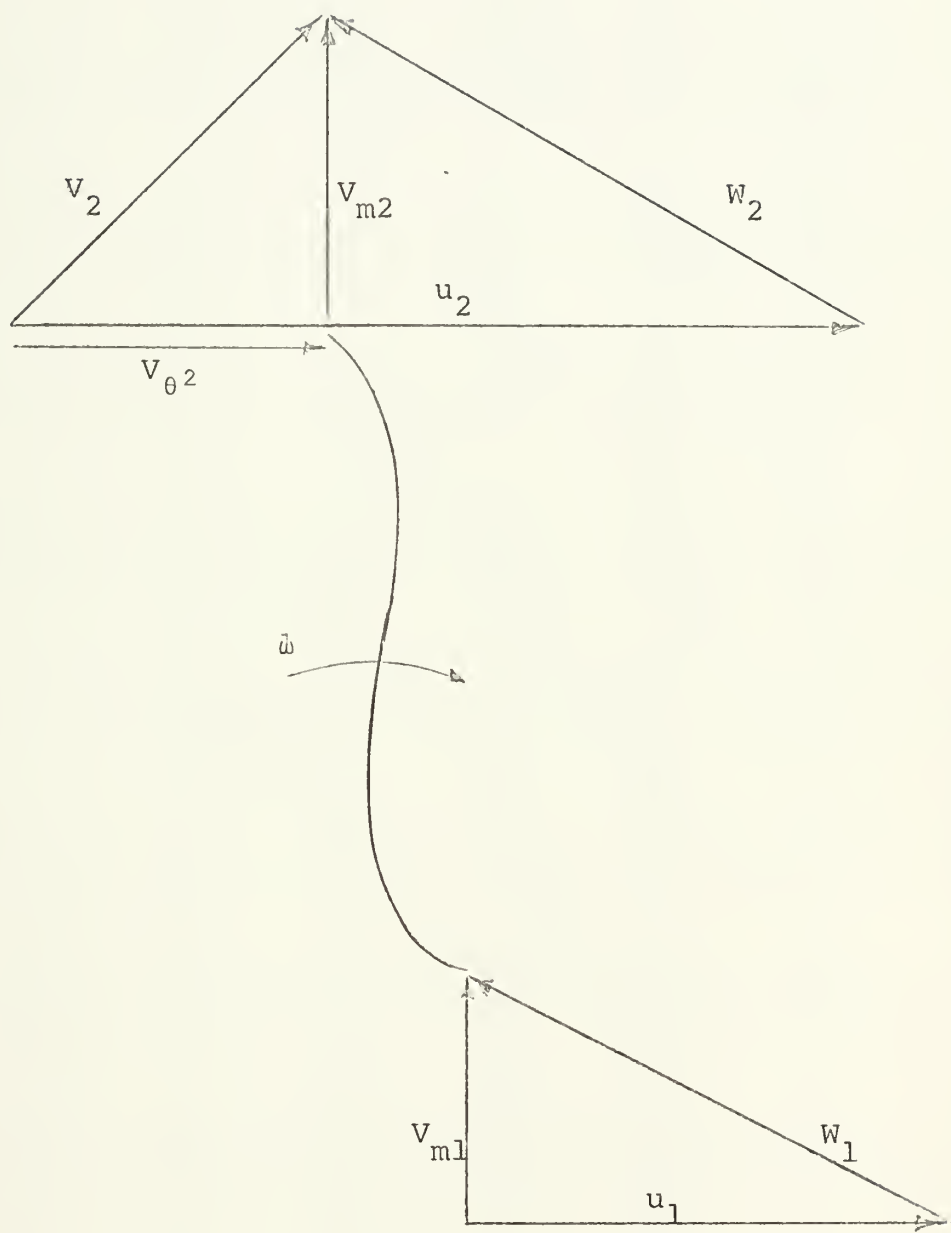


Figure 3. Impeller Flow Velocity Diagram

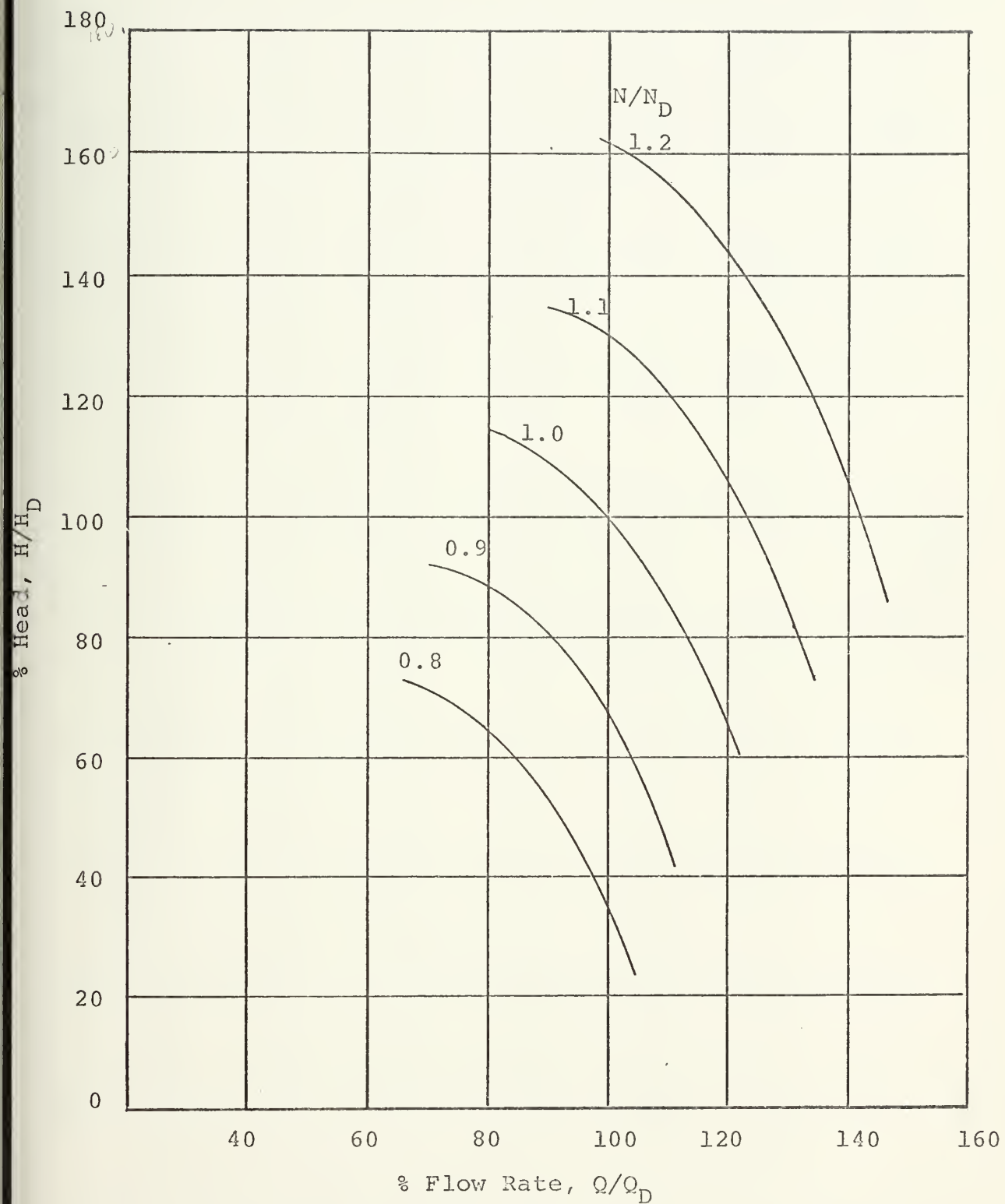


Figure 4. Inducer Stage Performance Map

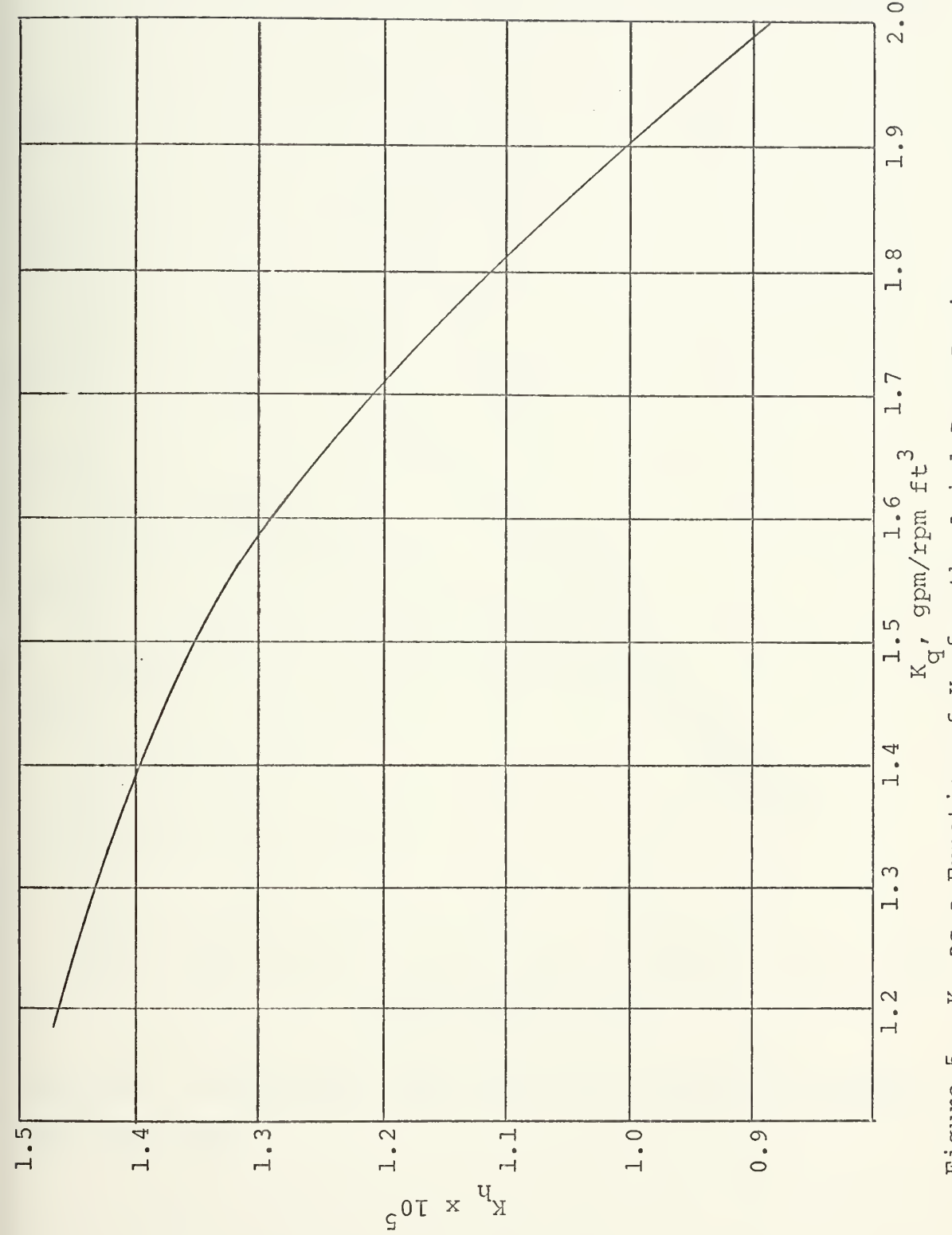


Figure 5. K_h as a Function of K_q for the Axial Pump Design

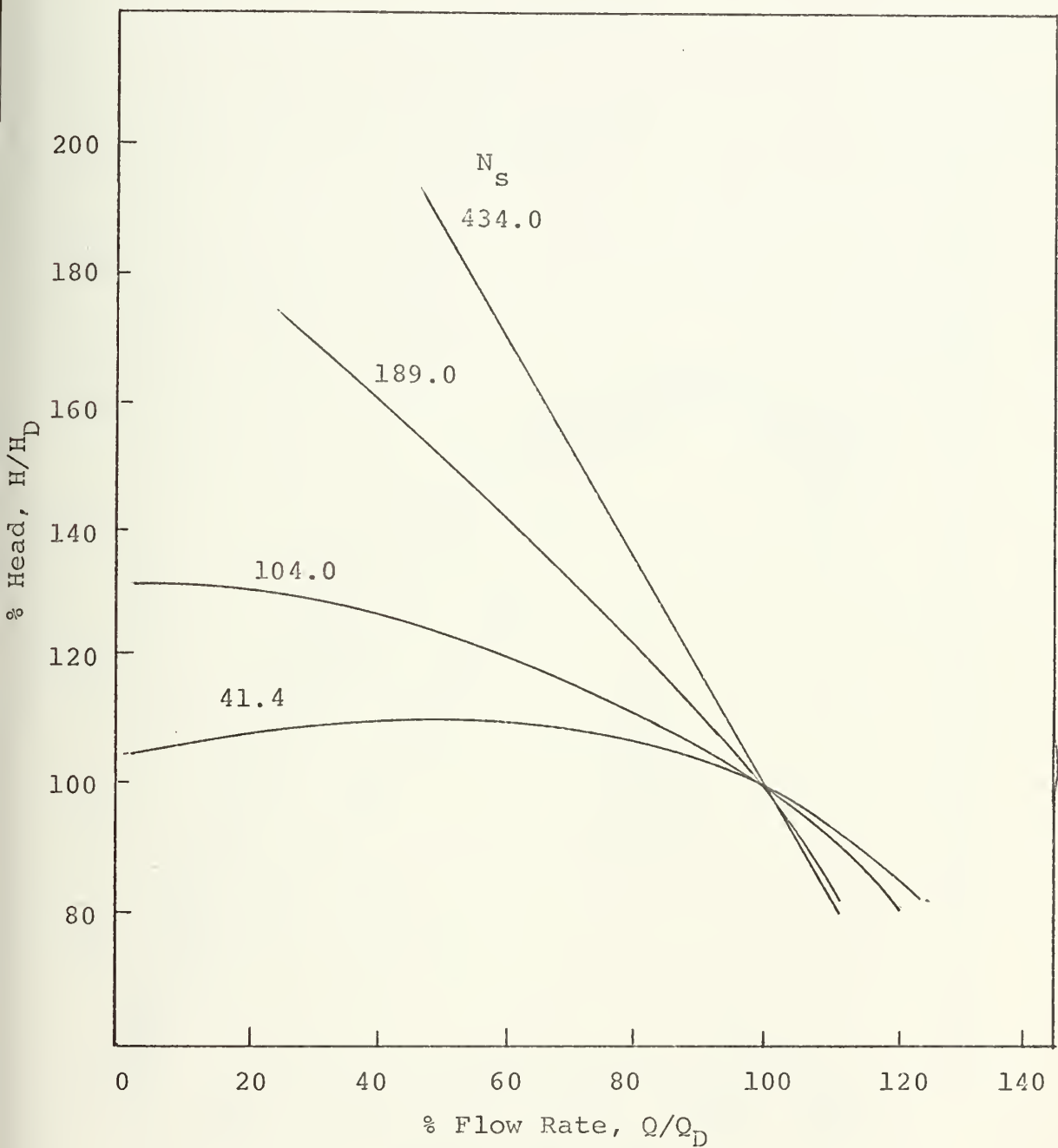


Figure 6. Centrifugal Pump Flow Rate vs Head for Changes in Specific Speed

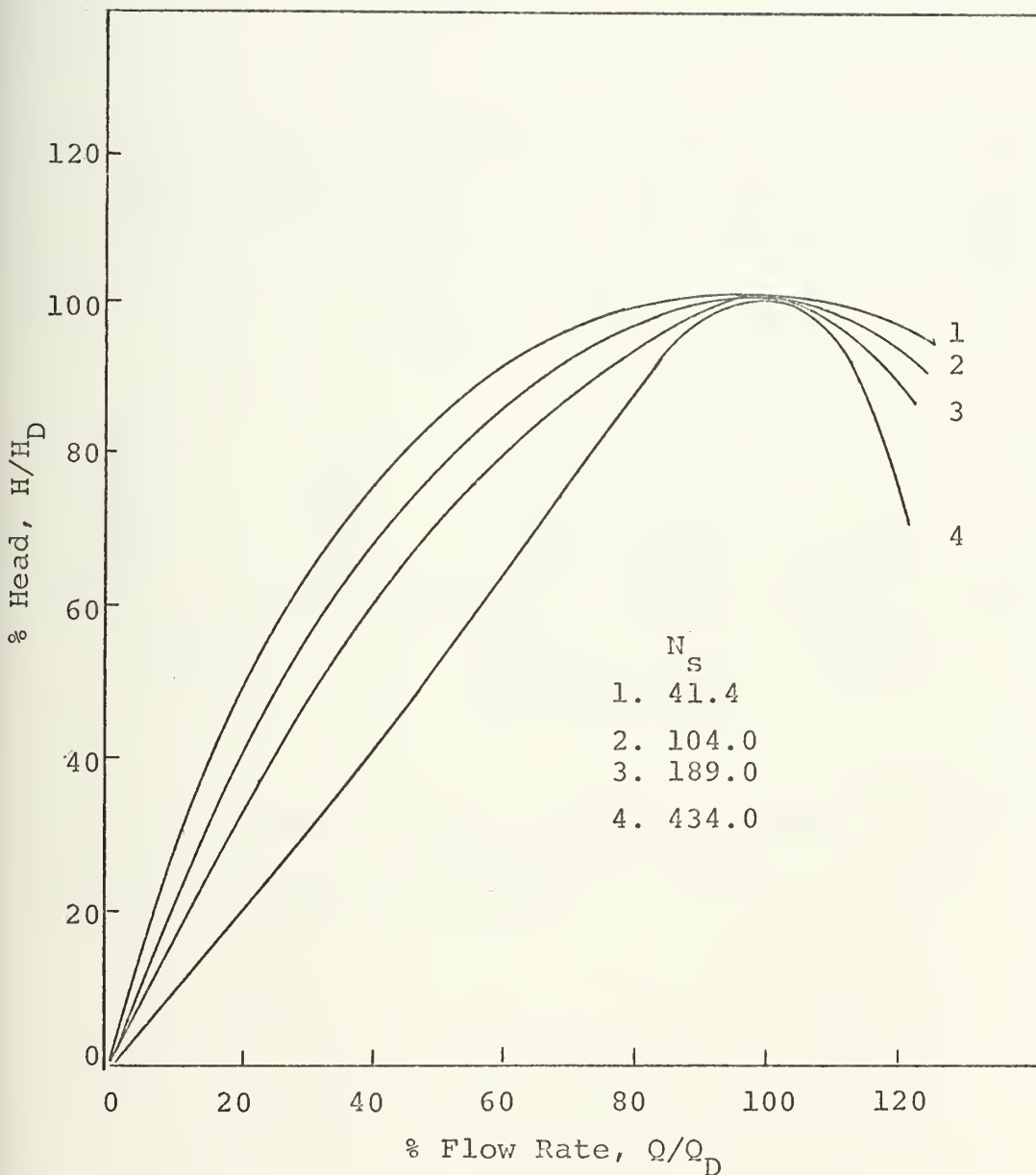


Figure 7. Centrifugal Pump Efficiency Curves for Various Values of Specific Speed

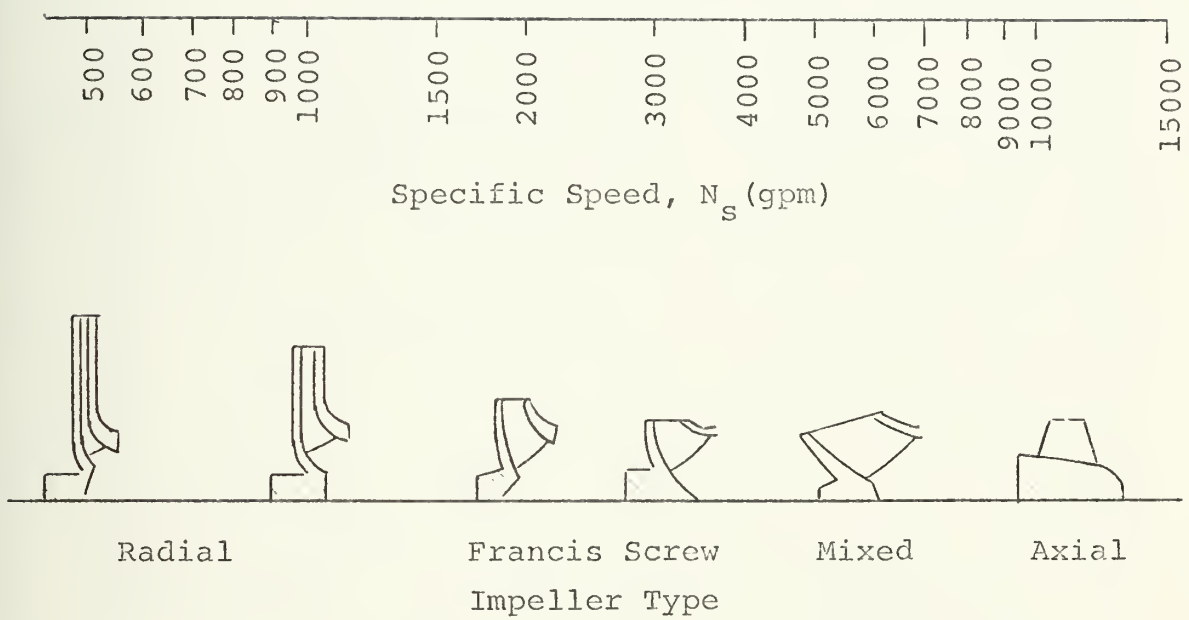


Figure 8. Pump Impeller Profiles for Range in Specific Speed from the Hydraulic Institute

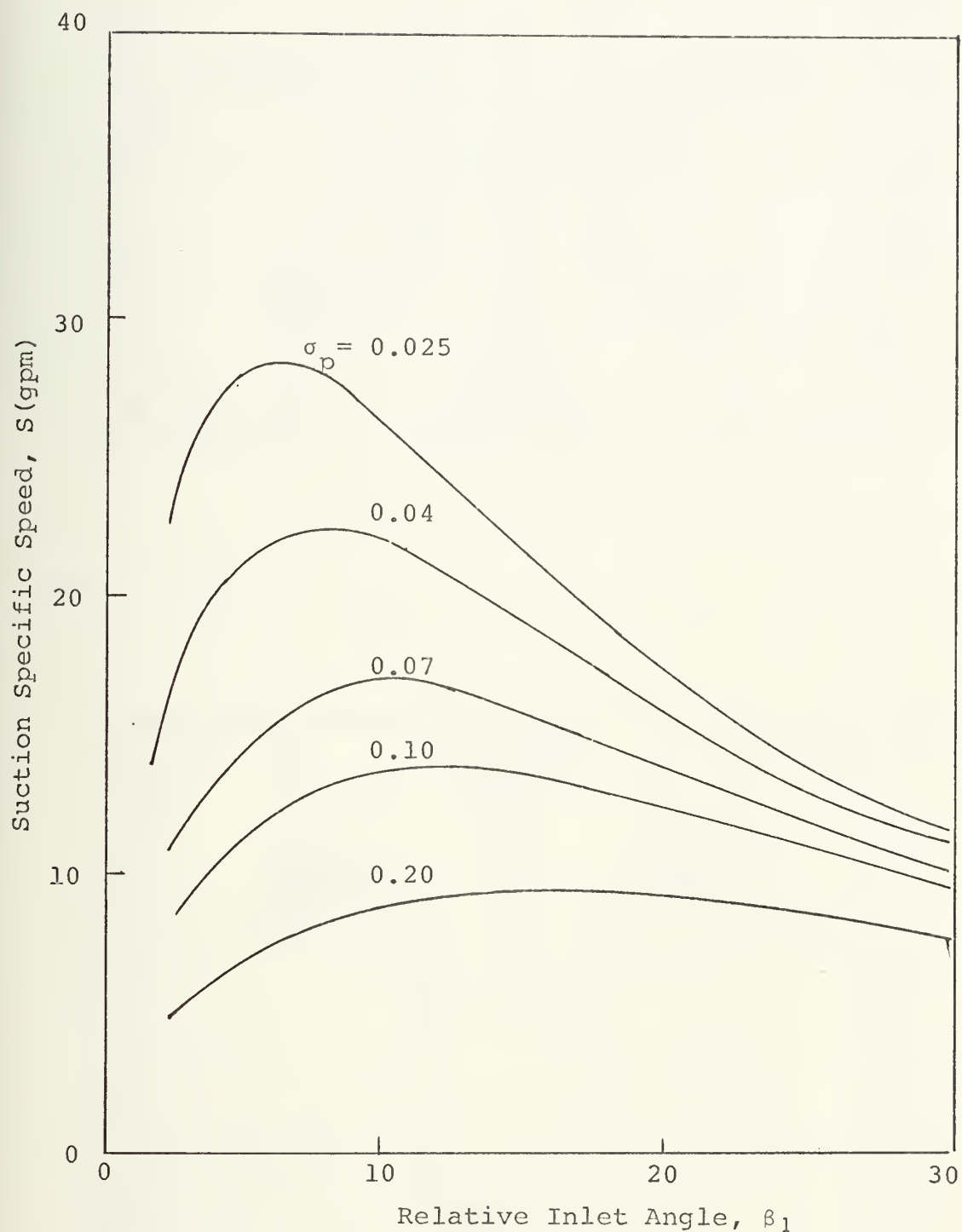


Figure 9. Relative Inlet Angle as a Function of Suction Specific Speed

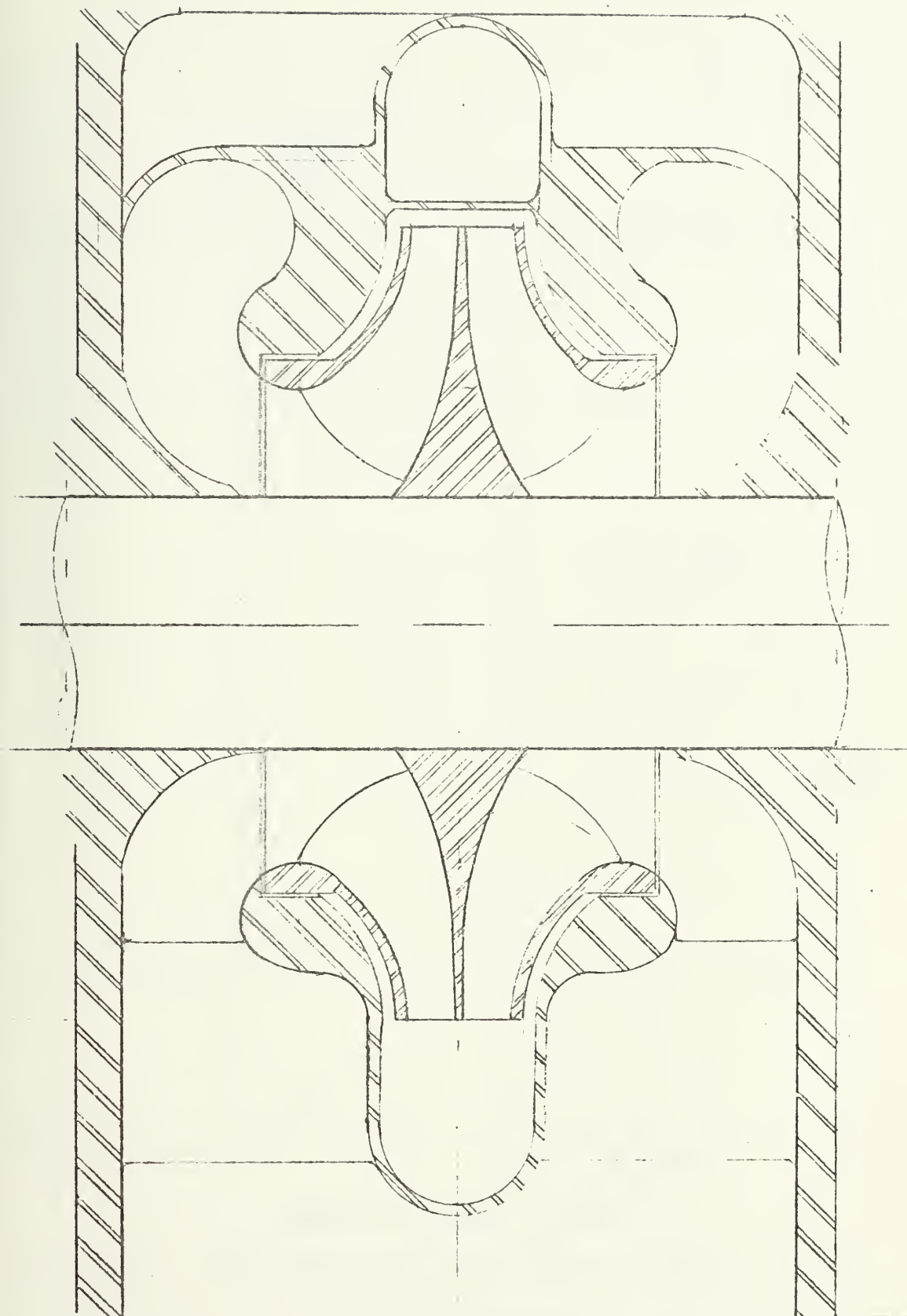


Figure 10. Centrifugal Pump Section for One Impeller

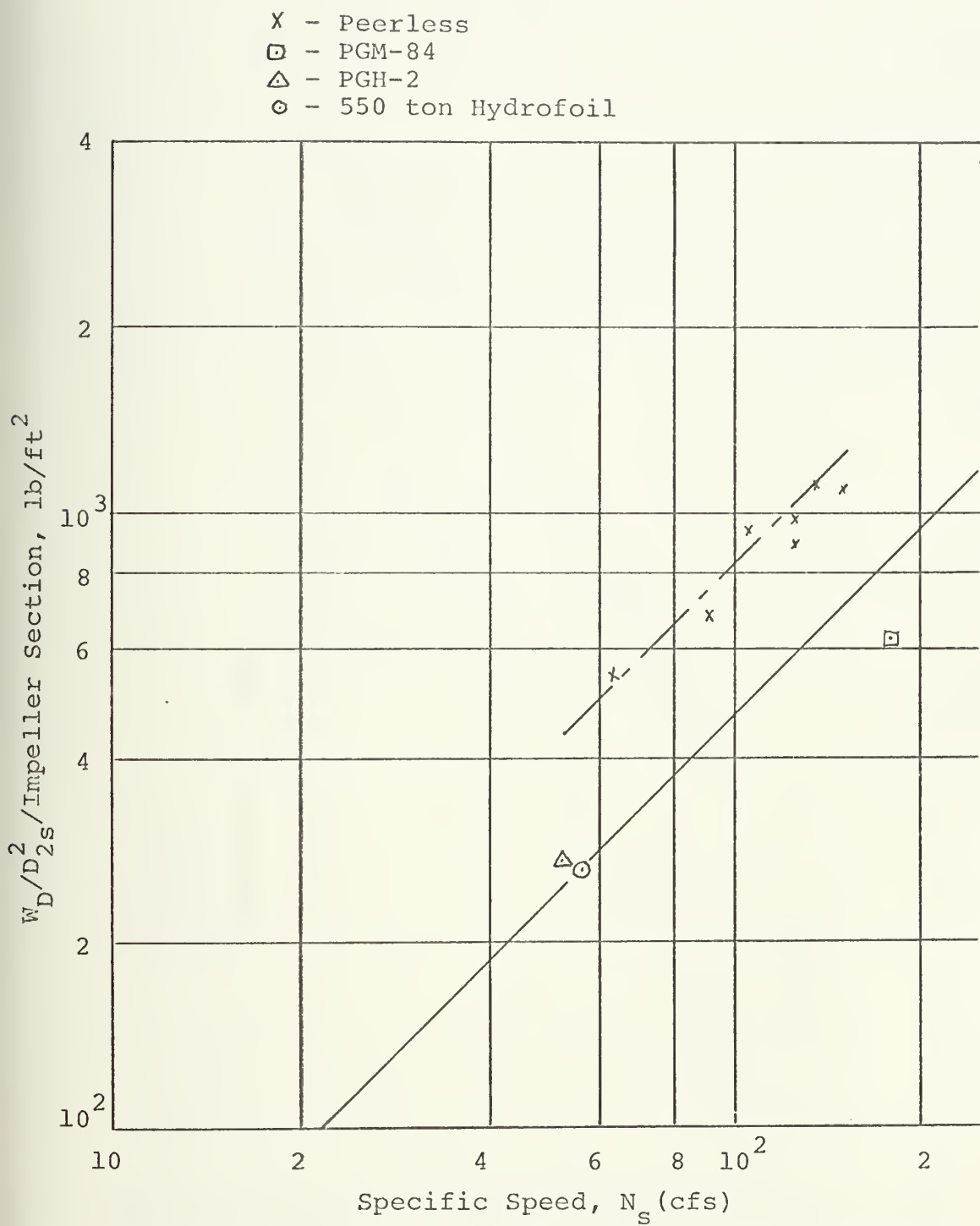


Figure 11. Centrifugal Pump Section Dry Weight to Exit Diameter Ratio as a Function of Specific Speed

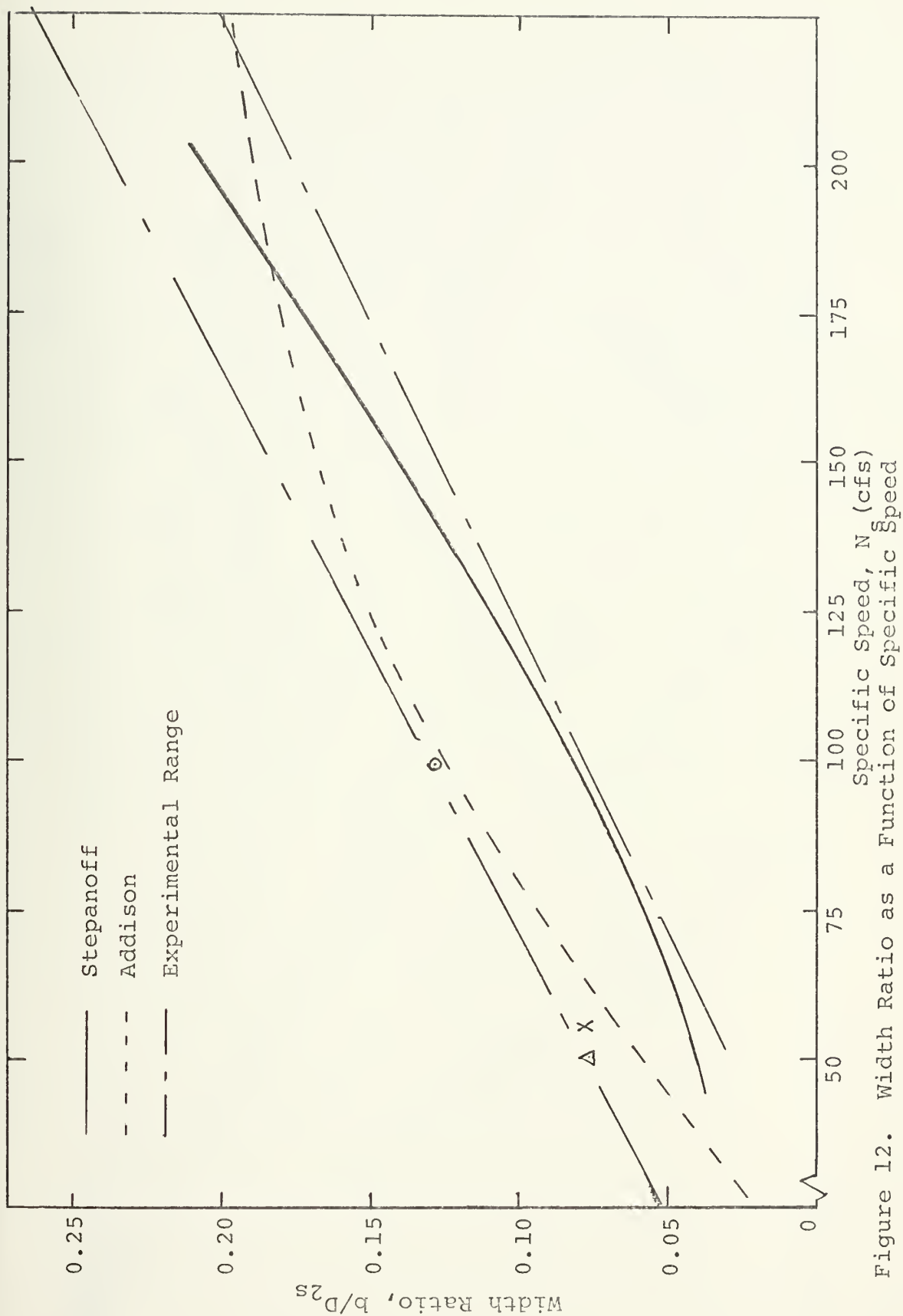


Figure 12. Width Ratio as a Function of Specific Speed

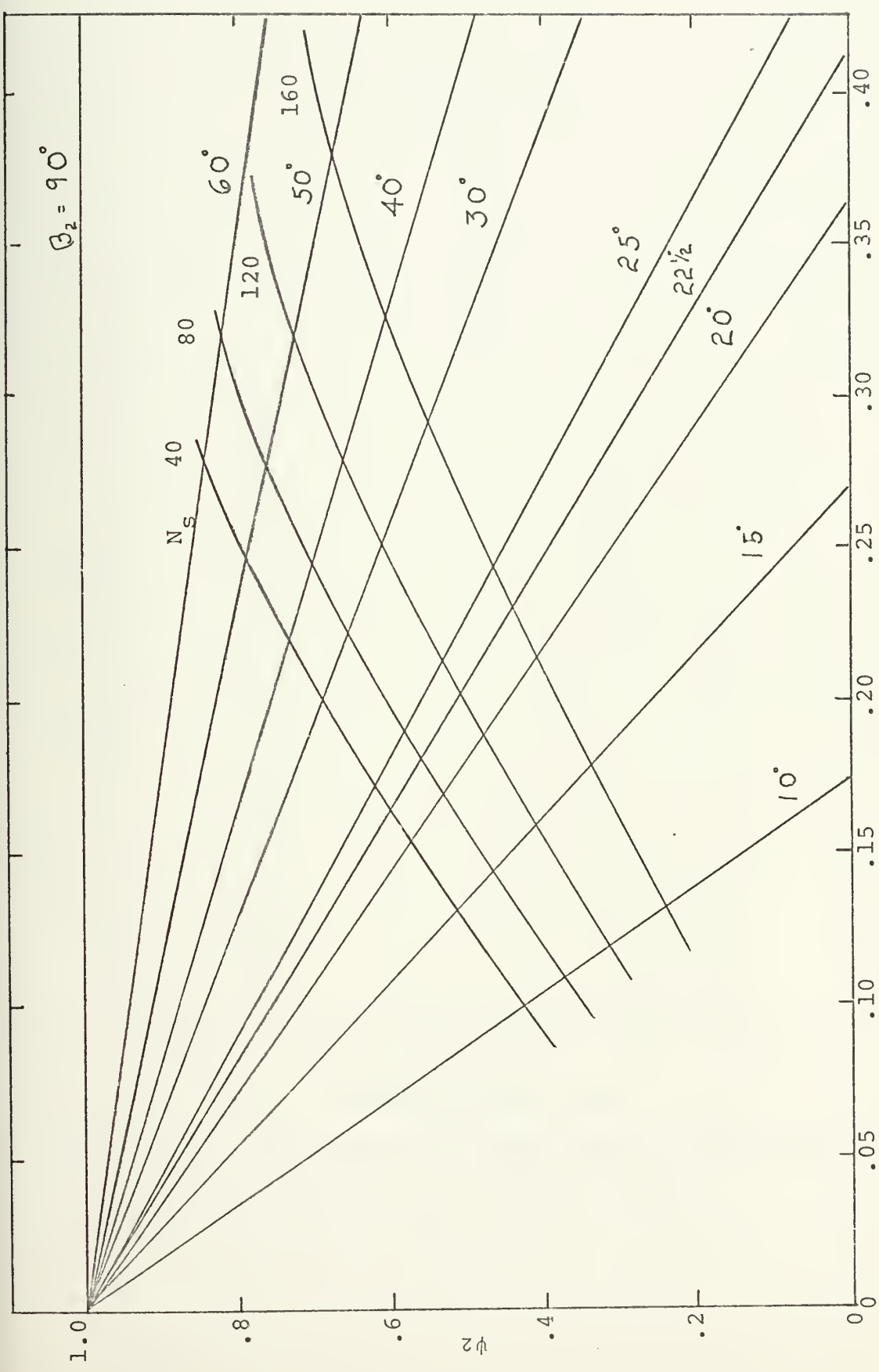


Figure 13. Centrifugal Impeller Design Chart for $b/D_{2s} = 0.001$, $N_s = 0.025$

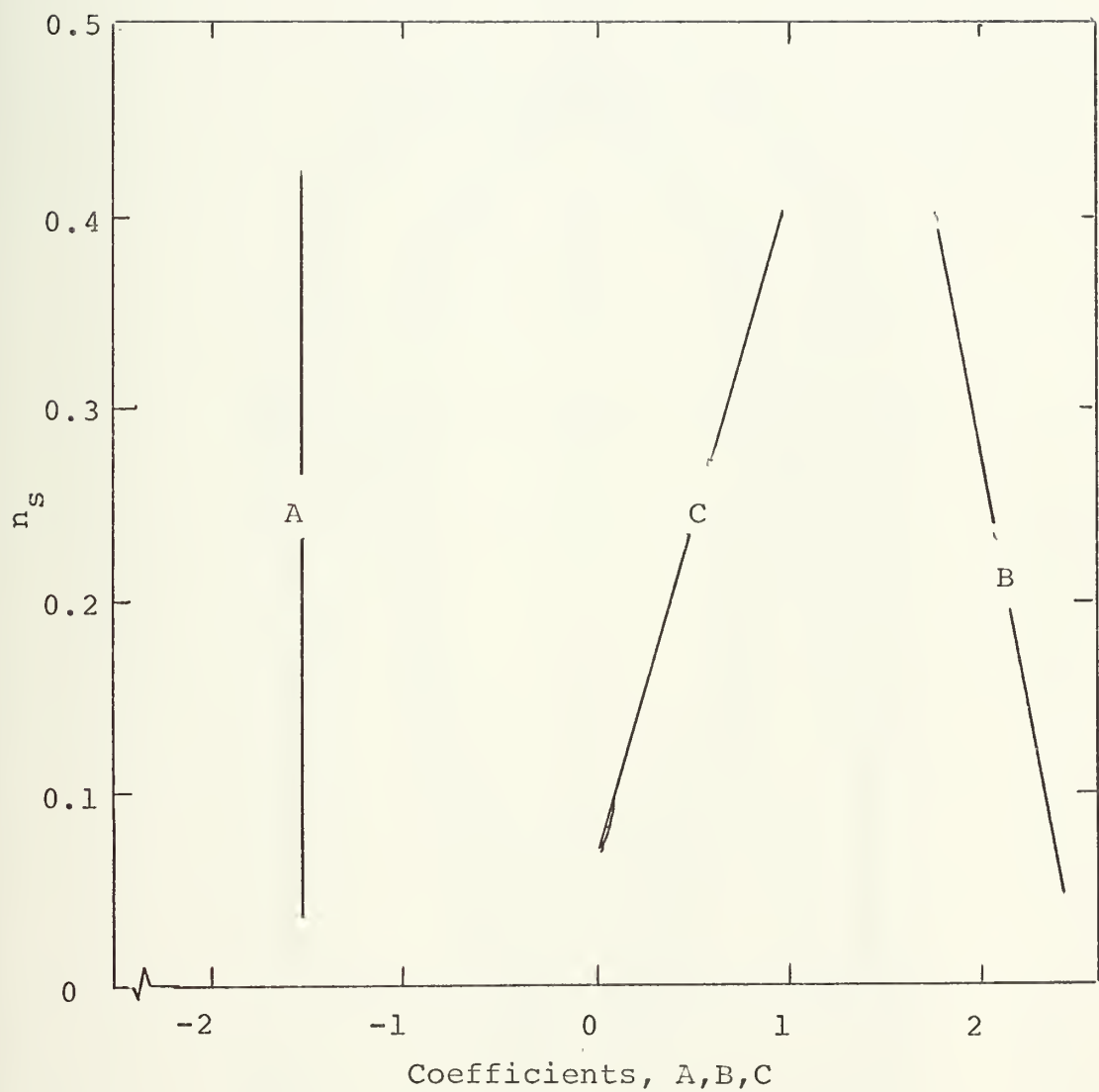


Figure 14. Centrifugal Pump Head Curve Coefficients as a Function of Non-Dimensional Specific Speed

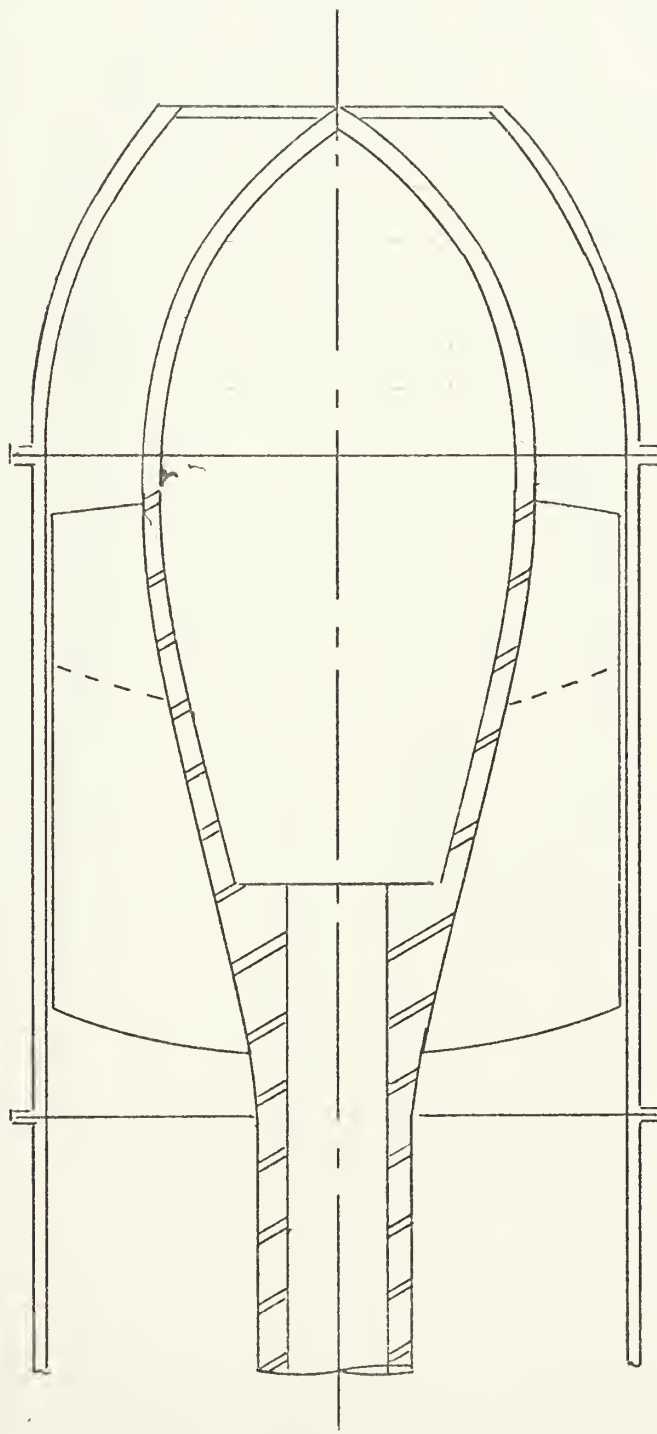


Figure 15. Inducer Stage Axial Pump Design

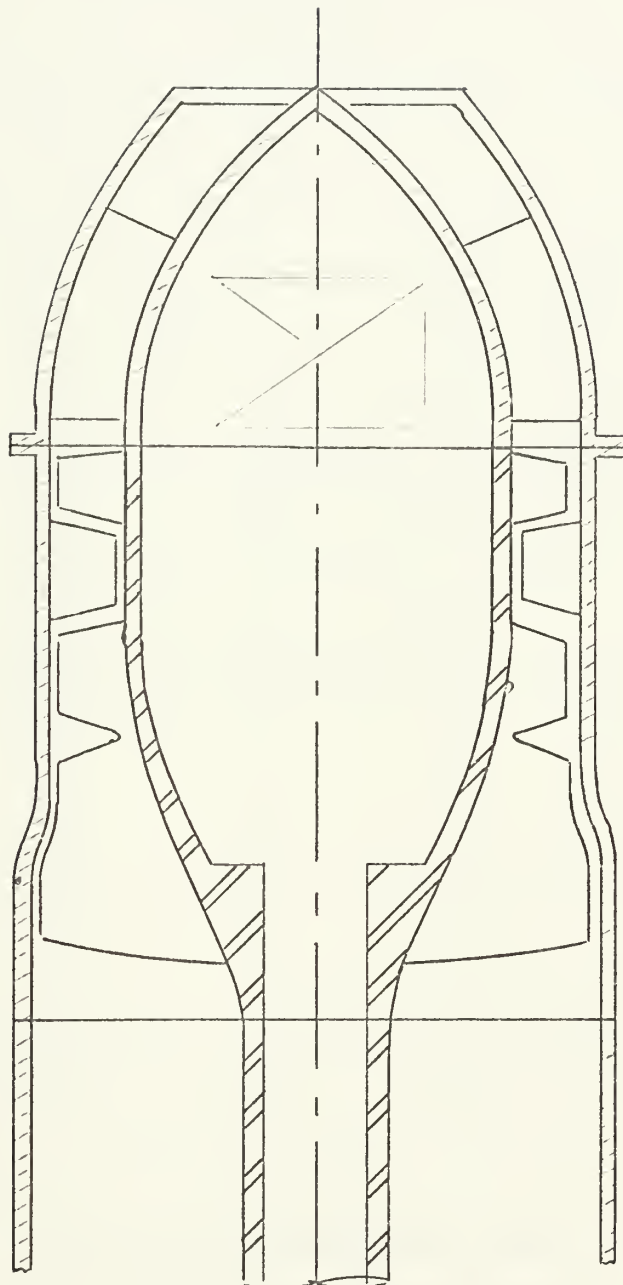


Figure 16. Inducer Plus One Axial Stage, Axial Pump Design

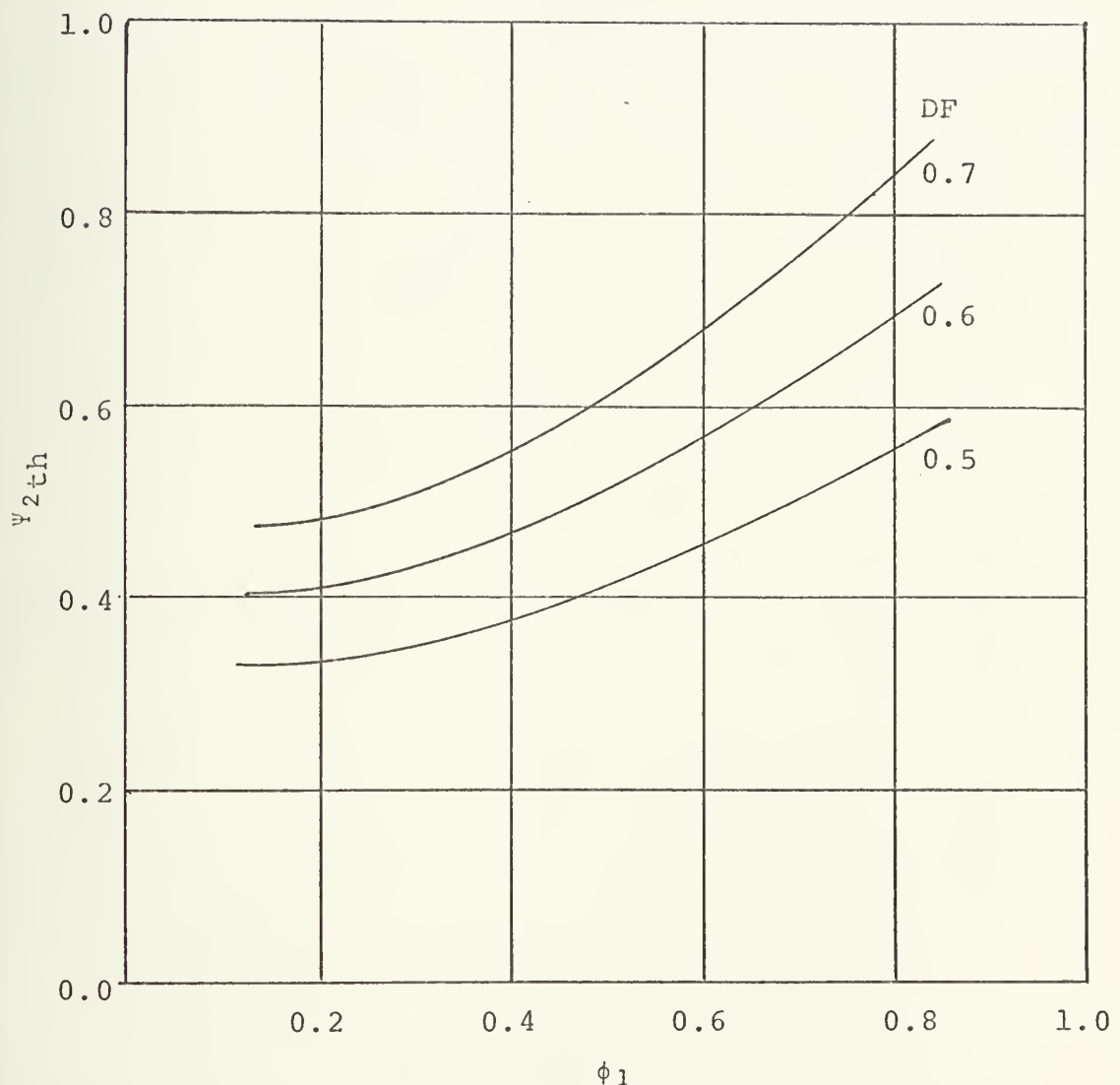


Figure 17. Theoretical Head Coefficient vs Flow Coefficient for Value of Diffusion Factor

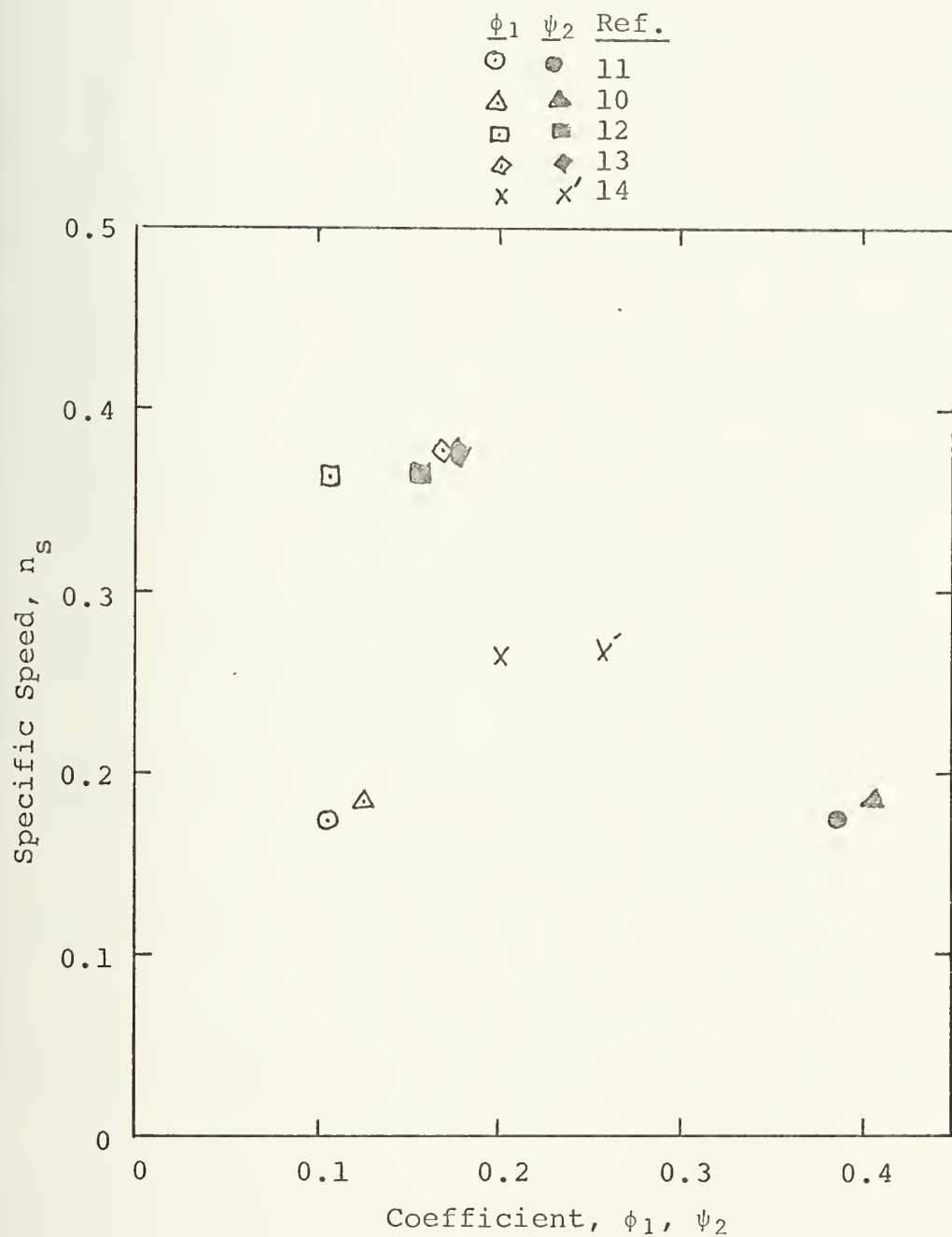


Figure 18. Inducer Inlet Flow Coefficient and Head Coefficient as a Function on Non-Dimensional Specific Speed for Various Designs

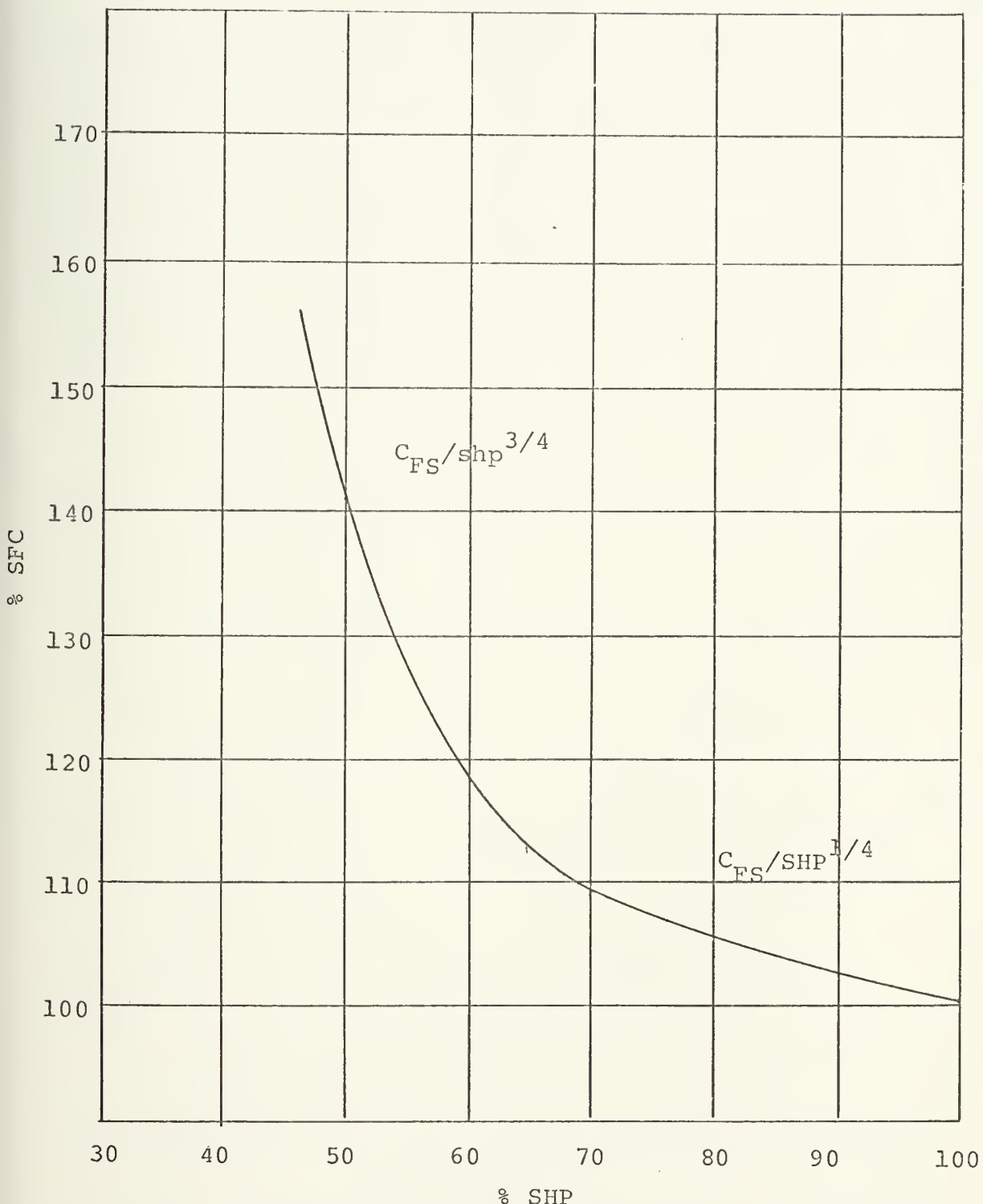


Figure 20. Percent SHP vs Percent SFC with Respect to Normal Power Approximation for Gas Turbine

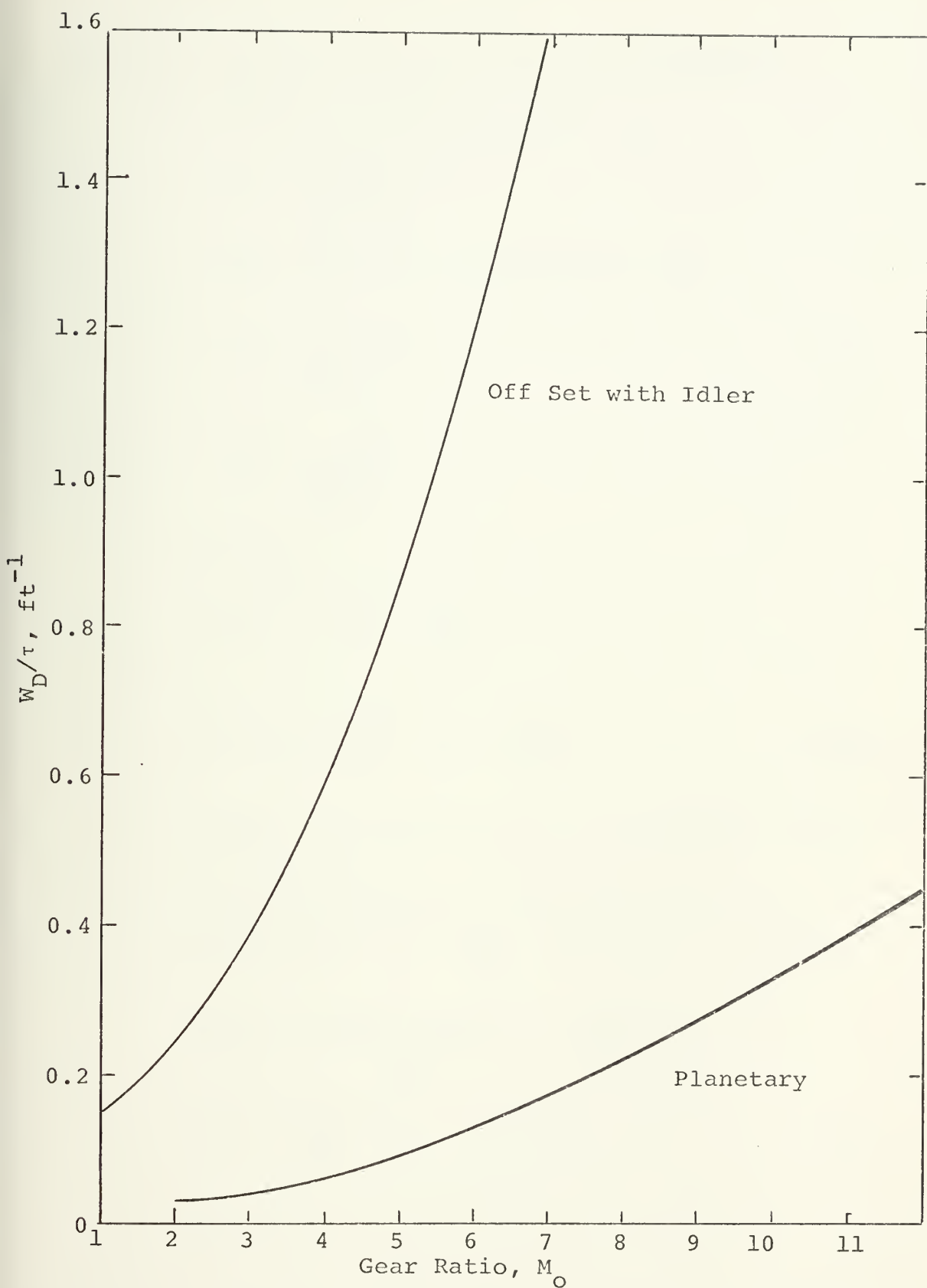


Figure 19. Gear Weight to Input Torque Ratio as a Function of Reduction Gear Ratio for $\text{FAC} = 1.0$

Appendix A. Development Of Cavitation Parameters

(1.) Prandlt's Cavitation Number Is:

$$\sigma_1 = \frac{p - p_v}{\frac{1}{2}\rho V^2}$$

when related to the impeller inlet

$$\sigma_p = \frac{p_1 - p_v}{\frac{1}{2}\rho W_{1s}^2} \quad (A.1)$$

$$\sigma_p = \frac{h - hv}{W_{1s}^2/2g}$$

relating σ_p to H_{sv}

$$H_{sv} = h - hv + \frac{V_{ml}^2}{2g}$$

$$H_{sv} = \sigma_p \frac{W_{1s}^2}{2g} + K_1 \frac{V_{ml}^2}{2g} \quad (A.2)$$

where K_1 is an allowance for induced prewhirl at the inlet and is typically (1.1).

Substituting for $\frac{V_{ml}}{u}$ to give H_{sv} in terms of ϕ_1

$$H_{sv} = \sigma_p \left(\frac{U_1^2 + V_{ml}^2}{2g} \right) + K_1 \frac{V_{ml}^2}{2g}$$

$$H_{sv} = \frac{V_{ml}^2}{2g} \{ \sigma_p (1 + 1/\phi_1^2) + 1 \} \quad (A.3)$$

for $K_1=1.0$

(2.) Relating S to σ_p and ϕ_1 :

$$S = \frac{N Q^{\frac{1}{2}}}{H_{SV}^3/4}$$

$$N = 60 U_1 / \pi D_{1s}$$

$$Q = Ka\pi/4 D_{1s}^2 (1-r_{h1}^2) V_{m1}$$

$$S(\text{cfs}) = \frac{60 U_1 / \pi D_{1s} \{ Ka\pi/4 V_{m1} D_{1s}^2 (1-r_{h1}^2) \}^{\frac{1}{2}}}{(V_{m1}^2/2g \{ \sigma_p (1+1/\phi_1^2) + 1 \})^{3/4}}$$

$$S(\text{cfs}) = \frac{Ka^{\frac{1}{2}} 60/2\pi^{\frac{1}{2}} \{ 1-r_{h1}^2 \}^{\frac{1}{2}}}{\phi_1 \{ 1/2g (1+\sigma_p + \sigma_p^2/\phi_1^2) \}^{3/4}} \quad (\text{A.4})$$

$$S^1 = S / (1-r_{h1}^2)^{\frac{1}{2}}$$

$$C = Ka^{\frac{1}{2}} 30/\pi^{\frac{1}{2}} = 16.5 \text{ (for } Ka = 0.95)$$

$$S^1 = C/\phi_1 \{ 1/2g (1+\sigma_p + \sigma_p^2/\phi_1^2) \}^{3/4} \quad (\text{A.5})$$

(3.) For maximum suction specific speed given a constant σ_p

$$\{ \phi_1^{4/3} (1+\sigma_p + \sigma_p^2/\phi_1^2) \}^{3/4} = \text{minimum}$$

$$d/d\phi_1 \{ \phi_1^{4/3} (1+\sigma_p + \sigma_p^2/\phi_1^2) \}^{3/4} = 0$$

$$4/3 \phi_1^2 (1+\sigma_p) - 2/3 \sigma_p = 0$$

$$\phi_1 = \{ \frac{1}{2} (\sigma_p / 1 + \sigma_p) \}^{\frac{1}{2}} \quad (\text{A.6})$$

for $\sigma_p = 0.03$, $K_1 = 1$

$\phi_1 = 0.120$

for $\sigma_p = 0.03$, $K_1 = 1.1$

$\phi_1 = 0.116$

Appendix B. Development Of Specific Speed As A Function Of Head and Flow Coefficients.

(1.) Non-dimensional specific speed is defined:

$$n_s = n Q^{1/2} / (gH)^{3/4} \quad (B.1)$$

$$n_s = N_s (cfs) / 811.3$$

(2.) Exit area of impeller equals:

$$A = K_a \pi b D_{2s} \quad (B.2)$$

where K_a is the blockage factor

(3.) The pump speed equals:

$$n = U_2 / \pi D_{2s} \quad (B.3)$$

(4.) Flow coefficient is defined at exit as:

$$\phi_2 = V_{m2} / U_2 \quad (B.4)$$

(5.) Head coefficient is defined as:

$$\psi_2 = gH / U_2^2 \quad (B.5)$$

(6.) Substituting equation B.2 and B.3 into B.1 gives:

$$n_s = U / \pi D_{2s} (V_{m2} K_a \pi b D_{2s})^{1/2} / (gH)^{3/4}$$

$$n_s = 1 / \pi^{1/2} (K_a b / D_{2s})^{1/2} U_2 V_{m2}^{1/2} / (gH)^{3/4}$$

$$n_s = 1 / \pi^{1/2} (K_a b / D_{2s})^{1/2} (V_{m1} / U_2)^{1/2} / (gH / U_2^2)^{3/4}$$

(7.) Substituting for definitions of B.4 and B.5:

$$n_s = 1 / \pi^{1/2} (K_a b / D_{2s})^{1/2} \phi_2^{1/2} / \psi_2^{3/4} \quad (B.6)$$

(5.) The gas turbine SFC to SHP relationship is approximated by:

$$SFC = C_{FS} / SHP^n \quad (E.6)$$

where:

$$n = 1/4$$

for 100% to 70% of normal power

$$n = 3/4$$

for less than 70% of normal power.

(6.) Substituting E.6 for E.5 gives:

$$W_F = C_{FS} \cdot SHP^{(1-n)} \cdot t \quad (E.7)$$

(7.) Using a discrete step approach where the time, t , is equal to the range over speed:

$$\Delta t = \frac{R}{V_O N}$$

$$W_F = \sum_{i=1}^N W_{fi} \quad (E.8)$$

where:

$$W_{fi} = C_{FS} \cdot SHP^{(1-n)} \cdot \Delta t \quad (E.9)$$

$$\text{for } V_j = -V_O/2 + \left\{ \frac{V_O^2/2 + \frac{(\Delta - W_{f(i-1)})D/L}{\rho A_j}^{1/2}}{\rho A_j} \right\} \quad (E.10)$$

Appendix C. Sample Calculation For The Centrifugal Pump Design.

(1.) Input to test routine:

Displacement: 100 tons
Cruise Speed: 45 Kts
Range: 750 n. mi.
Configuration: 2 pumps, 2 engines
Engine: Tyne RM-1A
Jet Velocity Ratio: 2.0

(2.) Input to the pump solution from the test routine:

	<u>Cruise</u>	<u>Takeoff</u>	
Q	123.42	126.89	cfs
H	304.66	393.80	ft
H _{SV}	91.02	22.56	ft

(3.) Pump design solution at takeoff:

$$\sigma_T = H_S/H$$

$$\sigma_T = 22.56/393.80$$

$$\sigma_T = 0.057$$

$$N_S (\text{cfs}) = S (\text{cfs}) \sigma_T^{3/4}$$

$$\text{for } S_{\max} = 424.5$$

$$N_S (\text{cfs}) = 49.72 \text{ (for single suction)}$$

for the number of double suction impellers $n=10$

$$Q/IMP = 126.89/2 \cdot 10 \cdot 2$$

$$Q/IMP = 3.172 \text{ cfs}$$

$$N = N_s H^{3/4} / Q/IMP^{1/2}$$

$$N = 2467 \text{ rpm}$$

for values of ϕ_2 & ψ_2 enter the design chart

for $n_h = 0.90$, the chart is based on $b/D_{2s} = 0.001 N_s - 0.025$ for $\beta_2 = 22^\circ$:

$$\phi_2 = 0.16$$

$$\psi_2 = 0.552$$

$$D_{2s} = \frac{60}{\pi N} \left(\frac{gH}{\psi} \right)^{1/2}$$

$$D_{2s} = \frac{60}{\pi 2465} \left(\frac{g}{0.552} \frac{398.8}{0.552} \right)^{1/2}$$

$$D_{2s} = 1.172 \text{ ft}$$

$$D_{1s} = \left\{ \frac{240}{\pi_2 K a \phi_1} \frac{Q/IMP}{(1-r_{h1}^2) N} \right\}^{1/2}$$

for: $r_{h1} = 0.5$, $\beta_1 = 14^\circ$, $Ka = 0.95$

$$\phi_1 = \tan 14^\circ = 0.25$$

$$D_{1s} = 0.558 \text{ ft}$$

$$\eta_p = 1 - \left\{ \left(\frac{2.333}{1.172} \right)^{0.165} (1-0.88) \right\}$$

$$\eta_p = 0.866$$

$$\text{SHP/ENG} = \frac{\rho \ g \ Q \ H}{550 \ n_p \ (\text{No. Eng})}$$

$$\text{SHP/ENG} = 3354.931 \text{ Shp}$$

If takeoff SHP is less than maximum intermittent power then calculation is continued:

$$A_{in} = \frac{Q}{V_{in} \ (\text{no. pump})}$$

$$V_{in} = 0.75 \ V_{ml}$$

$$V_{in} = (0.75) (0.25) \pi D_{1s} N / 60$$

$$A_{in}/\text{Pump} = 109 \ Q / N D_{1s} \ (\text{No. Pump})$$

$$A_{in}/\text{Pump} = \frac{(109) (126.89)}{(2467) (.558) (2)}$$

$$A_{in}/\text{Pump} = 5.03 \text{ ft}^2$$

$$L_p = \left(\frac{A_{in}}{n \ 0.866} \right) (2+n)$$

$$L_p = 6.85 \text{ ft}$$

$$W_D = (0.725n + 0.275) C_w D_{2s}^2 N_s$$

$$W_D = (7.525) (4.66) (1.17)^2 (49.72)$$

$$W_D = 2395.1 \text{ lbs.}$$

$$W_w = 0.55 W_D$$

$$W_w = 1317.3 \text{ lbs.}$$

(4.) Off design calculations at cruise:

$$H/H_D = A(Q/Q_D)^2 + B Q/Q_D N/N_D + C(N/N_D)^2$$

$$N/N_D = \frac{B}{2C} Q/Q_D \pm \left\{ \frac{B}{2C} (Q/Q_D)^2 - \frac{A}{C} (Q/Q_D)^2 + \frac{H}{H_D C} \right\}^{\frac{1}{2}}$$

$$A = -1.5$$

$$C = 2.85 n_s - 0.17$$

$$B = 1 + 1.5 - C$$

$$N/N_D = 0.904$$

$$N = 2225 \text{ rpm}$$

$$\eta_p = \eta_{pD} (A(Q/Q_D)^2 + B Q/Q_D + C)$$

$$A = -0.75, B = 1.51, C = 0.24$$

$$\eta_p = 0.865$$

$$SHP/ENG = \frac{\rho g Q H}{550 \eta_p (\text{No. Eng})}$$

$$SHP/ENG = 2530.39 \text{ shp}$$

Appendix D. Sample Calculations for Axial Pump Design.

(1.) Input to test routine:

Displacement: 100 tons
Cruise Speed: 45 Kts
Range: 750 n. mi.
Configuration: 2 pumps, 2 engines
Engine: Tyne RM-1A
Jet Velocity Ratio: 2.0

(2.) Input to the pump solution from the test routine:

	<u>Cruise</u>	<u>Takeoff</u>
Q	123.42	126.89 cfs
H	304.66	393.80 ft
H _{sv}	91.02	22.56 ft

(3.) Pump design solution at takeoff:

$$\sigma_T = H_s/H$$

$$\sigma_T = 0.057$$

$$N_s (\text{cfs}) = 149.5$$

$$Q/\text{pump} = 63.447 \text{ cfs}$$

$$N = N_s H^{3/4} (Q/p)^{1/2}$$

$$N = (149.5) (398.8)^{3/4} / (63.45)^{1/2}$$

$$N = 1659.17 \text{ rpm}$$

$$M_o = N_p / N$$

$$M_{\odot} = 1.874$$

for $\phi_1 = 0.11$, $r_{h1} = 0.3$

$$D_{1s} = \left\{ \frac{240 Q/\text{pump}}{\pi^2 K a \phi_1 N (1 - r_{h1}^2)} \right\}^{1/3}$$

$$D_{1s} = 2.131 \text{ ft}$$

$$A_{in} = 0.785 D_{1s}^2 (1 - r_{h1}^2)$$

$$A_{in} = 3.275 \text{ ft}^2$$

$$L_p = C_L D_{1s}$$

$$L_p = (1.79) (2.131)$$

$$L_p = 3.81 \text{ ft}$$

$$\eta_p = \left(\frac{3.66}{2.13} \right)^{0.165} (1 - 0.915)$$

$$\eta_p = 0.907$$

$$SHP/ENG = \frac{\rho g Q H}{550 \eta_p^2}$$

$$SHP/ENG = 3271.7$$

SHP/ENG < Maximum Intermittent Power

$$W_D = C_w D_{1s}^{2.3}$$

$$W_D = 347.1 (2.131)^{2.3}$$

$$W_D = 1477.98 \text{ lbs.}$$

$$W_w = 0.523 A_{in} L_p \rho g$$

$$W_w = 414.28 \text{ lbs.}$$

(4.) Off design calculations at cruise for:

$$A = -3.0, B = 4.8, C = -0.8$$

$$N = 1528.16 \text{ rpm}$$

$$\eta_p = \eta_{pD} (A (Q/Q_D)^2 + B Q/Q_D + C)$$

$$\text{for } A = -1.7, B = 3.42, C = -0.72$$

$$\eta_p = 0.907$$

$$\phi_1/\phi_D = \frac{Q_D}{N_D} - \frac{N}{Q} = 1.060$$

Appendix E. Fuel Weight Calculation Method

$$(1.) \quad \text{SHP} = \rho g Q H / 550 \eta_p \eta_g \quad (\text{E.1})$$

(2.) assuming D/L to be constant:

$$(D/L) \Delta = \rho Q (V_j - V_o) , \quad (\Delta-\text{lbs})$$

$$\Delta (D/L) = \rho A_j V_j (V_j - V_o)$$

as fuel is burned V_j is reduced with Δ for D/L , A_j , V_o remain constant.

$$V_j = -V_o / 2 + \{V_o^2 / 4 + \Delta (D/L) / \rho A_j\}^{1/2} \quad (\text{E.2})$$

(3.) Pump head is a function of losses and dynamic head. Assuming the losses ΔH_L to be only a function of jet velocity:

$$\Delta H_L = K_a V_j^2 / 2g$$

$$H = K_D V_j^2 / 2g + h_L - V_o^2 / 2g \quad (\text{E.3})$$

therefore

$$H = f(V_j)$$

$$Q = f(V_j)$$

giving

$$\text{SHP} = f(V_j)$$

$$\text{SHP} = \frac{\rho g V_j A_j}{550 \eta_p \eta_g} (K_D V_j^2 / 2g + h_L - V_o^2 / 2g) \quad (\text{E.4})$$

(4.) Fuel weight burned for a constant SHP is:

$$W_F = \text{SFC SHP } t \quad (\text{E.5})$$

where t is time in hours.

Appendix F. Program Flow Diagram

CHART TITLE - PRIMROSES

PAGE 02

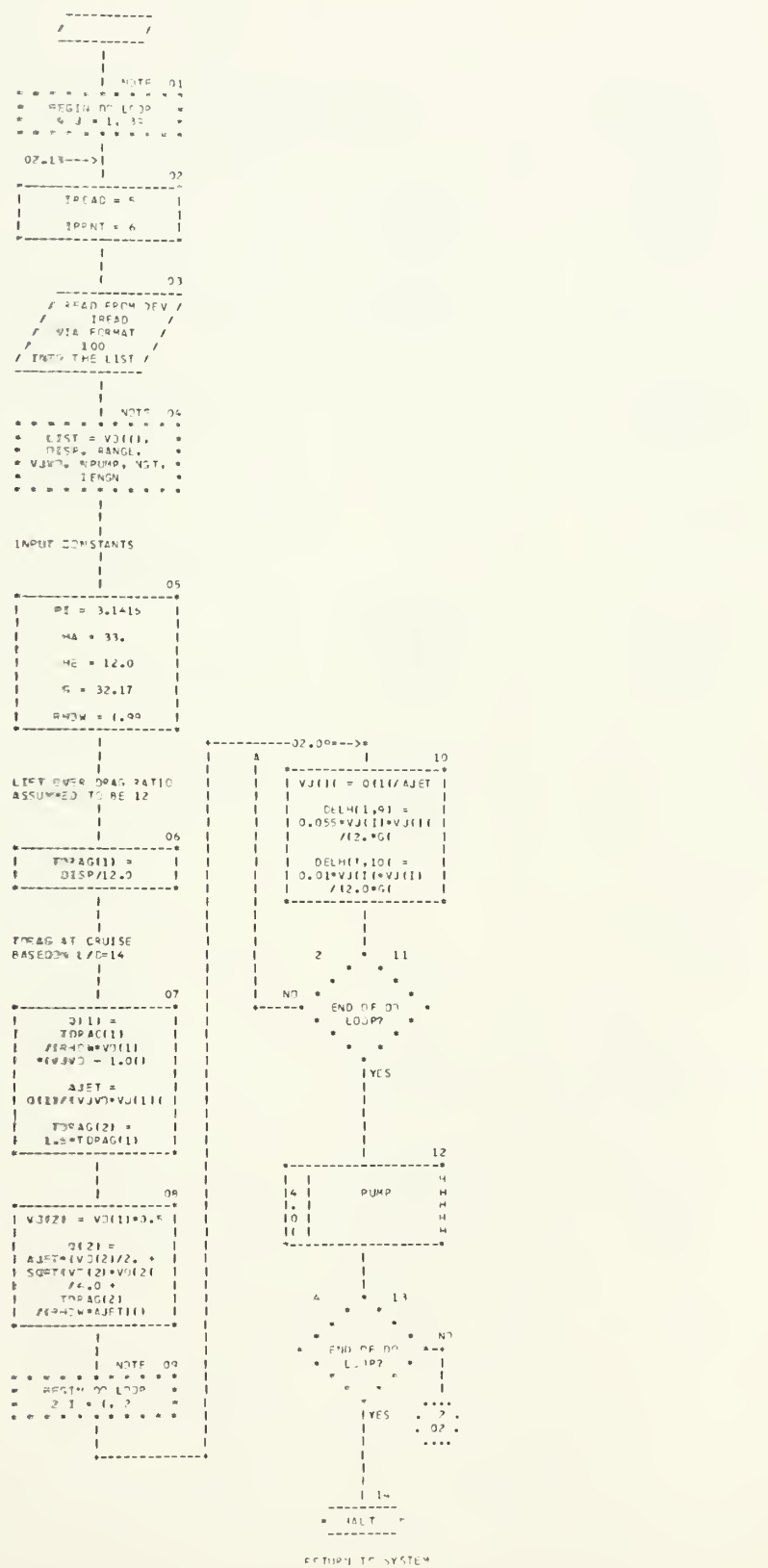


CHART TITLE - SWIRL JETTING PUMP

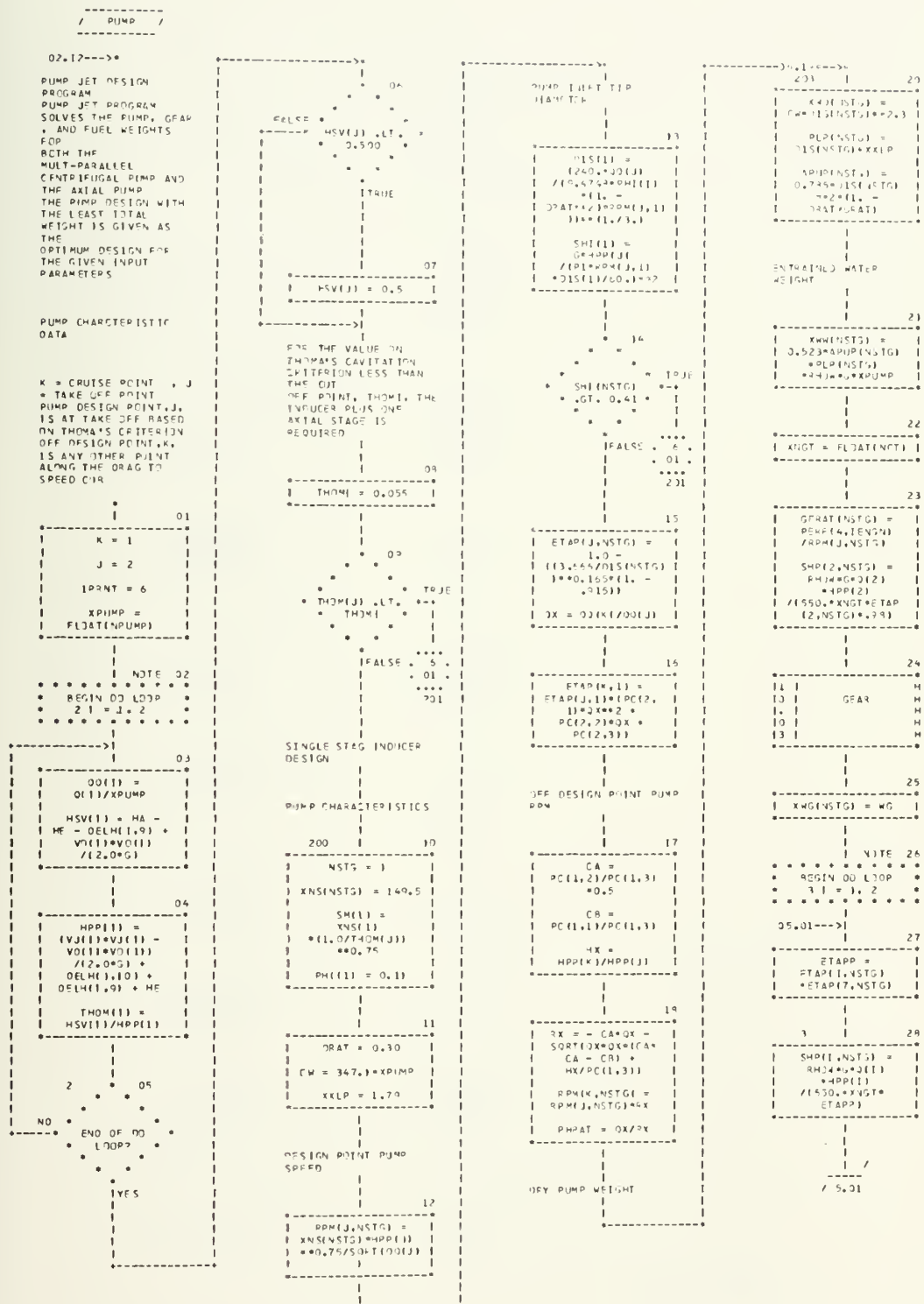


CHART TITLE - SUBROUTINE PUMP

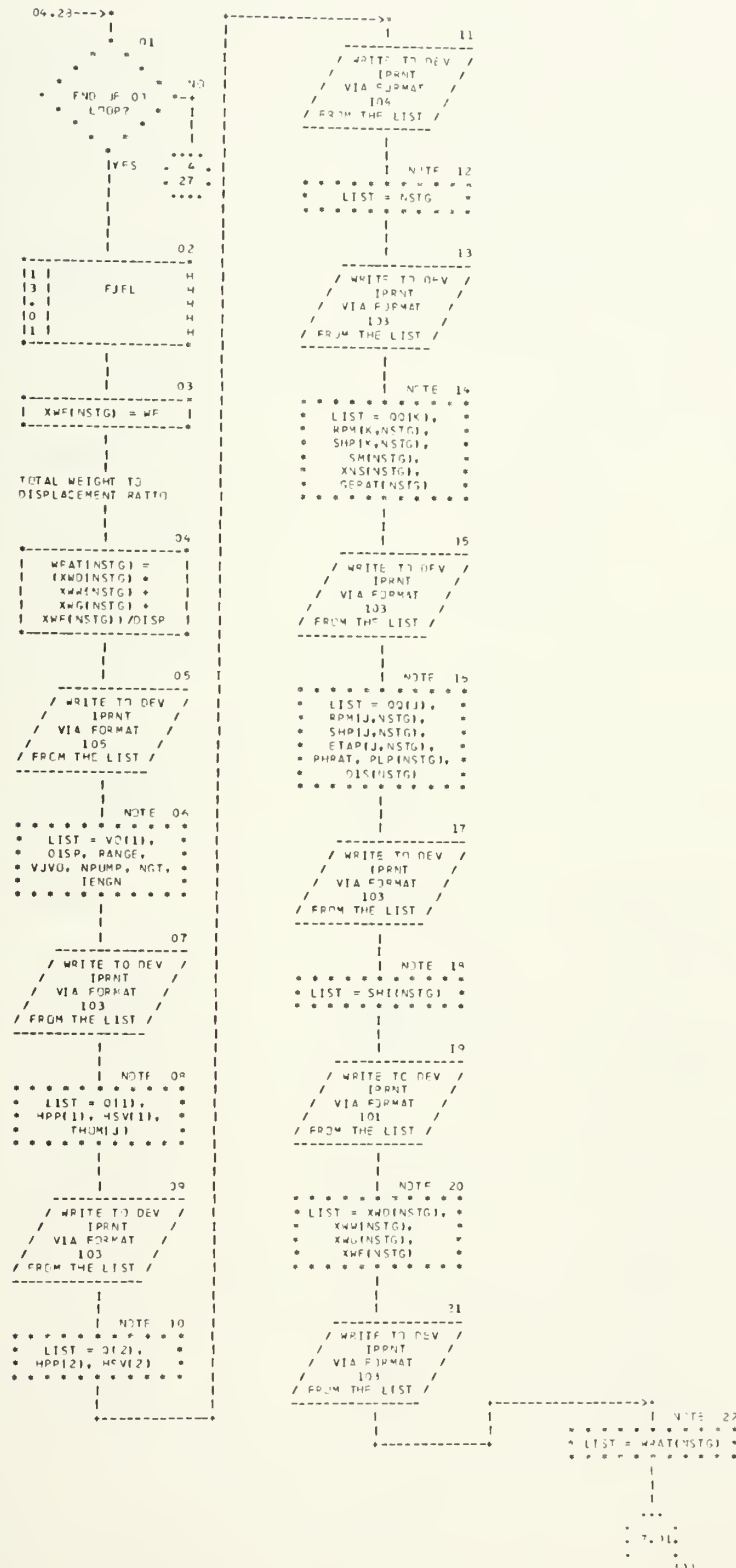


CHART TITLE = SUBROUTINE PUMP

INDUCER PLUS MF
AXIAL STAGE DESIGN

```
04.09-->*
201 1 01
*-----*
| THMT = 0.058 |
| NSTG = 2 |
| HP = HSV(J)/THMT |
*-----*
```

THMT IS THOMAS
CAVITATION CRITERION
FOR THE AXIAL STAGE
BASED IN A MAXIMUM S
OF 10,000 AND NS=3419

```
02
*-----*
| THMTS = 0.258 |
*-----*
```

INDUCER SPECIFIC
SPEED AND FLOW COEFF.

```
03
*-----*
| XNS(NSTG) = 142.5 |
| PHI(2) = 0.15 |
| DRAT = 0.3 |
| XXLP = 1.71 |
| CW = 393.5*XPUMP |
*-----*
```

DESIGN PUMP SPEED

```
04
*-----*
| RPM(J,NSTG) = |
| XNS(NSTG) |
| *HP*0.75/SORT |
| (Q1(J)) |
*-----*
```

PUMP INLET TIP
DIAMETER

```
05
*-----*
| DIS(2) = |
| (240.0*Q1(J)) |
| /(9.4748*PHI(2)) |
| *0.1 |
| DRAT*2*PHI(2) |
| *(1/3) |
| SH1(2) = |
| G*HP/(P1*PPH(J,2)) |
| *0.1*DIS(2)/60.0*2 |
*-----*
```

```
06
*-----*
| ETAP(J,NSTG) = |
| 1.0 - |
| ((3.666/0.15*NSTG) |
| *0.165*(1.0 - |
| .915)) |
| QX = 00*K1/Q01(J) |
*-----*
```

```
07
*-----*
| FTAP(X,NSTG) = |
| ETAP(J,NSTG) |
| *(PCA12,1) |
| *QX*2 + |
| PCA12,2*QX + |
| PCA12,3) |
*-----*
```

OFF DESIGN POINT RPM

```
09
*-----*
| CA = |
| PCA(1,2)/PCA(1,3) |
| *0.5 |
| CB = |
| PCA(1,1)/PCA(1,3) |
| HX = |
| HPP(K)/HPP(J) |
*-----*
```

INDUCER PLUS TWO
AXIAL STAGES DESIGN

```
202 1 12
*-----*
| H4P = (HPP(J) - |
| HP)/2.0 |
| NSTG = 3 |
| XXLP = 2.03 |
| CW = 432.5*XPUMP |
| XNS(3) = XNS(2) |
*-----*
```

```
10
*-----*
| PHRAT = QX/RX |
| SN(NSTG) = |
| XNS(NSTG) |
| *(HP/4*SV(J)) |
| *0.75 |
*-----*
```

```
11
*-----*
| = (HSV(J) + = TRUE) |
| * HP1/(HPP(J)) - = |
| * HP1 * LT. - |
| * THMTS * |
| = |
| IF FALSE |
| = |
| *** |
| *** 4.21 |
| *** 203 |
*-----*
```

```
14
*-----*
| RPM(K,3) = |
| RPM(K,2) |
| ETAP(J,3) = |
| ETAP(J,2) |
| FTAP(K,3) = |
| FTAP(K,2) |
*-----*
```


CHART TITLE - SUBROUTINE PUMP

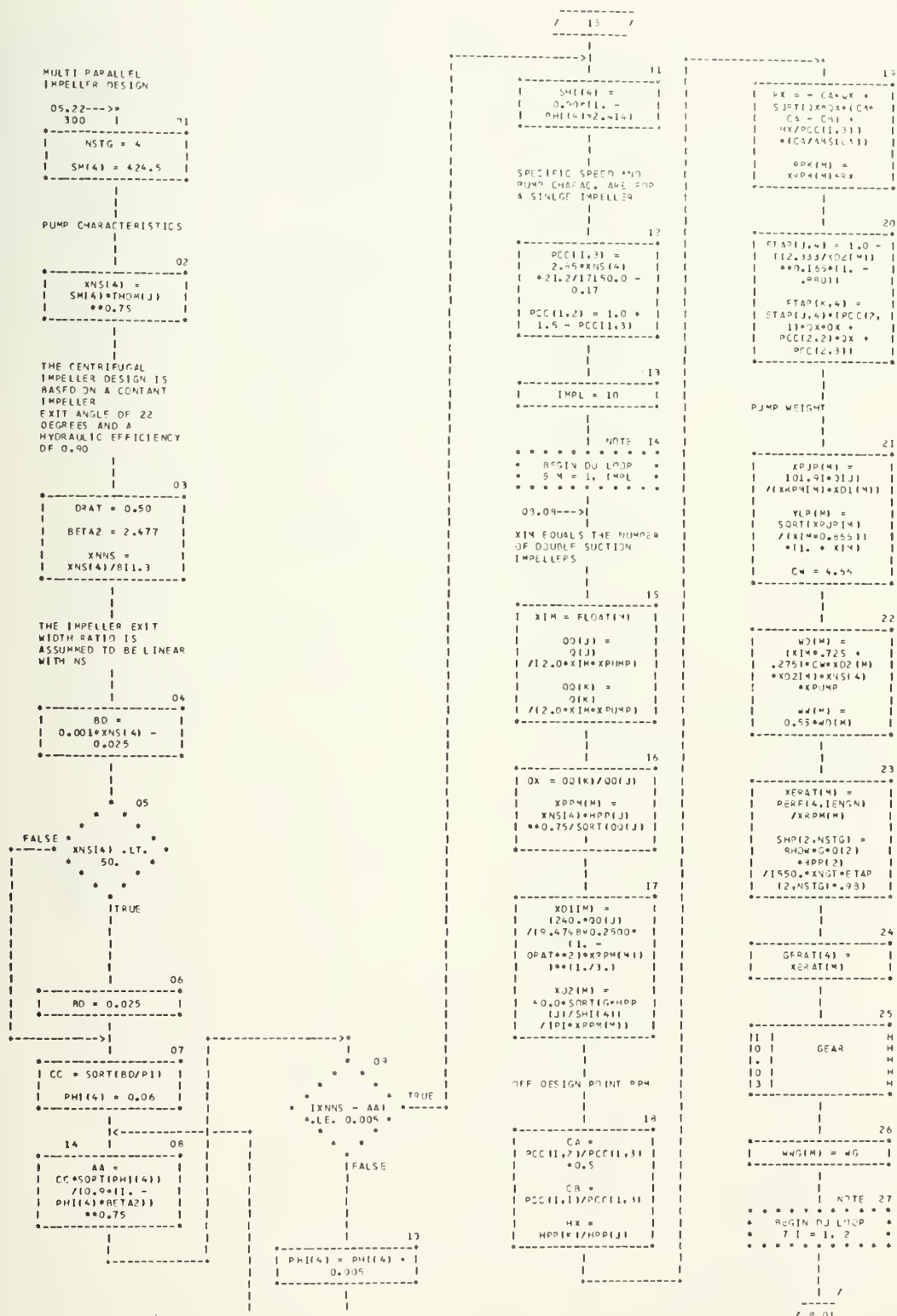


CHART TITLE - SURGE DUTING PUMP

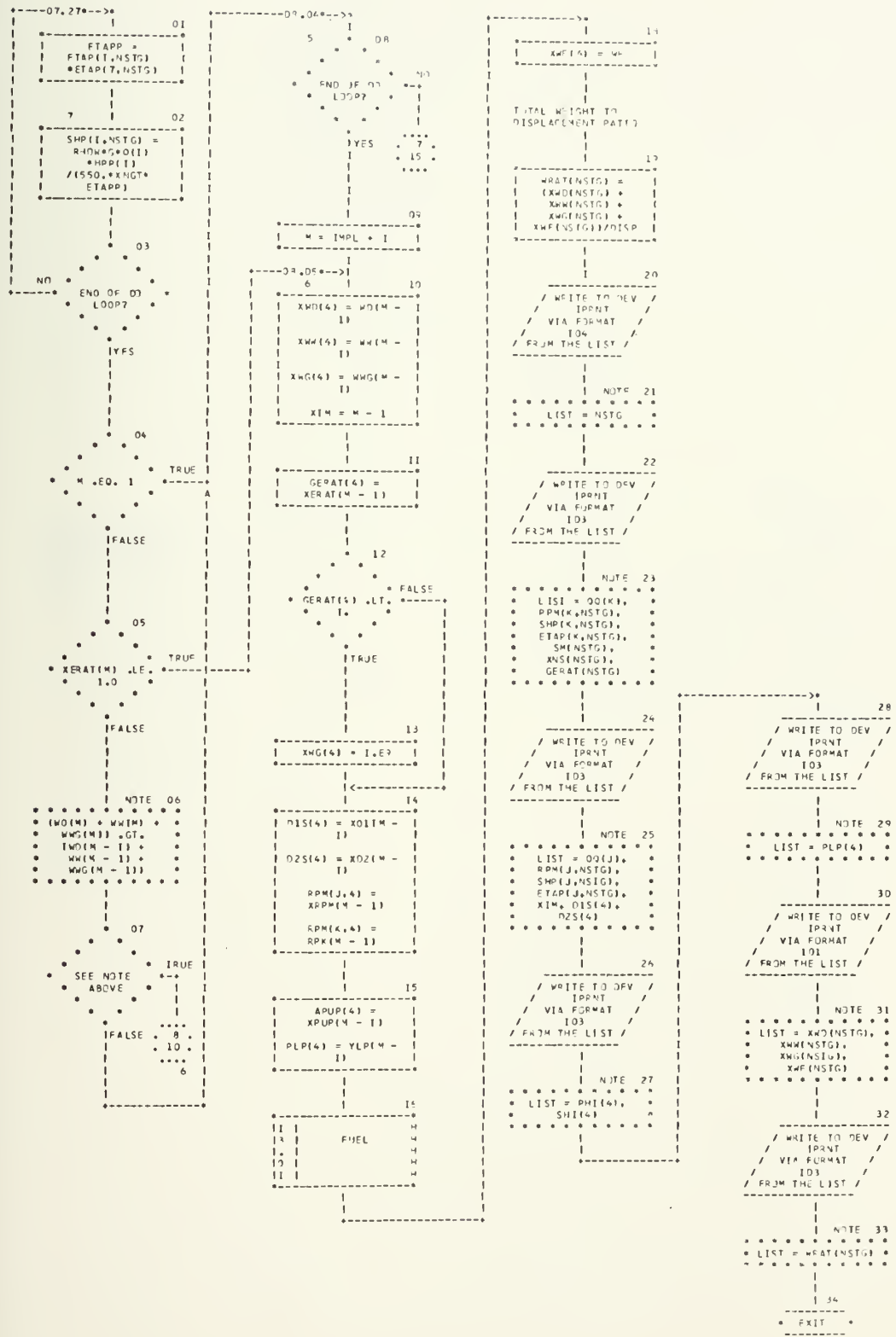


CHART TITLE - SUBROUTINE GEAR

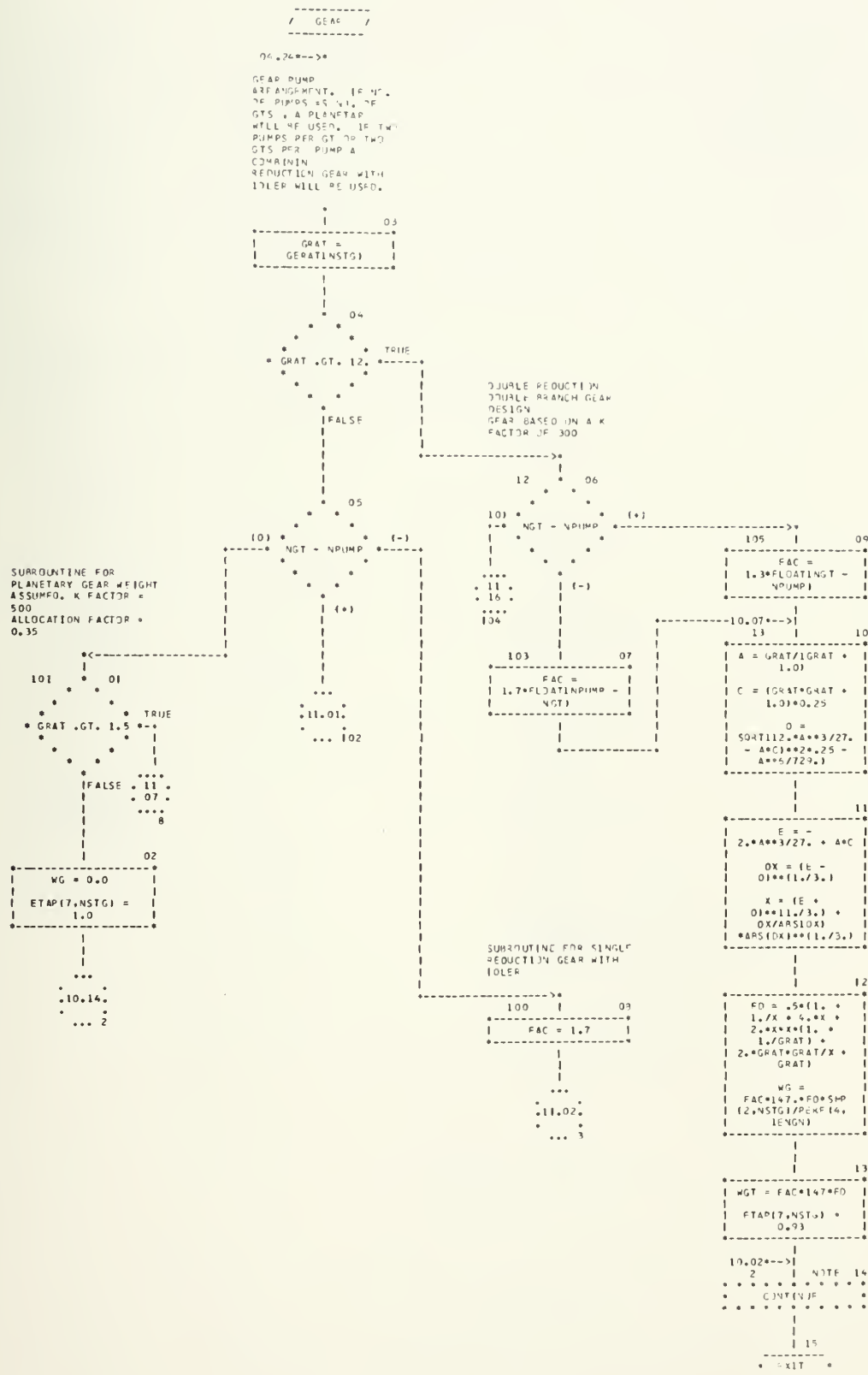


CHART TITLE = SUBROUTINE GEAR

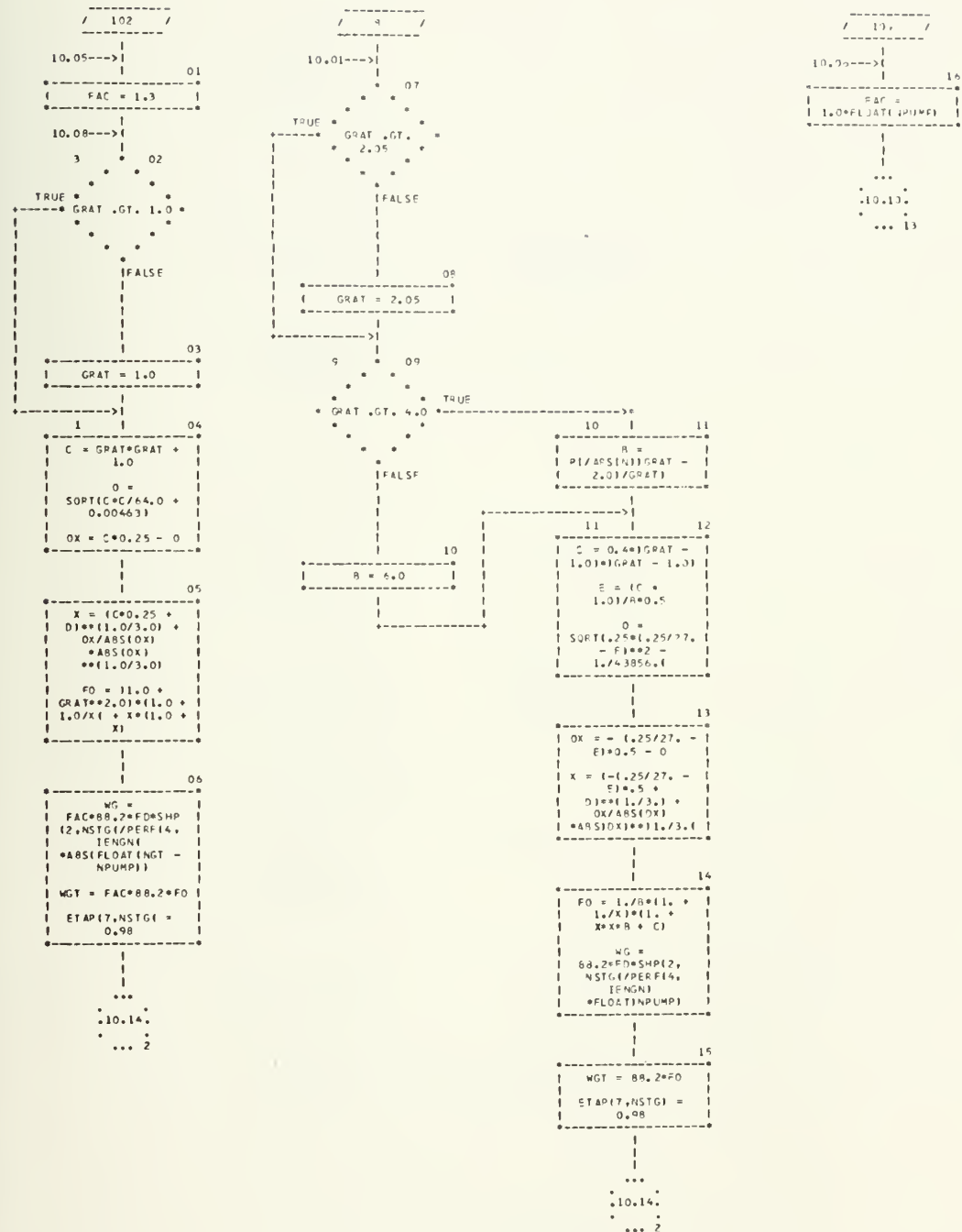
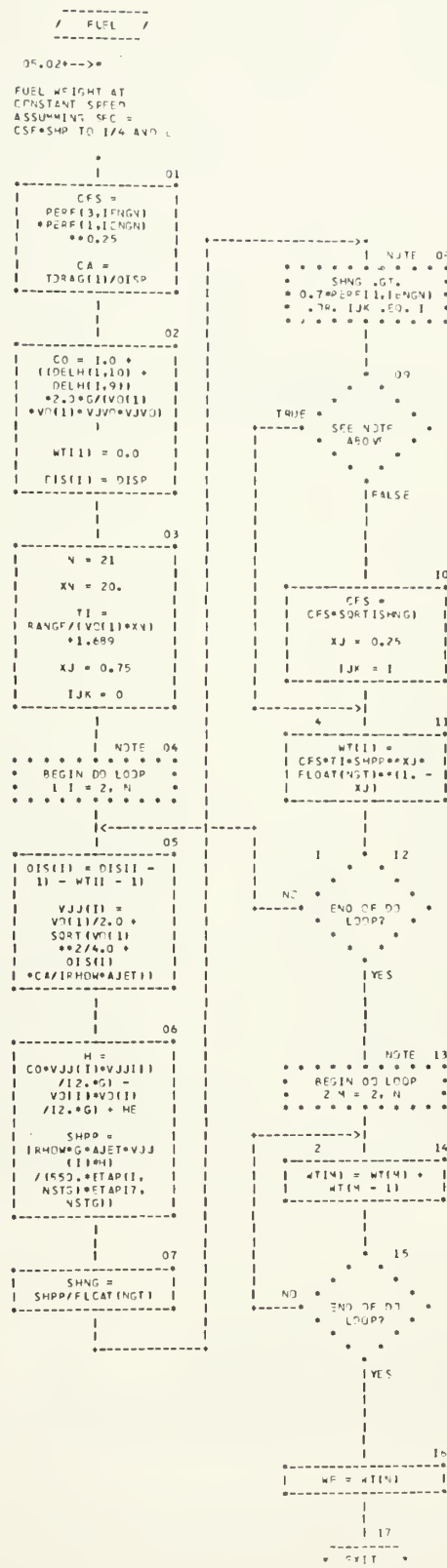


CHART TITLE - SUBROUTINE FUEL



LIST OF PROGRAM SYMBOLS

NOTE - NOT ALL VARIABLES IN TABLE COMMON ARE USED IN PUMP SUBROUTINE

SYMBOL	DESCRIPTION	UNITS
I	INDEX. 1-CRUISE, 2-TAKE OFF	
N	POSITION INDEX FOR SYS COMPONENT	
NSTG	INDEX TO PUMP TYPE	
PI	CONSTANT EQUAL TO 3.1416	
G	GRAVITATIONAL CONSTANT	
RHOW	DENSITY OF SEA WATER	LB/FT ³
PV	WATER VAPOR PRESSURE	FT
HA	ATMOSPHERIC PRESSURE	FT
HE	HEIGHT OF PUMP ABOVE WATER LINE	FT
DISP	HYDRODIL DISPLACEMENT	LB
RANGE	CRUISE RANGE	N. MILES
TDRAC(I)	DRAg	LB
AJET	JET EXHAUST AREA	FT ²
AREA(N)	AREA AT POSITION N	FT ²
VC(I)	HYDROFOIL VELOCITY	FPS
VJ(I)	JET VELOCITY	FPS
VJVO	JET VELOCITY TO HYDRO. VELOCITY RATIO	
DElh(I,N)	SYSTEM LOSSES AT POSITION (I,N)	FT
ENGN	ENGINE INDEX	
NGT	NUMBER JF ENGINES	
NPUMP	NUMBER JF PUMPS	
Q(I)	TOTAL FLOW RATE	CFS
QG(I)	FLOW RATE PER PUMP IMPELLER	CFS
HPP(I)	PUMP HEAD	FT
HSV(I)	NET POSITIVE SUCTION HEAD AT IMP INLET	FT
HP	INDUCER HEAD	FT
THOM(I)	THOMA'S CAVITATION CRITERION	
THOMI	MINIMUM VALUE OF THOMA FOR INDUCER	
THOMS	MINIMUM VALUE OF THOMA FOR AXIAL STAGE	
XNS(NSTG)	IMPELLER SPECIFIC SPEED	

C	S^4	SUCTION SPECIFIC SPEED AT TAKE OFF		
C	$D1(NSTG)$	IMPELLER INLET DIAMETER	FT	
C	$D2(NSTG)$	IMPELLER EXIT DIAMETER	FT	
C	$PLP(NSTG)$	PUMP LENGTH	FT	
C	$PHI(NSTG)$	IMPELLER FLOW COEFFICIENT		
C	$SHI(NSTG)$	IMPELLER HEAD COEFFICIENT		
C	$DRAT$	HUB TO TIP DIAMETER RATIO AT PUMP INLET	1/FT	
C	$XXLP$	PUMP LENGTH COEFFICIENT		
C	CW	PUMP WEIGHT COEFFICIENT		
C	$RPM(I, NSTG)$	PUMP SPEED	RPM	
C	$APUP(NSTG)$	PUMP INLET AREA FOR ONE PUMP	FT ²	
C	$PHRAT$	OFF DESIGN FLOW COEFF. TO DESING COEFF.		RATIO
C	RD	IMPELLER EXIT WIDTH RATIO, B/D ₂ S		
C	$IMPL$	MAX NO. OF CENTRIFUGAL IMPELLERS		
C	XIM	NUMBER OF CENTRIFUGAL IMPELLERS		
C	$GERAT(NSTG)$	REDUCTION GEAR RATIO		
C	$SHP(I, NSTG)$	POWER AT CONDITION I	SHP	
C	$PERF(M, IENGN)$	ENGINE CHARACTERISTIC WHERE M =		
C		1 - NORMAL ENGINE POWER	SHP	
C		2 - MAX INTERMITTENT POWER	SHP	
C		3 - ENGINE SFC AT 1		
C		4 - ENGINE RPM		
C		5 - ENGINE DRY WEIGHT	IB	
C	$FTAP(I, M)$	EFFICIENCY FOR M =		
C		1 - 4 IS NSTG		
C		7 - GEAR		
C	$PC(2,3)$	COEFFICIENTS TO HEAD AND EFF. CURVES		
C	$PCA(2,3)$	COEFFICIENTS TO HEAD AND EFF. CURVES		
C	$PCC(2,3)$	COEFFICIENTS TO HEAD AND EFF. CURVES		
C	$XWD(NSTG)$	PUMP DRY WEIGHT	LB	
C	$XWW(NSTG)$	PUMP ENTRAINED WATER WEIGHT	LB	
C	$XWG(NSTG)$	GEAR WEIGHT	LB	
C	$XWF(NSTG)$	FUEL WEIGHT	LB	
C	$WPAT(NSTG)$	SUM OF WEIGHTS TO DISP RATIO		
C	$WSTS(M, N)$	LIGHTEST SYSTEM WEIGHTS	LB	
C	$CGS(M, N)$	CENTER OF GRAVITY	FT	

XLP PUMP LENGTH OF LIGHTEST PUMP

C C TEST PROGRAM FOR SUBROUTINE PUMP
C C PROGRAM BASED ON CONSTANT LIFT TO DRAG RATIO AND INLET AND
C DUCKING LOSSES AFUNCTION OF JET VELOCITY ONLY

COMMON /PARMS/VJVD,VVVO,ARATO
COMMON /CHARS/WGTS(2,15),CGS(4,15),DELH(5,15)
COMMON /DRAG/TDRAG(5),STRD(5),POD(5),SPRAY(5),REST(5),VO(5),
1 TRIM(5)
COMMON /H2D/TEMP,PV,RHOM,GNU,HA
COMMON /SHIP/ DISP,RANGE,BEAM,HS,HE,HCL,XLS,XLPF,XLP
COMMON /CONST/PI,G,RHOD
COMMON /FLDW/Q(5),AIN,AJET,AREA(11),VJ(5),VI(5)
COMMON /INDEX/I EVAL,IEQPT,ISTRT,NUMB,IFENGN,ITYPF,ICOMP,NPUMP,NGT
COMMON /EECT/XWD(5),XWW(5),XWG(5),XWF(5)
DO 4 J=1,39
IREAD=5
IPPNNT=6
READ(IREAD,100) VJ(1),DISP,RANGE,VJVO,NPUMP,NGT,IFENGN
FORMAT(4F8.2,3I2)
C INPUT CONSTANTS
PI=3.1416
HA=33.
HE=12.C
G=32.17
RHOM=1.99
C LIFT OVER DRAG RATIO ASSUMED TO BE 12
TDRAG(1)=DISP/12.0
C DRAG AT CRUISE BASED ON L/D=14
O(1)=TDRAG(1)/(RHOM*VJ(1)*(VJVO-1.0))
AJET=O(1)/(VJVO*VJ(1))
TDRAG(2)=1.6*TDRAG(1)
VJ(2)=VO(1)*C.5
Q(2)=AJET*(VJ(2)/2.+SQRT((VO(2)*VJ(2)/4.+TDRAG(2)/(RHOM*AJET)))
DO2 I=1,2


```
VJ(I)=Q(I)/AJET
DELH(I,9)=C*0.55*VJ(I)*VJ(I)/(2.*G)
DELH(I,10)=0.01*VJ(I)*VJ(I)/(2.*G)
2 CONTINUE
  CALL PUMP
4 CONTINUE
  STOP
END
```


SUBROUTINE PUMP
PUMP JET DESIGN PROGRAM

C PUMP JET PROGRAM SOLVES THE PUMP, GEAR, AND FUEL WEIGHTS FOR
 C BOTH THE MULTI-PARALLEL CENTRIFUGAL PUMP AND THE AXIAL PUMP
 C THE PUMP DESIGN WITH THE LEAST TOTAL WEIGHT IS GIVEN AS THE
 C OPTIMUM DESIGN FOR THE GIVEN INPUT PARAMETERS

COMMON /PAPMS/VJVO,VIVO,ARATO
 COMMON /CHARS/AGTS(2,15),CGS(4,15),DELH(5,15)
 COMMON /DRAG/DTDRAG(5),STRTD(5),POD(5),SPRAY(5),REST(5),VO(5),
 1 TRIM(5)

COMMON /420/TEMP,PV,RHOM,HA
 COMMON /SHIP/ DISP,RANGE,BEAM,HS,HE,HCL,XLS,XLP
 COMMON /CONST/PI,G,RHOD

COMMON /FLDW/Q(5),ATN,AJET,AREA(11),VJ(5),VI(5)
 COMMON /INDEX/I EVAL,IEQPT,ISTRRT,NUM3,LENGN,ITYPE,ICOMP,NPUMP,NGT
 COMMON /WEIGT/XW(5),XWW(5),XWF(5)

COMMON /PSUB3/GERAT(5),SHP(5,5),RPM(5,5),PERF(5,12),ETAP(8,5)
 COMMON /PUAM/QO(5),DIS(5),D2S(5),XNS(5),SM(5),PLP(5),NSTG,SHI(5)

COMMON /HEAD/HPP(5),HSV(5),THOM(5),PHI(5),WF,WG,WRAT(5)
 DIMENSION WO(10),WW(10),WWG(10)

DIMENSION PC(2,3),PCA(2,3),PCC(2,3)
 DIMENSION XROM(11),XDI(11),XDO(11),RDK(11),XPUP(11),YLP(11),
 SXERAT(11)

DIMENSION APUP(5)

C PUMP CHARACTERISTIC DATA

DATA PC/-3.0,-1.7,4.3,3.42,-0.8,-0.720/
 DATA PCA/-1.0,-1.7,1.0,3.42,1.0,-0.72/
 DATA PCC/-1.5,-0.75,1.0,1.51,1.0,0.24/

C K = CRUISE POINT, J = TAKE OFF POINT
 C PUMP DESIGN POINT, J, IS AT TAKE OFF BASED ON THOMAS CRITERION

OFF DESIGN POINT, K , IS ANY OTHER POINT ALONG THE DRAG TO SPEED CURVE

۲۲

```

IPRNT=6
XPUMP=FLD AT (NPUMP)
D02 I=1,2
  Q(I)=Q(I)/XPUMP
  HSV(I)=HA-HE-DELH(I,9)+VO(I)*VO(I)/(2.0*G)
  HPP(I)=(VJ(I)*VJ(I)-VO(I)*VO(I))/(2.0*G)+DELH(I,10)+DELH(I,9)+HE
  THOM(I)=HSV(I)/HPP(I)
  2 CONTINUE
  IF(HSV(J),LT.0.500) HSV(J)=0.5

C FOR THE VALUE ON THOMA'S CAVITATION CRITERION LESS THAN THE CUT
C OFF POINT, THOM, THE INDUCER PLUS ONE AXIAL STAGE IS REQUIRED
C
C THOMI=0.055
C IF(THOM(J).LT.THOMI) GO TO 201

C SINGLE STAG INDUCER DESIGN

C PUMP CHARACTERISTICS
C
C 200 NSTG=1
  XNSIN(STG)=149.5
  SM(1)=XNS(1)*(1.0)/THOM(J)**0.75
  PHI(1)=0.11
  DRAT=C.30
  CW=347.1*XPUMP
  XXLP=1.79

C DESIGN POINT PUMP SPEED
  RPM(J,NSTG)=XNS(NSTG)*HPP(J)**0.75/SQRT(QQ(J))

C PUMP INLET TIP DIAMETER
  DIS(1)=(24C.*QQ(J)/(9.4748*PHI(1)*(1.-DRAT**2))*RPM(J,1))***(1./3.)

```



```

SHI(1)=G*HPP(J)/(PI*RPM(J,1)*DIS(1)/60.)***2
IF(SHI(NSTG).GT.0.41) GO TO 201
ETAP(J,NSTG)=1.0-((3.666/DIS(NSTG))*C.165*(1.0-.915))
QX=QQ(K)/QQ(J)
ETAP(K,1)=ETAP(J,1)*(PC(2,1)*QX**2+PC(2,2)*QX+PC(2,3))

C OFF DESIGN POINT PUMP RPM
CA=PC(1,2)/PC(1,3)*C.5
CB=PC(1,1)/PC(1,3)
HX=HPP(K)/HPP(J)
PX=-CA*QX-SQRT((JX*QX*(CA*CA-CB)+HX)/PC(1,3))
RPM(K,NSTG)=RPM(J,NSTG)*RX
PHPAT=QX/RX

C DRY PUMP WEIGHT
2C3 XWD(NSTG)=C*N*DIS(NSTG)**2.3
PLP(NSTG)=DIS(NSTG)*XXLP
APUP(NSTG)=J.785*DIS(NSTG)**2*(1.-DRAT*DRAAT)

C ENTAINED WATER WEIGHT
XWW(NSTG)=C.523*APUP(NSTG)*PLP(NSTG)*RHOW*G*XWPUMP

C XNGT=FLOAT(NGT)

C GENERATION(NSTG)=PERF(4,LENGN)/RPM(J,NSTG)
SHP(2,NSTG)=RHOW*G*Q(2)*HPP(2)/(550.*XNGT*ETAP(2,NSTG)*.98)
CALL GEAR
XWG(NSTG)=WG
DO 3 I=1,2
ETAPP=ETAP(I,NSTG)*ETAP(7,NSTG)
SHP(I,NSTG)=RHOW*G*Q(I)*HPP(I)/(550.*XNGT*ETAPP)
3 SHP(I,NSTG)=XWD(NSTG)+XWW(NSTG)+XWF(NSTG)/DISP

C CALL FUEL
XWF(NSTG)=WF
TOTAL WEIGHT TO DISPLACEMENT RATIO
RATIO(NSTG)=(XWD(NSTG)+XWW(NSTG)+XWF(NSTG))/DISP

```



```

      WRITE((IPRNT,105) V(J(1),DISP,RANGE,VJVO,NPUMP,VGT,IENG)
      WRITE((IPRNT,103) Q(1),HPP(1),THOM(J))
      WRITE((IPRNT,103) Q(2),HPP(2),HSV(2))
      WRITE((IPRNT,104) NSTG
      WRITE((IPRNT,103) QQ(K),RPM(K,NSTG),SHP(K,NSTG),SM(NSTG),
      5 XNS(NSTG),GERAT(NSTG)
      WRITE((IPRNT,103) QQ(J),RPM(J,NSTG),SHP(J,NSTG),ETAP(J,NSTG),
      4 PHRAT,PLP(NSTG),DIS(NSTG)
      WRITE((IPRNT,103) SAI(NSTG)
      WRITE((IPRNT,101) XWD(NSTG),XWW(NSTG),XWG(NSTG),XWF(NSTG)
      WRITE((IPRNT,103) WRAT(NSTG)
      101 FORMAT(* XWD=*,F11.3,* XWW=*,F11.3,* XWG=*,F11.3,* XWF=*,F11.3)
      103 FORMAT(8F10.2,3I2)
      104 FORMAT(3I5)
      105 FORMAT(4F10.2,3I2)
      GO TO 330

C C INDUCER PLUS JNE AXIAL STAGE DESIGN
C C
C 201 THOMI=0.058
C NSTG=2
C HP=HSV(J)/THOMI
C THOMS IS THOMA'S CAVITATION CRITERION FOR THE AXIAL STAGE
C BASED ON A MAXIMUM S OF 10,000 AND NS=3619
C THOMS=0.253
C C INDUCER SPECIFIC SPEED AND FLOW COEFF.
C C
C XNS(NSTG)=149.5
C PHI(2)=0.15
C DRAFT=0.3
C XXLP=1.71
C CW=393.5*XUMP
C C DESIGN PUMP SPEED
C C

```


C RPM(J,NSTG)=XNS(NSTG)*HP**0.75/SORT(QO(J))

C PUMP INLET TIP DIAMETER

C C DIS(2)=(24)*QQ(J)/(9.4748*PHI(2)*(1.0-DRAT**2)*RPM(J,2))***(1.0/3.0)
SHI(2)=G*HP/(PI**RPM(J,2)*DIS(2)/60.0)**2
ETAP(J,NSTG)=1.0-((3.666/DIS(NSTG))**0.165*(1.0-.915))
QX=QQ(K)/QQ(J)
ETAP(K,NSTG)=ETAP(J,NSTG)*(PCA(2,NSTG)**QX**2+PCA(2,2)*QX+PCA(2,3))

C C OFF DESIGN POINT RPM
CA=PCA(1,2)/PCA(1,3)*0.5
CB=PCA(1,1)/PCA(1,3)
HX=HPP(K)/HPP(J)
RX=-CA*QX+SQR((QX*QX*(CA*CA-CB)+HX/PCC(1,3))*(CA/ABS(CA)))
RPM(K,NSTG)=RPM(J,NSTG)*RX

C PHRAT=QX/RX
SM(NSTG)=XNS(NSTG)*(HP/HSV(J))**0.75
IF((HSV(J)+HP)/(HP*(J)-HP).LT.THOMS) GO TO 202
GO TO 203

C INDUCER PLUS TWO AXIAL STAGES DESIGN

C 202 HHP=(HPP(J)-HP)/2.0
NSTG=3
XXLP=2.03
CW=4.39.5*XPUMP
XNS(3)=XNS(2)
SM(3)=SM(2)
DIS(3)=DIS(2)
SHI(3)=SHI(2)
RPM(J,3)=RPM(J,2)
RPM(K,3)=RPM(K,2)


```
ETAP(J,3)=ETAP(J,2)
ETAP(K,3)=ETAP(K,2)
GO TO 203
```

```
C MULTI PARALLEL IMPELLER DESIGN
```

```
C 307 NSTG=4
C SM(4)=424.5
C PUMP CHARACTERISTICS
C XNS(4)=SM(4)*THOM(J1)**0.75
C
C THE CENTRIFUGAL IMPELLER DESIGN IS BASED ON A CONSTANT IMPELLER
C EXIT ANGLE OF 22 DEGREES AND A HYDRAULIC EFFICIENCY OF 0.90
C
C DRAT=0.50
C RETA2=2.477
C XNNS=XNS(4)/811.3
C
C THE IMPELLER EXIT WIDTH RATIO IS ASSUMED TO BE LINEAR WITH NS
C BD=0.001*XNS(4)-J.025
C IF(XNS(4).LT.50.) BD=0.025
C CC=SQRT(BD/PI)
C PHI(4)=C.05
C AA=CC*SQRT(PHI(4))/(J.9*(1.-PHI(4))*BETA2)**0.75
C IF((XNNS-AA).LE.J.005) GO TO 15
C PHI(4)=PHI(4)+D.005
C GO TO 14
C 15 SHI(4)=C.90*(1.-PHI(4)**2.414)
C SPECIFIC SPEED AND PUMP CHARAC. ARE FOR A SINGLE IMPELLER
C
C PCC(1,3)=2.85*XNS(4)*21.2/17150.0-0.17
C PCC(1,2)=1.0+1.5-PCC(1,3)
C
C IMPL=10
C DO5 M=1,IMPL
```


C XIM EQUALS THE NUMBER OF DOUBLE SUCTION IMPELLERS
 XIM=FLOAT(M)

QQ(J)=Q(J)/(2.0*XIM*XPUUMP)
 QQ(K)=Q(K)/(2.0*XIM*XPUUMP)
 QX=QQ(K)/QQ(J)
 XPPM(N)=XNS(4)*HPP(J)*0.75/SQRT(QQ(J))
 XD1(M)=(240.0*QQ(J)/(9.4748*C.2500*(1.0-DRAT**2))*XPPM(M))***(1.0/3.0)
 XD2(M)=6.0*SQRT(G*HPP(J)/SHI(4))/(PI*XPPM(M))
 C DFF DESIGN POINT RPM
 CA=PCC(1,2)/PCC(1,3)*0.5
 CR=PCC(1,1)/PCC(1,3)
 HX=HPP(K)/HPP(J)
 RX=-CA*QX+SQRT(QX*QX*(CA*CA-CB)+HX/PCC(1,3))*(CA/ABS(CA))
 RPK(M)=XPPM(M)*RX

C
 ETAP(J,4)=1.0-(2.333/XD2(M))*0.165*(1.0-.889)
 ETAP(K,4)=ETAP(J,4)*(PCC(2,1)*QX*QX+PCC(2,2)*QX+PCC(2,3))

C PUMP WEIGHT

C
 XPPM(M)=1.09.*Q(J)/(XPPM(M)*XDI(M))*XPUUMP
 YLP(M)=SQRT(XPPM(M)/(XIM*0.866))*((2.0+XIM))
 CW=4.66
 WD(M)=(XIM*.725+.275)*CW*XD2(M)*XNS(4)*XPUUMP
 WN(M)=0.55*WD(M)

C
 XERAT(M)=PERF(4,ILENG)/XPPM(M)
 SHP(2,NSTG)=RHO*W*G*Q(2)*HPP(2)/(550.*XNGT*ETAP(2,NSTG)*.98)
 GERAT(4)=XERAT(M)
 CALL GEAR
 WWG(M)=WG
 DO 7 I=1,2
 ETAPP=ETAP(I,NSTG)*ETAP(7,NSTG)
 7 SHP(I,NSTG)=RHO*W*G*Q(I)*HPP(I)/(550.*XNGT*ETAPP)
 IF(M.EQ.1) GO TO 5


```

IF(XERAT(M).LE.1.0) GO TO 6
IF((WD(M)+WN(4)+WG(M)).GT.(WD(M-1)+WN(M-1)+WG(M-1))) GO TO 6
5 CONTINUE

```

```

M=IMPL+1
6   XWD(4)=WD(M-1)
     XWN(4)=WN(M-1)
     XWG(4)=WG(M-1)
     XIM=M-1
     GERAT(4)=XERAT(M-1)
     IF(GERAT(4).LT.1.) XWG(4)=1.E9
     D1S(4)=XD1(4-1)
     D2S(4)=XD2(M-1)
     RPM(J,4)=XRPM(M-1)
     RPM(K,4)=RPK(M-1)
     APUP(4)=XPUP(M-1)
     OLP(4)=YLP(M-1)
     CALL FUEL
     XWF(4)=WF
     TOTAL WEIGHT TO DISPLACEMENT RATIO
     WRAT(NSTG)=(XAD(NSTG)+XW(M(NSTG))+XWG(NSTG))/NSTG
N=4
DO 3 M=1,3
  IF(WRAT(M).NE.C.) GO TO 9
  9 CONTINUE
  8 CONTINUE
  IF(WRAT(M).GT.WRAT(N)) M=N
  NSTG=M
  XLP=PLP(NSTG)
  IPUMP=NCT*IPUMP
  WGTS(1,8)=XWD(M)
  WGTS(2,8)=XWN(M)
  WGTS(1,10)=XWG(M)
  WGTS(2,11)=XWF(M)
  CGS(1,ICMP)=HCL
  CGS(2,ICOMP)=XLP+XLP*.5

```



```

CGS(3,ICOMP)=4CL
CGS(4,ICOMP)=CGS(2,ICOMP)
AREA(8)=APUP(NSTG)*XPUMP
WRITE(IPRNT,104) NSTG
WRITE(IPRNT,103) QQ(K),RPM(K,NSTG),SHP(K,NSTG),ETAP(K,NSTG),
7 SM(NSTG),XNS(NSTG),GERAT(NSTG)
WRITE(IPRNT,103) Q(J),RPM(J,NSTG),SHP(J,NSTG),ETAP(J,NSTG),
6 XIM,D1S(4),D2S(4)
WRITE(IPRNT,103) PHI(4),SHI(4)
WRITE(IPRNT,103) PLP(4)
WRITE(IPRNT,101) XWD(NSTG),XWW(NSTG),XWF(NSTG)
WRITE(IPRNT,103) WRAT(NSTG)
RFTURN
END

```



```

SUBROUTINE GEAR
COMMON /INDEX/IEQPT,IEQVAL,ISTRRT,NUMB,IENGN,ITYPE,ICOMP,NPUMP,NGT
COMMON /CONST/PI,G,RHOD
COMMON /PSUBJ/GERAT(5),SHP(5,5),RPM(5,5),PERF(5,12),ETAP(8,5)
COMMON /PUMPS/QQ(5),DIS(5),D2S(5),XNS(5),SN(5),PLP(5),NSTG,SHI(5)
COMMON /HEAD/HPP(5),HSV(5),THOM(5),PHI(5),WF,WG,WRAT(5)
C GFAR PUMP ARRANGEMENT. IF NO. OF PUMPS =S NO. OF GTS, A PLANETARY GEAR
C WILL BE USED. IF TWO PUMPS PER GT OR TWO GTS PER PUMP A COMBINING SINGLE
C REDUCTION GEAR WITH IDLER WILL BE USED.
C GRAT=GERAT(NSTG)
IF(GRAT.GT.12.) GO TO 12
IF(NGT-NPUMP) 100,101,102
C SUBROUTINE FOR SINGLE REDUCTION GEAR WITH IDLER
100 FAC=1.7
GO TO 3
102 FAC=1.3
103 IF(GRAT.GT.1.0) GO TO 1
GRAT=1.0
1 C=GRAT*GRAT+1.0
D=SQRT(C*C/64.0+3.0463)
DX=C*0.25-D
X=(C*0.25+D)**(1.0/3.0)+DX/ABS(DX)*ABS(DX)**(1.0/3.0)
FD=(1.0+GRAT**2.0)*(1.0+C+1.0/X)+X*(1.0+X)
WG=FAC*89.2*FD*SHP(2,NSTG)/PERF(4,IENGN)*ABS(FLOAT(NGT-NPUMP))
NGT=FAC*89.2*FD
FTAP(7,NSTG)=0.93
GO TO 2
C SUBROUTINE FOR PLANETARY GEAR WEIGHT
C ASSUMED. K FACTOR = 500
C ALLOCATION FACTOR = 0.35
C 101 IF(GRAT.GT.1.5) GO TO 3
WG=0.0
FTAP(7,NSTG)=1.0
GO TO 2
C 8 IF(GRAT.GT.2.05) GO TO 9
GRAT=2.05

```


SUBROUTINE FUEL
 FUEL WEIGHT AT CONSTANT SPEED ASSUMMING SFC = CSF*SHP TO 1/4 AND ETAP = CO
 COMMON /PARMS/VJVO,VIVO,ARATO
 COMMON /CHARS/WGTS(2,15),CGS(4,15),DELH(5,15)
 COMMON /DRAG/TDRAG(5),STRTD(5),POD(5),SPRAY(5),REST(5),VO(5),
 1 TRIM(5)

COMMON /H2O/TEMP,PV,RH0W,GNU,HA
 COMMON /SHIP/DISP,RANGE,REAM,HS,HE,HCL,XLS,XLPE,XLP
 COMMON /CONST/PI,G,RHOD
 COMMON /FLOW/Q(5),AIN,AJET,AREA(11),VJ(5),VI(5)
 COMMON /INDEX/IEVAL,IEQPT,ISTRT,NUMB,IENGN,ITYPE,ICOMP,NPUMP,NGT
 COMMON /PSUB/GERAT(5),SHP(5,5),RPM(5,5),PERF(5,12),ETAP(8,5)
 COMMON /PUM/QQ(5),DIS(5),D2S(5),XNS(5),SM(5),PLP(5),NSTG,SHI(5)
 COMMON /HEAD/HPP(5),HSV(5),THOM(5),PHI(5),WF,WG,WRAT(5)
 DIMENSION WT(21),DIS(21),VJJ(21)
 CFS=PERF(3,IENGN)*PERF(1,IENGN)**0.25
 CA=TDRAG(1)/DISP
 C=1.0+((DELH(1,1)+DFLH(1,9))*2.0*G/(VO(1)*VJ(1)*VJVO))
 WT(1)=C
 DIS(1)=DISP
 N=21
 XN=20.
 TI=RANGE/(VO(1)*XN)*1.589
 XJ=0.75
 IJK=C
 DO1 I=2,N
 DIS(I)=DIS(I-1)-WT(I-1)
 VJJ(I)=VO(1)/2.0+SQRT(VO(1)**2/4.0+DIS(I)*CA/(RH0W*AJFT))
 H=C*VJJ(I)*VJJ(I)/(2.*G)-VO(1)*VJ(1)/(2.*G)+HE
 SH0P=(RH0W*G*A*JET*VJJ(I)*H)/(550.*ETAP(1,NSTG)*ETAP(7,NSTG))
 SHNG=SHPP/FLDAT(NGT)
 IF(SHNG.GT.0.7*PERF(1,IENGN).OR.IJK.EQ.1) GO TO 4
 CFS=CFS*SQRT(SHNG)
 XJ=0.25
 IJK=1
 4 WT(I)=CFS*TI*SH0P**XJ*FLOAT(NGT)**(1.-XJ)


```

1 1 CONTINUE
 002 M=2 ,N
2  WT(M)=WT(M)+WT(M-1)
  WF=WT(N)
  RETURN
END

BLOCK DATA
COMMON /PSUB/GERAT(5),SHP(5,5),RPM(5,5),PERF(5,12),ETAP(8,5)
ENGINE PERFORMANCE DATA
DATA PERFD2220.,284.,59,14500.,1050.,2850.,3060.,55,14500.,
11050.,2930.,351.,63,1500.,3200.,2800.,3510.,63,1000.,3300.,
23320.,4250.,49,3110.,2800.,4160.,5300.,47,3110.,2800.,
32220.,2940.,79,900.),1010.,12500.,14000.,575,5500.,7500.,
422200.,22500.,41,3400.,10500.,19150.,24200.,52,3600.,14200.,
521750.,26950.,52,3600.,14200.,27600.,34400.,48,3600.,14200./
END
C

```



3 OCT 74
24 JUL 75

22321
8200

Thesis 135293
P3345 Percival
Optimization of water-
jet propulsion pumps for
hydrofoil application.

19 SEP 72
3 OCT 74
4 JUL 75

DISPLAY
22321
8200

Thesis 135293
P3345 Percival
Optimization of water-
jet propulsion pumps for
hydrofoil application.

thesP3345
Optimization of waterjet propulsion pump



3 2768 001 97965 1
DUDLEY KNOX LIBRARY